The Dissertation Committee for Rachel Marie Snyder Certifies that this is the approved version of the following dissertation:

Investigation of the Effects of α-TEA, MSA and *t*-RES Alone and in Combination on Human MDA-MB-435 Breast Cancer Cells *in Vitro* and *in Vivo*

Committee:

Bob G. Sanders, Co-Supervisor

Kimberly Kline, Co-Supervisor

Michelle Lane

Vishwanath Iyer

Claudio Conti

Investigation of the Effects of α-TEA, MSA and *t*-RES Alone and in Combination on Human MDA-MB-435 Breast Cancer Cells *in Vitro* and *in Vivo*

by

Rachel Marie Snyder, B.S.

Dissertation

Presented to the Faculty of the Graduate School of

The University of Texas at Austin

in Partial Fulfillment

of the Requirements

for the Degree of

Doctor of Philosophy

The University of Texas at Austin

December 2006

Dedication

To Michael-for giving me the strength to continue and who lifts me up when I am down, for loving me unconditionally, for being infinitely patient, and for being my best friend and the best husband ever.

Acknowledgements

I would like to thank Dr. Bob G Sanders and Dr. Kimberly Kline for their continued guidance and support over the years. I would like to thank present and past members of the Kline/Sanders lab for their help, support, friendship and willingness to pass on valuable information. I would like to thank Dr. Rajenda Mehta and Dr. Henry Thompson and the members of their labs who have collaborated with us in order to complete the chemoprevention studies, Dr. LuZhe Sun and Dr. John Richburg for providing cells for my experiments and allowing me to use equipment in their labs, and my committee members for their helpful suggestions and guidance. I would like to thank my family for the support through the years and my husband Michael for his unending support and love.

Investigation of the Effects of α-TEA, MSA and *t*-RES Alone and in Combination on Human MDA-MB-435 Breast Cancer Cells *in Vitro* and *in Vivo*

Publication No._____

Rachel Marie Snyder, Ph.D.

The University of Texas at Austin, 2006

Supervisor: Bob G. Sanders and Kimberly Kline

Cancer is the leading cause of death in U.S. women under 85. It is becoming increasingly clear that individual treatments will not cure cancer and that combination approaches may be more effective. Our goal was to further understand the molecular mechanisms of α-TEA's anticancer effects, and to explore its potential in combination with two other agents, MSC/MSA and *t*-RES. Data support the efficacy of α-TEA as a chemopreventive and chemotherapeutic agent in human breast cancer cells. We first determined that α-TEA, *t*-RES, and MSC/MSA inhibit cell proliferation, induce differentiation, and synergize when used in combination to induce apoptosis. Treatment enhanced cell death was seen in other cancer cell lines and no cell killing was seen in HMECs. Next, the ability of these agents to reduce tumor burden, induce apoptosis, and prevent proliferation of MDA-MB-435-F-L cells was investigated *in vivo*. α-TEA and

low doses of *t*-RES reduce tumor burden in athymic nude mice but combinations of the three compounds were not as effective as α-TEA or *t*-RES alone. The three treatments significantly reduced visible and micrometastatic tumor foci. We showed that the efficacy of *t*-RES administered at low (10 mg/kg bw) and high (100 mg/kg bw) concentrations was diet-related. Our third aim was to determine if these compounds could effectively inhibit the formation of DMBA and MNU-induced lesions in the MMOC and rat mammary carcinogenesis models. Each compound inhibited cancer lesions in these models but α-TEA and *t*-RES were better than MSA, and a combination of α-TEA and *t*-RES was best. Next, we examined apoptotic and survival signaling events that could lead to synergy after α-TEA and *t*-RES treatment. Pre-treatment sensitized the cancer cells to cell membrane receptor-mediated apoptosis. α-TEA and co-treatment induced cell death was caspases-dependent while that for *t*-RES was not. Next, decreases in prosurvival survivin and c-FLIP proteins were shown to be significant to treatment induced apoptosis. Based on the results reported here, we propose a signaling model where the synergy between α-TEA and *t*-RES is due to a combination of apoptosis and caspase-independent cell death (CICD).

Table of Contents

List of Tables

List of Figures

Chapter 1: Introduction and Literature Review

INTRODUCTION AND CANCER STATISTICS

In the last 50 years there have been numerous advances in medicine and the understanding of human diseases and disorders. Epidemiological data shows significant decreases in the United States for death rates from cardiovascular, cerebrovascular, and infectious diseases. Despite the many advances that have been made in the understanding of cancer progression and targeted drug development, cancer incidence and cure rates have remained relatively unchanged [1-2]. Among U. S. women under the age of 85, cancer is the most common cause of death, followed closely by cardiovascular disease. Specifically, it is estimated that breast cancer specifically will have the highest incidence of reported new cases in 2006 (31%) and will be responsible for approximately 15 percent of cancer deaths in women [1].

The cause of all diseases can be classified into one of three categories: diet, environment, or genetics. It is estimated that 75-85% of all chronic illnesses and diseases are directly linked to lifestyle choices and not genetics [2], and while it is difficult to change some environmental factors and nearly impossible to change genetic factors, it is relatively easy to change diet and therefore reduce the risk of many diseases by a large factor. In recent years there has been a scientific evaluation of many natural and biologically active compounds found in the human diet, many of which have their roots in traditional medicines from around the world. Many of these natural agents have little toxicity and a high potential for use against human disease. With this in mind, we evaluated the anti-tumor effects of three natural-based compounds, α-tocopherol ether analog (α-TEA), *trans*-resveratrol (*t*-RES), and methylseleninic acid (MSA), against human breast cancer cells and examined their potential in human therapy.

CELL DEATH

Schleiden and Schwann first introduced the concept of a cell to the scientific community in 1839. Soon after this initial report was the identification of cell death by Carl Vogt in 1842. Since that time, cell death has continually been studied in order to understand the conditions that lead to cellular demise and the mechanisms by which it occurs [3-4]. Cell death and cell division are essential parts of the normal development and maintenance of multi-cellular organisms [4-5]. Disruption of either process can lead to disturbed embryogenesis, neurodegenerative diseases or cancer [5].

Cells are constantly exposed to external and internal signals, some of which are pro-survival and some of which are anti-survival. For this reason, the balance between life and death is highly regulated in the cell so that cell fate depends on how these signals are interpreted. Melino *et al* [6] describe 11 types of cell death currently known. While there is some overlap between characteristics of the different types, there are also unique characteristics and circumstances under which they occur. In our evaluation of α-TEA, *t*-RES and MSA on human breast cancer cells we will focus primarily on apoptosis and autophagy.

Apoptosis

Description

Apoptosis is a highly regulated form of programmed cell death (PCD) that's name is derived from the Greek term for "dropping off" of petals or leaves from a healthy plant. First recognized in 1842 by Vogt, it has since become recognized as one of many types of cell death and is referred to as Type 1 PCD [4]. Characteristics include cell shrinkage, DNA fragmentation, chromatin condensation, and controlled blebbing of the nucleus and cytosolic cellular fractions into apoptotic bodies [4-5, 7-10], which are

engulfed by phagocytic cells *in vivo* [5, 7-9]. Often, apoptosis is associated with the activation of a group of cysteine proteases known as caspases and there is an absence of lysosomal involvement [4, 7-8, 11].

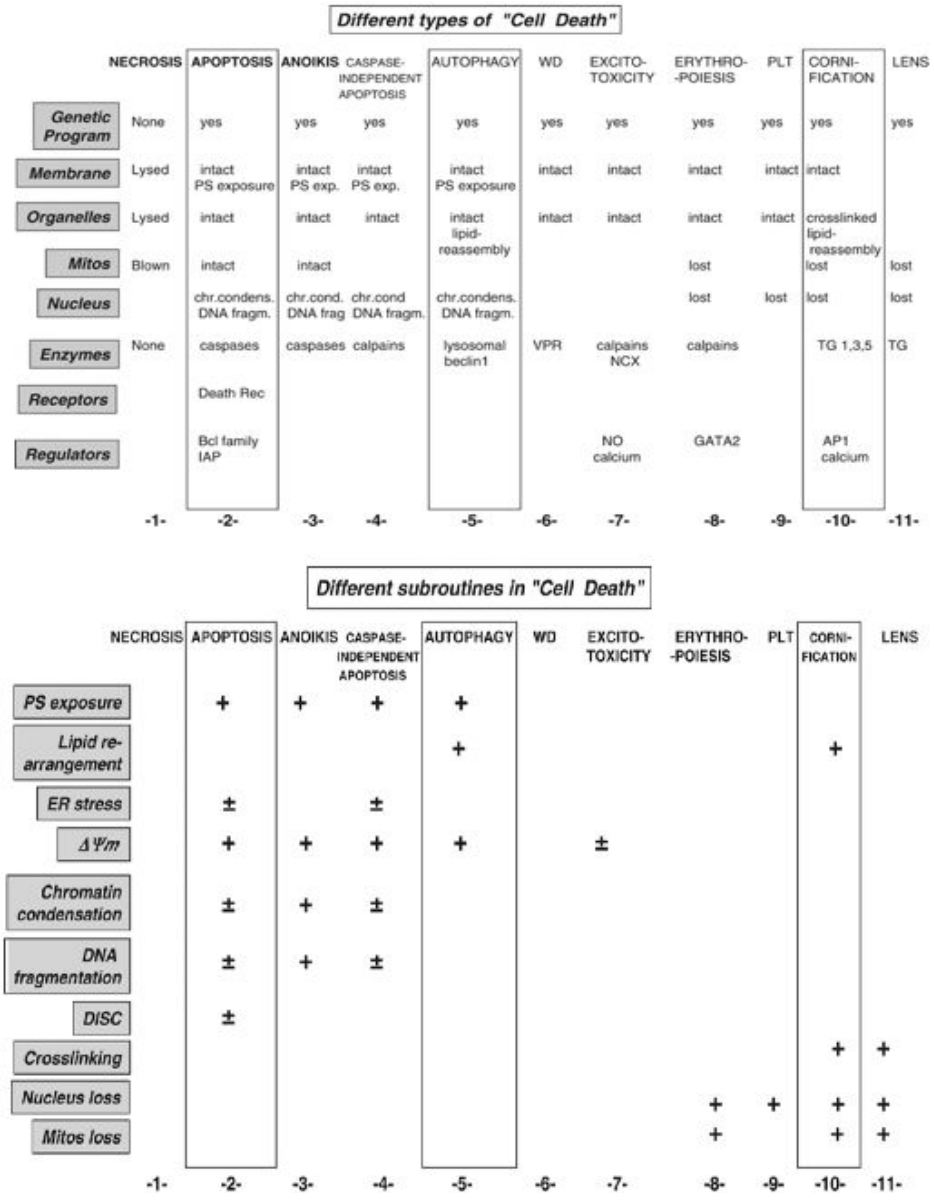

FIGURE 1.1: CHARACTERISTICS OF DIFFERENT TYPES OF CELL DEATH. Adapted from [6].

Signaling Pathways

For a cell to undergo apoptosis, precise signaling pathways must be activated either intrinsically or extrinsically. In addition to the intermediate proteins in the signaling pathways, there are groups of proteins that can promote or block apoptotic pathways, justly named anti-apoptotic and pro-apoptotic proteins. Some cancer therapeutic agents act to induce or sensitize cells to apoptosis by down-regulating anti-apoptotic proteins and/or by upregulating pro-apoptotic proteins.

Apoptosis begins when either an extracellular ligand binds to a death receptor on the cell surface or intracellulary via DNA damage [5, 9-15]. There are six known death receptors, including Fas(CD95), TNFR1, DR3(TRAMP), DR4(TRAIL-R1), DR5(TRAIL-R2), and DR6 [11] with ligands FasL (Fas), TNFα (TNFR1), TRAIL(DR4 and DR5) and TWEAK(DR3) [4, 9, 11-15]. Binding of the ligand induces homotrimerization of the receptor and recruitment of FADD and pro-caspase-8 to the cytosolic part of the receptor to form the DISC, or death inducing signaling complex. Once formed, the DISC cleaves pro-caspase-8 to active caspase-8, which then cleaves and activates substrates in either the mitochondrial independent (type I) or dependent pathways (type II), both of which lead to apoptosis. In the mitochondrial independent pathway (type I), caspase-8 directly activates caspase-3. A slower activation of caspase-3 is accomplished via the mitochondrial dependent pathway (type II). In this pathway, caspase-8 cleaves Bid to tBid, which can then bind to and inhibit anti-apoptotic Bcl-2, allowing Bax to form pores in the mitochondria and release cytochrome c from the intermembrane space [4, 9, 11-15]. Once released, cytochrome c associates with apaf-1 and pro-caspase-9 to form the apoptosome [4-5, 9, 11-15]. Apoptosome formation activates caspase-9, leading to activation of caspase-3 [4, 9, 11-15], which in turn

activates many proteins responsible for the morphological and chemical changes that lead to apoptotic cell death [12-15].

Bcl-2 Family

The Bcl-2 family is a group of proteins that influence the permeability of the mitochondria and can be classified as pro-apoptotic or anti-apoptotic. Regardless of the type, all contain at least one Bcl-2 homology domain (BH) [4-5, 10]. The pro-apoptotic bcl-2 family members include Bax, Bak, Bok, Bid, Bad, Puma, Bmf, Bim, Bik, Noxa, and Hrk/DP5. Upon apoptotic signals, the activation of Bax and Bak results in mitochondrial permeability. The anti-apoptotic bcl-2 family members include Bcl-2, Bcl-XL, Bcl-w, and Mcl-1 [4, 10]. Bcl-2 and Bcl-XL form heterodimers with Bax-like proteins to inhibit mitochondrial permeabilization. Since these two classes have opposing functions they are often in competition and can inhibit each other through direct binding [5, 10].

Mitochondrial Proteins

Upon permeabilization of the mitochondria, there are several proteins released from the mitochondria in addition to cytochrome c. Two pro-apoptotic proteins, apoptosis-inducing factor (AIF) and endonuclease G (endo G), work to enhance DNA condensation and degradation by working with caspase-activated DNase CAD/DFF40 [4-5, 10-11]. Smac/DIABLO (second mitochondria-derived activator of caspase/direct IAP binding protein with low p*I*) and Omi/HtrA2 (high temperature requirement protein A2) are two other proteins released from the intermembrane space of the mitochondria and act to inhibit the activity of anti-apoptotic XIAP (see below) [4, 10-11]. Additionally, Omi/HtrA2 has protease function that can directly inhibit cytochrome c [5].

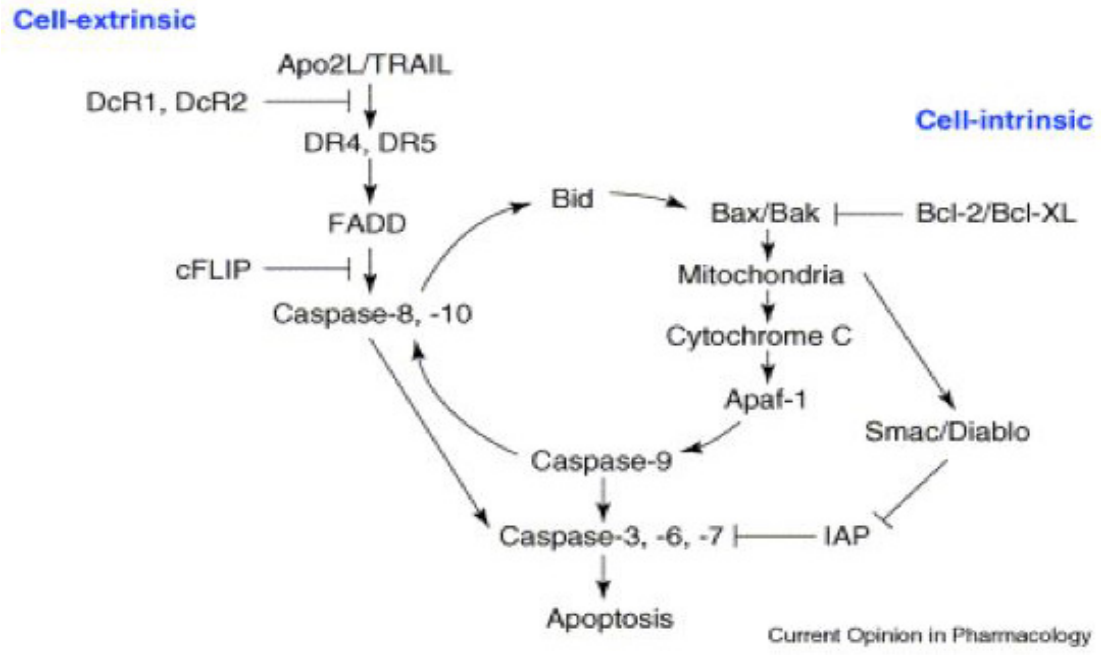

FIGURE 1.2: MODEL OF SIGNALING EVENTS LEADING TO APOPTOSIS. Adapted from [14].

Inhibitors of Apoptosis Proteins

Some cancer therapeutic agents can act to induce or sensitize cells to apoptosis by down-regulating inhibitor of apoptosis proteins (IAPs). This family of proteins includes cIAP1, cIAP2, livin, XIAP (X-linked inhibitor of apoptosis) and survivin, most of which are expressed at high levels in tumor cells. IAPs exert their anti-apoptotic activity by binding to the active form of caspases-3 and -9 [4, 11, 16]. To counteract the activity of IAPs, Smac/DIABLO and Omi/HtrA2 can bind to and inhibit their activity [4]. Cellular FLICE-inhibitory protein (c-FLIP), though not an IAP, is another anti-apoptotic protein that functions by competing with pro-caspase-8 for binding to FADD. c-FLIP is able to bind to FADD because it shares high sequence homology to caspase-8, however it

cannot signal as caspase-8 because it lacks a proteolytic domain required for downstream signaling [12, 15]. Several studies have shown that degradation of anti-apoptotic proteins can increase apoptosis [15]. Survivin, the smallest member of the IAP family, is down regulated by *t*-RES [11, 17] and α-TEA [18] in some cell types, and α-TEA can also down-regulate c-FLIP [18].

Autophagocytosis

Description

In contrast to apoptosis, is type II PCD, or autophagocytosis. It derives its name from the Greek word autophagy or "self eating." Characteristics primarily include the formation of autophagic vacuoles (AV), dilation of the endoplasmic reticulum (ER), and the enlargement of the Golgi [4-5, 7, 9, 19-20]. Once formed, autophagic vacuoles fuse with lysosomes to sequester cytoplasmic contents such as mitochondria and degrade them via lysosomal hydrolases [4-5, 7, 19-22]. Unlike apoptosis, autophagy depends on an intact cytoskeleton [8]. While the signaling events for autophagy are known in yeast, many of the mammalian homologs are yet to be found, so the exact signaling pathways are unknown [19, 21-23]. The general pathway begins with a signaling event that leads to the formation of a double membrane structure called an autophagosome, which fuses with cellular lysosomes to form an autolysosome, or autophagic vacuole (AV) [9, 19, 21-22, 24]. Often in autophagocytosis, caspases are not activated and DNA fragmentation does not occur.

Signaling Proteins

Autophagocytosis can be induced both by nutrient starvation or DNA damage, the former as a means of cellular survival and the latter a means to death [10]. It is thought to primarily be controlled by phosphoinositide 3-kinase (PI3K)/Akt, which is the

mammalian target of rapamycin (mTOR) [7, 10, 21]. Another protein that has been identified is beclin-1, the mammalian homolog to the yeast Atg6 protein that is involved in the early steps of autophagic vesicle formation and whose action can be inhibited by bcl-2 [7, 10, 21, 25-26]. In addition to its role in autophagy, beclin-1 has also been shown to be a haplo-insufficient tumor suppressor gene, which supports the model of autophagy as a suppressor of tumorigenesis [7, 18]. It is mono-allelically deleted in 40-75% of sporadic human breast and ovarian cancers, is frequently expressed at low levels in human breast epithelial carcinoma cell lines, and ubiquitously expressed at high levels in normal breast epithelial cells [27].

Another autophagy gene is microtubule-associated protein light-chain 3 (MAP-LC3), which is the mammalian homolog to Apg8p/Aut7p. MAP-LC3 is recruited to the pre-autophagosome membranes [19, 21, 24, 28] where it remains associated with the inner and outer phagosomal membrane [24]. MAP-LC3 can be proteolytically cleaved to smaller derivatives (LC3-I and LC3-II) that are found localized in either the cytosol (LC3-1) or the autophagosome membranes (LC3-2) [22]. The amount of LC3-II in cells is often used to estimate the abundance of autophagosomes in cells [19, 21-22].

LAMP-1 and LAMP-2 are structurally similar, highly N-glycosylated lysosomal proteins. Each of these transmembrane proteins is critical for transport to lysosomes in cells. Both LAMP-1 and LAMP-2 are ubiquitously expressed in cells and have been shown to be localized in late endosomes and lysosomes [29-30], and to serve as a receptor for the import and degradation of cytosolic proteins in the lysosome during autophagy [30]. This role is confirmed by studies that have shown that LAMP-2 deficient cells can block autophagy [24].

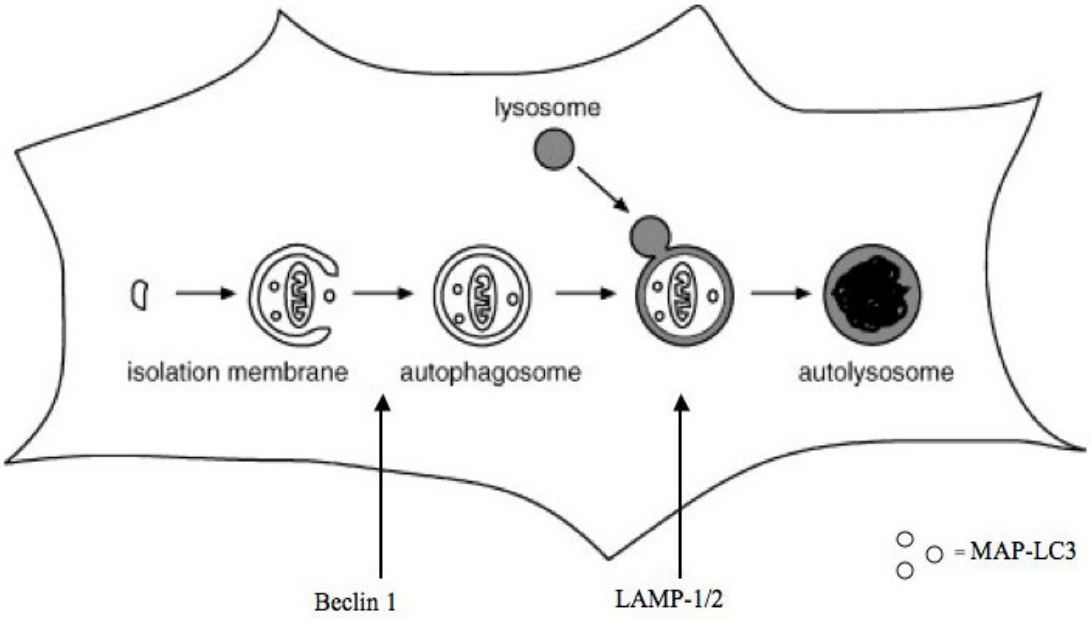

FIGURE 1.3: FORMATION OF AUTOPHAGIC VACUOLES. Adapted from [22, 24].

VITAMIN E

Vitamin E is a fat-soluble vitamin that serves as an antioxidant and is widespread in the human diet. It can be found in a variety of vegetable sources but is most abundant in vegetable oils and products made from vegetable oils. Wheat germ oil [~13 mg/Tb], sunflower oil [~6 mg/Tb], cottonseed oil [~5 mg/Tb], and safflower oil [~5 mg/Tb] contain some of the highest concentrations of RRR-α-tocopherol. Another form of vitamin E, tocotrienols, is highly concentrated in palm oil [~6 mg/Tb] and wheat germ oil [~3 mg/Tb] [32, 70].

The recommended dietary allowance (RDA) for adult males and females is 15 mg RRR-α-tocopherol/ day (22.4 IU) [32]. Because vitamin E is so prevalent in the human diet, it is rare for humans to be deficient. When it does occur, prolonged deficiency can

lead to neuromuscular dysfunction in the spinal cord and retina, loss of muscle coordination and reflexes, and impaired vision and speech, all of which can be corrected with vitamin E supplementation [33, 70]. Most cases of vitamin E deficiency occur in premature infants or as the result of genetic mutations in vitamin E binding proteins. Erthyrocyte hemolysis in premature infants occurs because the fetus has not yet reached the stage of development where the mother transfers vitamin E to the child, an event, which usually occurs in the last weeks of gestation [33-34, 70]. The most common genetic cause of vitamin E deficiency is Ataxia with vitamin E deficiency (AVED), which is an uncommon autosomal recessive neurodegenerative disease caused by mutations in α-tocopherol transfer protein (α-TTP) [34-35]. This mutation, along with others in proteins like apolipoprotein B (apoB), inhibits the proper uptake and metabolism of vitamin E [33-34, 70]. Symptoms include loss of deep tendon reflexes, cerebral ataxia, dysarthria, and mental retardation. Skeletal myopathy and retinitis retardation can also occur [33-34]. Supplementation with vitamin E can prevent the onset of both erythrocyte hemolysis or AVED before damage develops [33-35, 70].

In contrast to pathologies of vitamin E deficiency, there are also consequences to ingesting too much. The tolerable upper intake limit for vitamin E is 1000 mg (1492.5 IU) [32]. In these rare cases, extremely high doses can interfere with the role of vitamin K in blood clotting and can enhance the effects of anti-blood clotting drugs, leading to hemorrhaging [70].

Discovery

Evans and Bishop first discovered Vitamin E in 1922 when rats fed a semi-purified diet containing all the then known vitamins failed to reproduce [34-36]. They found that by feeding lettuce to the rats, resorption of the fetus was prevented, which suggested a missing nutrient in the diet of the rats [35-36]. Over the next few years,

deficiency of this unknown nutrient was shown to cause sterility in rats [31, 33, 36], nutritional encephalomalacia in chicks, and muscular dystrophy in guinea pigs, rabbits, and ducklings [36]. In 1936, Evans finally isolated the nutrient from wheat germ oil and named it tocopherol, from the Greek phrases "tokos" and "phorein" meaning "to bring forth offspring" [31, 35-36]. In 1938, the structural formula was published and the α, β, γ, and δ prefixes were given to distinguish the different molecules of the tocopherol family. In 1964, a second family of vitamin E was identified and named "tocotrienols" [36]. There is no clear relationship in humans between maternal vitamin E status and reproductive ability, but as a result of its discovery, vitamin E is now supplemented to farm animals [33].

Structure

Vitamin E is a general term often used to refer to both natural and synthetic vitamin E compounds. The 8 naturally occurring compounds can be evenly divided between tocopherols and tocotrienols [34, 36-37]. Tocotrienols differ from tocopherols through an unsaturated phytyl tail at chiral carbons 3', 7', and 11' [33, 36, 38]. Tocopherols and tocotrienols can be further distinguished within and between each other by the presence of methyl groups attached to the chroman head of the structure. Molecules with methyl groups at the 5, 7, and 8 positions are referred to as α; those with methyls at 5 and 8 or 7 and 8 are referred to as β and δ respectively. Molecules with a single methyl at the 8 position are referred to as γ [36, 38]. At room temperature, RRR-α-tocopherol is a lipophilic viscous oil [36].

Synthetic Vitamin E is a mixture of 8 stereoisomers of α-tocopherol, or molecules that contain the same number and types of atoms but which are arranged differently spatially. Sold commercially as dl-α-tocopherol or *all-rac*[emic]- α-tocopherol, only 12.5% is authentic RRR-α-tocopherol and 87.5% are stereoisomers that have no known

biological activity since liver hepatocytes selectively incorporate RRR-α-tocopherol over other vitamin E forms [34, 37].

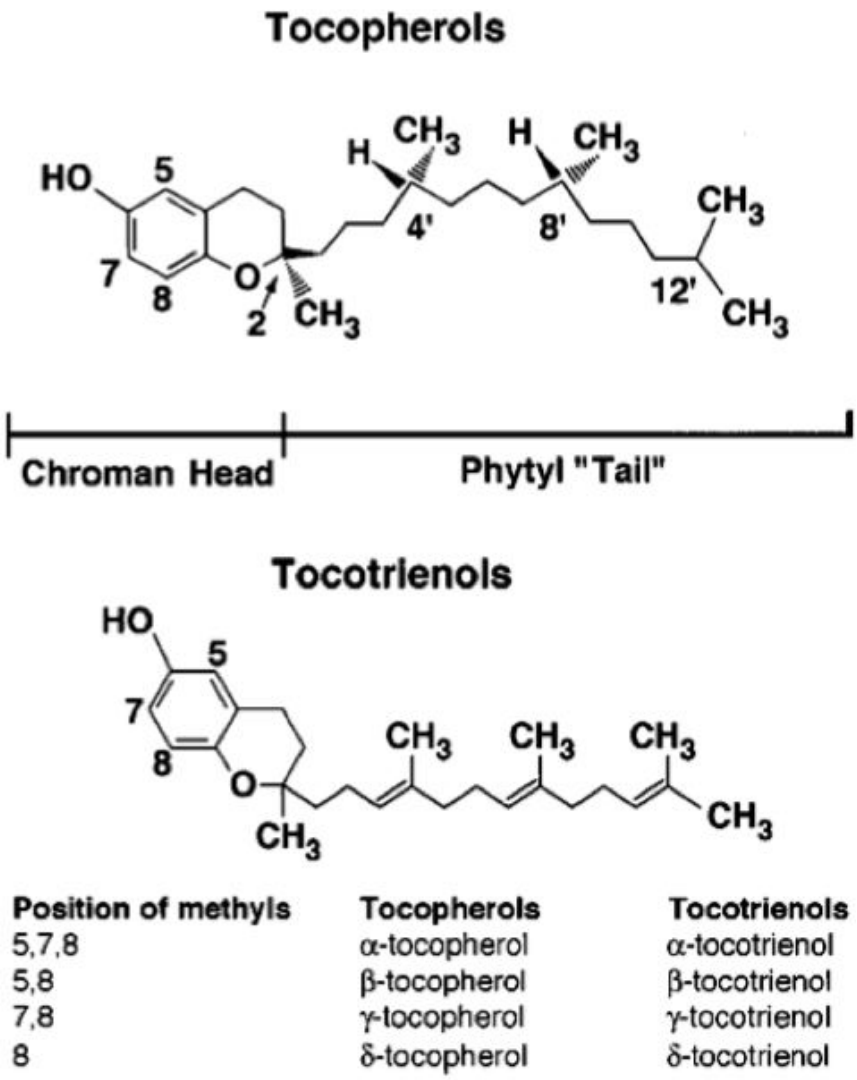

FIGURE 1.4: STRUCTURES OF NATURAL VITAMIN E COMPOUNDS. Adapted from [38].

Function

Cells are exposed to free radicals from endogenous and exogenous sources. Many biological re-dox reactions within cells can generate them as well as external drugs, pollutants, heavy metals, heat, UV, visible light, and other forms of ionizing radiation. Reactant species can cause reversible or irreversible damage to DNA, proteins, carbohydrates, and lipids, which can result in diseases such as cancer, arthritis, ageing, and heart disease. In many cases, the reactions that create free radicals are chain-reactions and a single reactive species can produce and propagate large numbers of free radical species to target many molecules and structures in the cell [36]. The primary role of Vitamin E is to serve as an antioxidant against free radical damage, thus protecting lipids and cell membranes from oxidation destruction from free radicals and singlet oxygen [31, 34, 36-37]. Its most notable role is to prevent oxidation of polyunsaturated fatty acids (PUFAs) [31, 36-37]. A second function is to stabilize membrane structures by forming complexes with destabilizing molecules, which prevents the disturbance of the amphipathic balance within the structure [36].

Once a lipid peroxyl radical (LO_2•) is formed, it attacks target lipids (L) by removing a hydrogen atom from the target lipid to form a lipid hydroperoxide (LOOH) and a carbon-centered lipid radical (L•). A chain reaction then begins where the carbon-centered lipid radical (L•) can react with oxygen (O_2) to generate another lipid peroxyl radical (LO_2•) which can go on to further damage more lipids. RRR-α-tocopherol (TOH) acts to scavenge lipid peroxyl radicals (LO_2•) before they are able to attack their target lipid substrates in a re-dox reaction that yields α-tocopheroxyloxyl radical (TO•) and a lipid hydroperoxide (LOOH). This newly formed radical is fairly stable due to the delocalization of the unpaired electron around the chroman head, which renders it relatively unreactive. RRR-α-Tocopherol is also very efficient because it can be

regenerated from the tocopheroxyl radical to α-tocopherol by vitamins A, C, and coenzyme Q. The reaction with coenzyme Q is a two-step process where the tocopheroxyl radical (TO•) first reacts with reduced coenzyme-Q (QH2) to form RRR-α-tocopherol (TOH) and semi-reduced ubisemiquinone (QH•). In a second step, a second tocopheroxyl radical (TO•) reacts with semi-reduced ubisemiquinone (QH•) to yield α-tocopherol (TOH) and coenzyme Q (Q). *In vitro* studies have shown that α-tocopherol can scavenge peroxyl radicals faster than peroxyl radicals can react with lipid substrates making them ideal for this purpose. Tocopherols have also been shown to react with other reactive species including singlet oxygen, alkoxyl radicals, peroxynitrite, nitrogen dioxide, ozone, and superoxide [36].

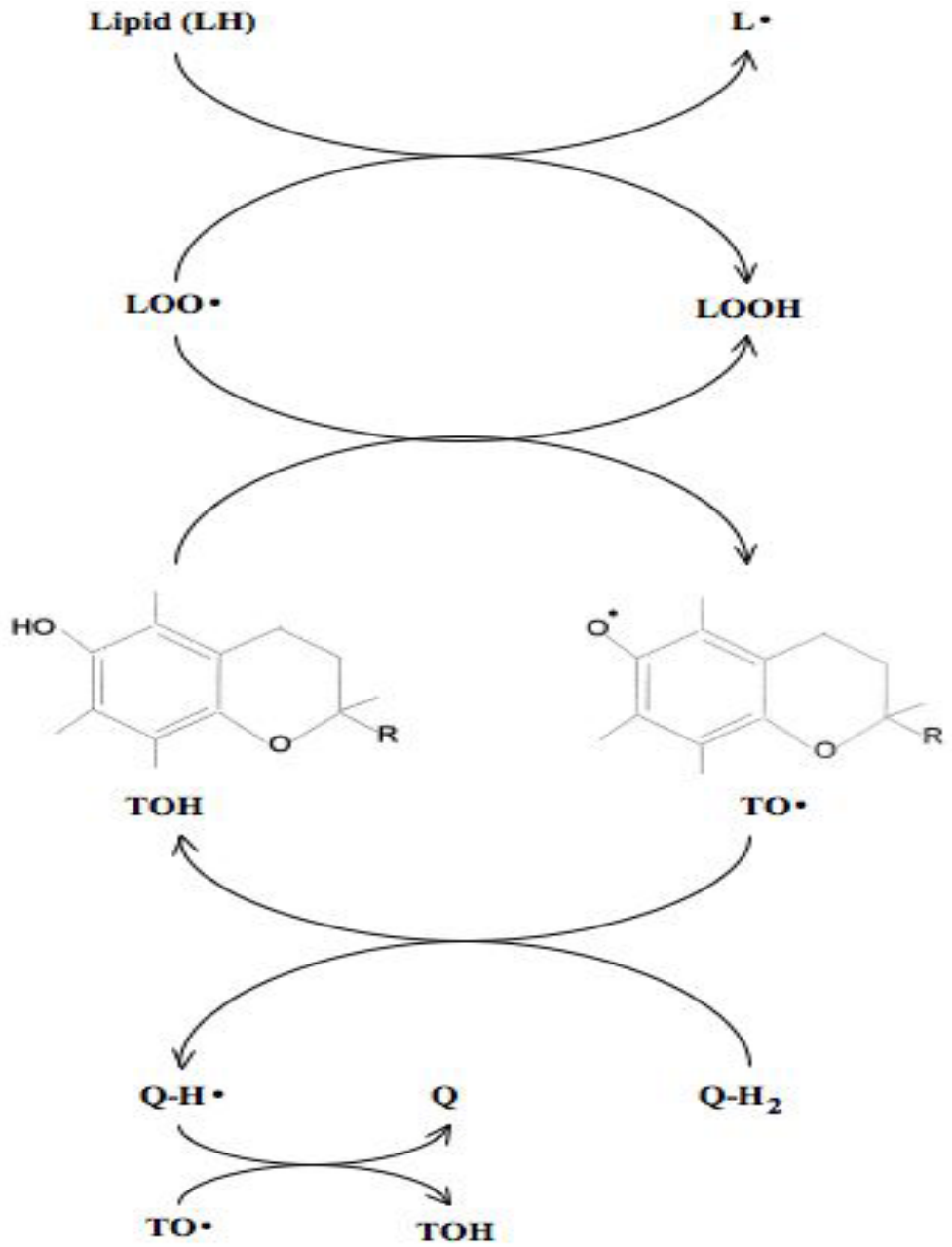

FIGURE 1.5: VITAMIN E AS AN ANTIOXIDANT. Adapted from [36]. LO_2•, lipid peroxyl radical; L, target lipid; LOOH, lipid hydroperoxide; L•, carbon-centered lipid radical; O_2, oxygen; TOH, α-tocopherol; TO•, α-tocopheroxyloxyl radical.

Absorption

The bioavailability differs for the different forms of vitamin E. γ-tocopherol is the most abundant form found in human diets but its plasma concentration is 1/10 that of α-tocopherol, the most abundant form in plasma [33]. All forms of vitamin E are absorbed by intestinal enterocytes and are secreted to the liver via the portal vein in chylomicrons [33-34, 36, 38]. In addition to α-tocopherol, triglycerides, phospholipids, cholesterol and apoliproteins can be found in the chylomicrons, which are made by the Golgi of the enterocytes. Once made they are stored as secretory granula until they are exocytosed into the lymphatic compartment where they make their way to the blood stream via the ductus thoracicus. In the bloodstream, HDLs exchange apoliproteins with the chylomicrons, which triggers the formation of remnants, a prerequisite for uptake by liver parenchyma by the endothelial lipoprotein lipase (LPL) [35].

Once the remnants arrive at the liver, the apoliproteins act as ligands to induce receptor-mediated endocytosis where they then fuse with lysosomes of the cell [35]. RRR-α-tocopherol is preferentially transported from the hepatic lysosomes to very low-density lipoproteins (VLDLs) by α-TTP and excreted into the bloodstream for transport to tissues [33, 35-36, 38]. Once in the blood, the plasma phospholipids transfer protein (PLTP) catalyses the exchange of α-tocopherol between HDL and LDL [35]. The binding affinity of α-TTP is $\alpha=\beta>\gamma>\delta$. LDL structures typically carry 6-12 molecules of α-tocopherol (0.5 mol/LDL). The structure of a LDL is that of a phospholipids monolayer with a core of neutral lipid including cholesterol esters with α-tocopherol positioned within the phospholipids monolayer [36].

α-TTP is a small protein that specifically selects α-tocopherol with a side chain linked to the chroman head in the R configuration at position 2 for incorporation into VLDL [33-34]. It is primarily expressed in the liver and its expression can be

upregulated by the presence of dietary tocopherols. In addition to being found in the liver, low concentrations have also been found in the brain, spleen, lung, and kidney [33]. Other forms of vitamin E that are not taken up are excreted in the bile or urine as carboxyethyl hydroxychromans (CEHCs) [33-35].

Transport of vitamin E occurs via binding to lipoproteins and intracellular transport may occur through binding to tocopherol-associated proteins (TAP). Several TAP proteins have been identified. One 46-kDa TAP may be responsible for intracellular transport by acting as a chaperone to move vitamin E between membranes compartments containing tocopherol-metabolizing enzymes. Another TAP is 15-kDa and may be responsible for intracellular distribution, and a third 75-kDa TAP is known to facilitate the exchange of α-tocopherol between HDL and LDL [33]. It is theorized that tissue specific retention and biological effects may be due to a cytosolic vitamin E binding to TAPs or supernatant protein factor (SPF) [38].

In humans, normal RRR-α-tocopherol plasma concentrations are around 25 μmol/L and it is difficult to increase this more than 2-3 fold, irrespective of amount or duration of supplement. This is due to the fact that RRR-α-tocopherol is absorbed at a constant rate and not due to limited absorption. Another limiting factor is that newly absorbed α-tocopherol replaces older α-tocopherol in plasma lipoproteins [33]. Studies have shown that TAP can selectively bind to RRR-α-tocopherol and that its presence can enhance the ability of vitamin E succinate (VES) to induce apoptosis [38].

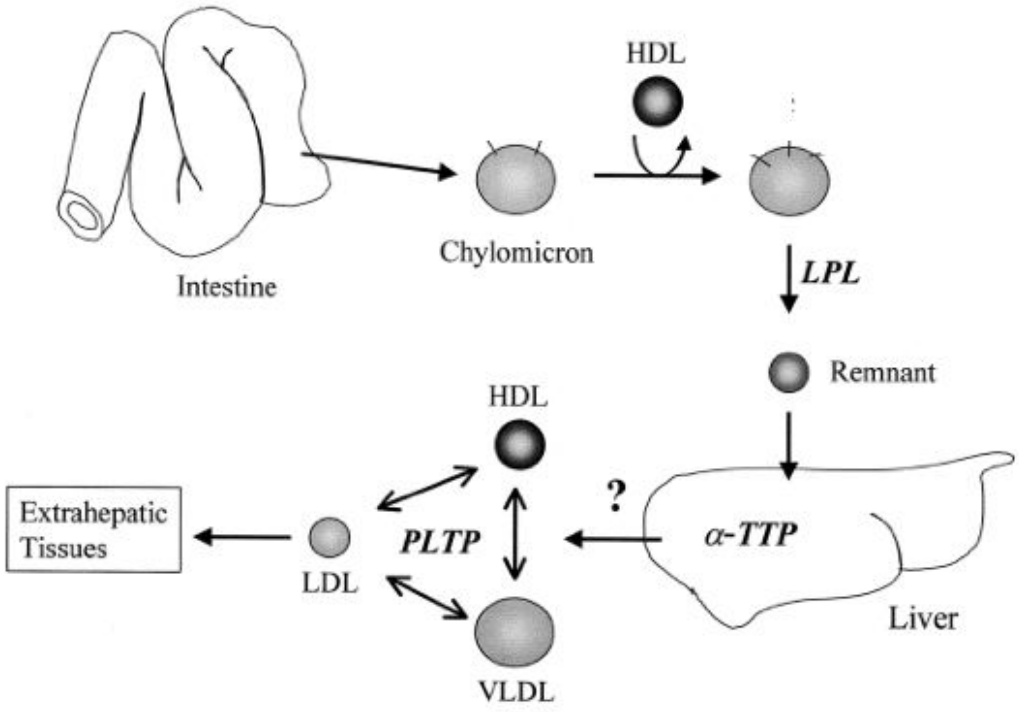

FIGURE 1.6: ABSORPTION OF VITAMIN E. Adapted from [35].

Metabolism

Vitamin E is highly metabolized by CYP3A prior to excretion. CYP3A is a cytochrome P450 enzyme with specificity for a wide range of substrates including steroids, antibiotics, and other pharmacological agents. The initial steps in the metabolism of RRR-α-tocopherol consist of two successive ω-oxidations (hydroxylations) on the phytyl tail by cytochrome P450 (CYP)-dependent hydroxylases. This is followed by several β-oxidation steps that result in two intermediates, α-2-[6'-carboxy-4'-methylhexyl]hydroxychroman (α-CMHHC) and α-2-[4'-carboxy-4'-methylbutyl]hydroxychroman (α-CMBHC) [33]. The final product of metabolism is α-2-[2'-carboxyethyl]hydroxychroman (α-CEHC) [33, 35]. Similar metabolism is seen for

β-, δ-, and γ- forms of vitamin E and synthetic dl-α-tocopherol is excreted at a 3-4 times higher rate than natural α-tocopherol [33].

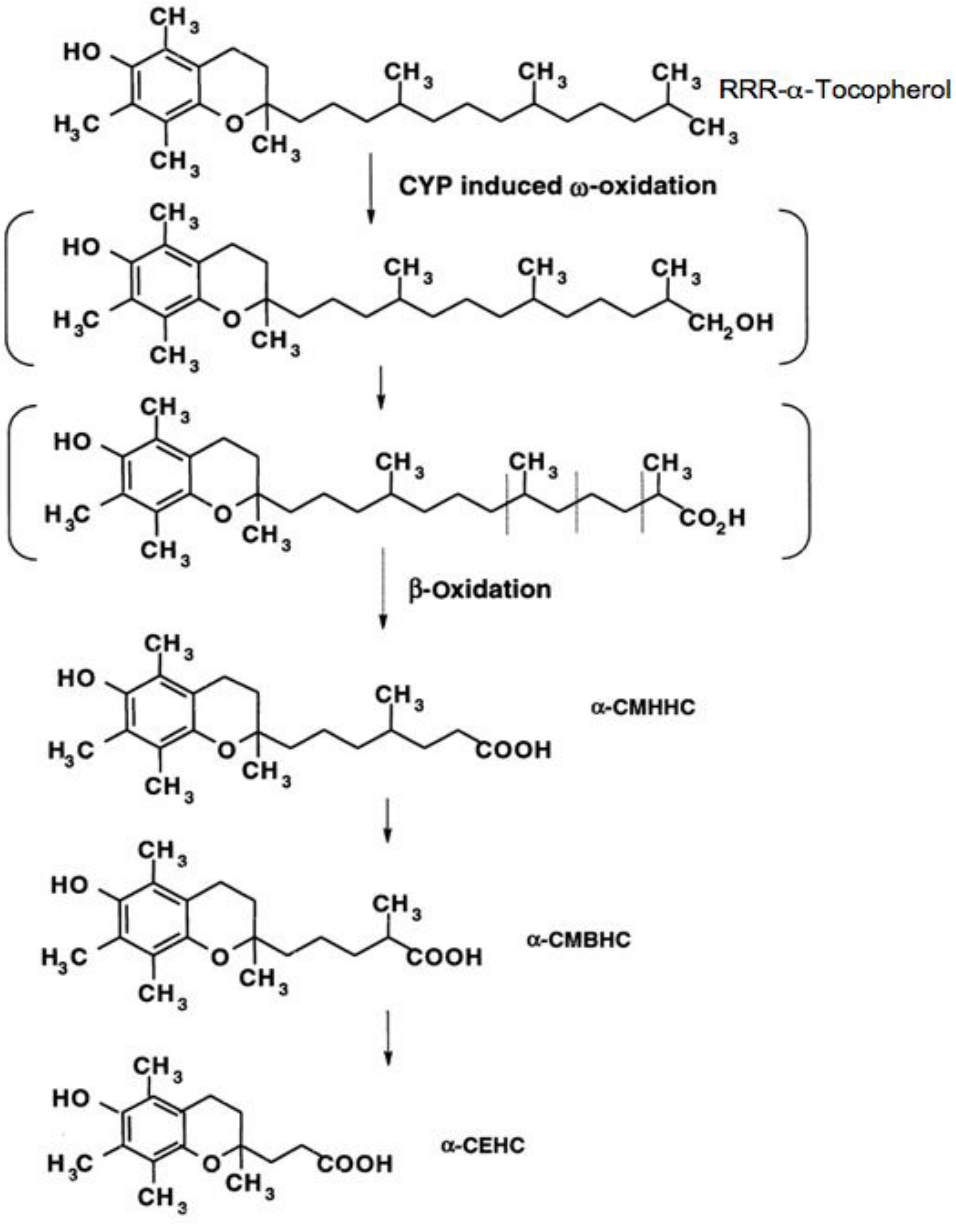

FIGURE 1.7: METABOLISM OF RRR-α-TOCOPHEROL. Adapted from [33].

Derivatives

Both natural RRR-α-tocopherol and synthetic vitamin E can be purchased as more stable acetate or succinate derivatives. Normally the hydroxyl moiety at the C-6 position is prone to oxidation when exposed to air. Since this hydroxyl moiety is responsible for the antioxidant effect of vitamin E, it must be removed in order to restore potency. In addition to these acetate and succinate forms, our lab has developed a non-hydrolyzable ether derivative referred to as α-tocopherol ether analog (α-TEA) [37].

Vitamin E Succinate

RRR-α-tocopherol succinate (vitamin E succinate, VES) is a commercially available derivative of vitamin E. It is effective against several cancer cell lines *in vitro*, including breast. It has previously been shown by our lab that VES induces apoptosis by restoring Fas/FasL signaling in cells. Unfortunately, it has also been shown that an intact molecule is necessary for activity *in vivo,* and since the succinate moiety is linked via an ester linkage, esterases *in vivo* can cleave and inactivate the molecule [37-38].

Alpha-tocopherol ether analog

α-TEA was developed with the hope of finding a clinically useful vitamin E-based chemotherapeutic agent that could be administered in a clinically relevant manner. It is a non-hydrolysable ether analog of RRR-α-tocopherol referred to as called RRR-α-tocopheryloxyacetic acid or RRR-α-tocopherol ether-linked acetic acid analog (α-TEA). The chemical name is 2,5,7,8-tetramethyl-2R-(4R, 8R-12-trimethyltridecyl)chroman-6-yloxyacetic acid [38]. α-TEA differs from RRR-α-tocopherol by an ether linked aecetic acid moiety at the phenolic oxygen at carbon 6 of the chroman head. Unlike VES, the ether linkage is unhydrolyzable and the molecule remains stable *in vivo*. For this reason, α-TEA is not known to have antioxidant properties [37-38].

α-TEA is capable of inducing human ovarian (A2780/cp-70), cervical (ME-180), breast (MCF-7, MDA-MB-231, MDA-MB-435), endometrial (RL-952), prostate (LNCaP, PC-3, DU-145), lung (A-549), colon (HT-29, DLD-1) and lymphoid (Raji, Ramos, Jurkat) cells to undergo apoptosis [39]. Also, α-TEA does not induce apoptosis in normal human mammary epithelial cells or normal PrEC human prostate epithelial cells [38]. Previous studies within our lab have also shown α-TEA to be effective at reducing tumor burden and metastasis *in vivo* [40-44].

Natural Vitamin E (RRR-α-tocopherol; d-α-tocopherol)

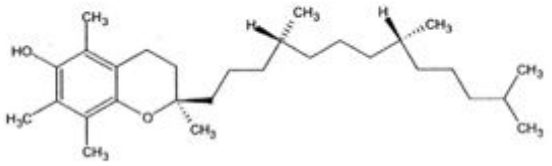

2R 4'R 8'R α-tocopherol

Synthetic Vitamin E (*all-rac*-α-tocopherol; dl-α-tocopherol)

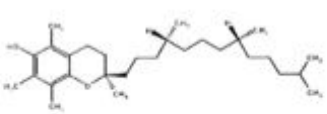

2R 4'R 8'R α-tocopherol

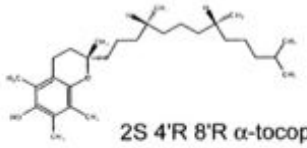

2S 4'R 8'R α-tocopherol

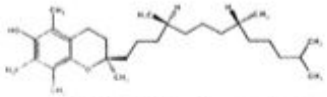

2R 4'S 8'R α-tocopherol

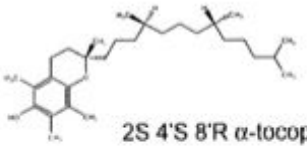

2S 4'S 8'R α-tocopherol

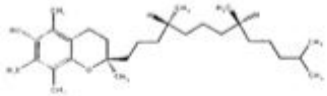

2R 4'R 8'S α-tocopherol

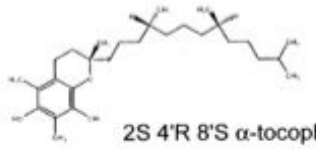

2S 4'R 8'S α-tocopherol

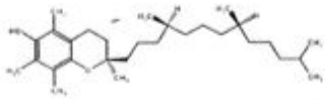

2R 4'S 8'S α-tocopherol

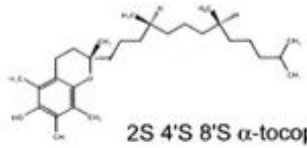

2S 4'S 8'S α-tocopherol

Analogs of RRR-α-tocopherol

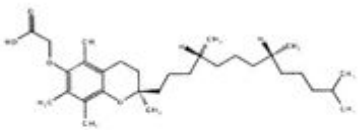

α-TEA

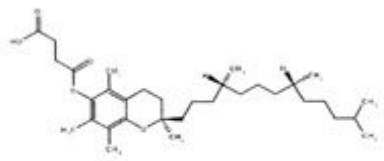

VES

FIGURE 1.8: STRUCTURAL ISOMERS AND ANALOGS OF RRR-α-TOCOPHEROL. Adapted from [37].

TRANS-RESVERATROL

Trans-resveratrol (3,5,4'-trihydroxy-*trans*-stilbene; *t*-RES) was first isolated in 1940 from the roots of white hellebore (*Veratrum grandiflorum O. Leos*), and later in 1963 from the roots of *Polygonum cuspidatum,* a plant used in traditional Chinese and Japanese medicine [45]. It is a naturally occurring phytoalexin that has since been found in a variety of foods such as grapes, wine, berries, and peanuts [45-53, 57]. *t*-RES is considered a promising chemotherapeutic agent based on its ability to inhibit free radical formation [46-48], and to induce cellular differentiation [46], autophagocytosis in human ovarian cancer cells [54], and apoptosis in human promyelocytic leukemia cells [46-47], human colon cancer cells [47-48], and human breast cancer cells [47, 49, 55] *in vitro*. *t*-RES has also been shown to have antitumor effects *in vivo* against the development of 7,12-dimethylbenz(a)anthracene (DMBA) induced hyperplasic and atypical preneoplasic lesions in the mouse mammary organ culture model (MMOC) [46-47, 52, 56], N-methyl-N-nitrosourea (NMU) induced mammary lesions in rats, and tumorigenesis in a two-stage mouse skin cancer model [46-48, 50, 52]. It has also been shown to reduce tumor growth and metastases in syngeneic mouse tumor models [57]. In addition to its anticancer effects, this pleotrophic compound has been shown to prevent or slow the progression of cardiovascular disease, ischemic injuries, enhance stress resistance, and extend the lifespan of various species including yeast and vertebrates [45], all without toxicity [45-48, 50, 52]. *In vivo* studies have shown such promise that there are now several Phase-I clinical trials for oral administration of *t*-RES to humans with the purpose of preventing cancer, HIV-1, and treating colon cancer [45].

Biosynthesis and Structure

Resveratrol and flavonoids are made in plants via a common synthetic pathway. The pathway begins when phenylalanine is converted to hydroxy-cinnamoic acid.

Depending on the number of cinnamoyl-radicals combined, chalcone synthase can form flavonoids (three required) or pinosylvin synthase can form resveratrol (two required). In plants, resveratrol functions both as an antioxidant and a free radical scavenger to protect plants against fungus and other types of stress [58].

Resveratrol is a polyphenolic derivative of plant stilbenes. Its structure is an alkene with two phenyl groups on either carbon. Resveratrol can exist as one of two structural isomers, *cis-(Z)* or *trans-(E)*. Due to the instability of the *cis* conformation caused by steric hindrance, most resveratrol is found in the *trans* conformation, though isomerisation can occur due to heat or UV irradiation. The structure of resveratrol contains three hydroxyl groups positioned on the phenyl groups at carbon 3, 5, and 4' positions, which give it its antioxidant properties [58].

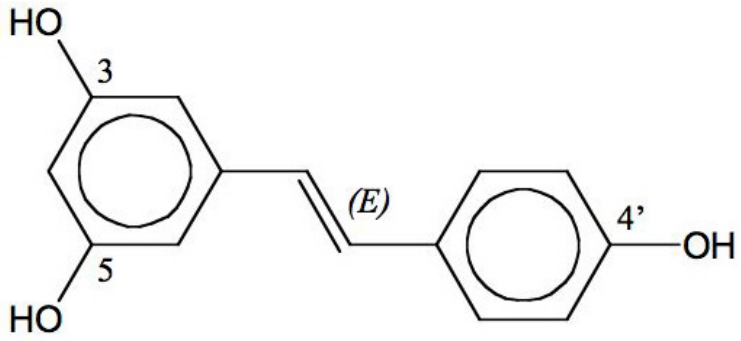

FIGURE 1.9: STRUCTURE OF *trans*-RESVERATROL. Adapted from [58].

Metabolism

Promising results have been seen *in vitro* over a wide range of concentrations (32 nM-100 μM) and *in vivo* ranging from 100 ng-1500 mg/kg bodyweight. Such large ranges question the bioavailability of *t*-RES and whether *in vivo* concentrations are large

enough to exert many of the effects seen *in vitro*. Pharmacokinetic studies have shown that the parental *t*-RES structure has a short half-life (8-14 min) and is extensively metabolized by cytochrome P450 enzymes in the liver [45]. When *t*-RES is administered intravenous to humans, the parental structure is primarily converted to sulphate conjugates within 30 min. Glucuronide conjugates can also be detected in the serum and up to four metabolites have been reported in urine. The most abundant urine metabolites are *trans*-resveratrol-3-*O*-glucuronide and *trans*-resveratrol-3-sulfate, followed by *trans*-resveratrol-4'-*O*-glucuronide and *trans*-resveratrol-4'-sulfate [59]. The serum half-life for *t*-RES metabolites is 9.2 h, which suggests that the efficacy of *t*-RES may actually arise from metabolites that retain biological activity [60]. It is clear from the many *in vivo* studies that *t*-RES has a high efficacy so further studies are needed to determine whether the metabolites retain activity and are responsible for the high efficacy of *t*-RES [45].

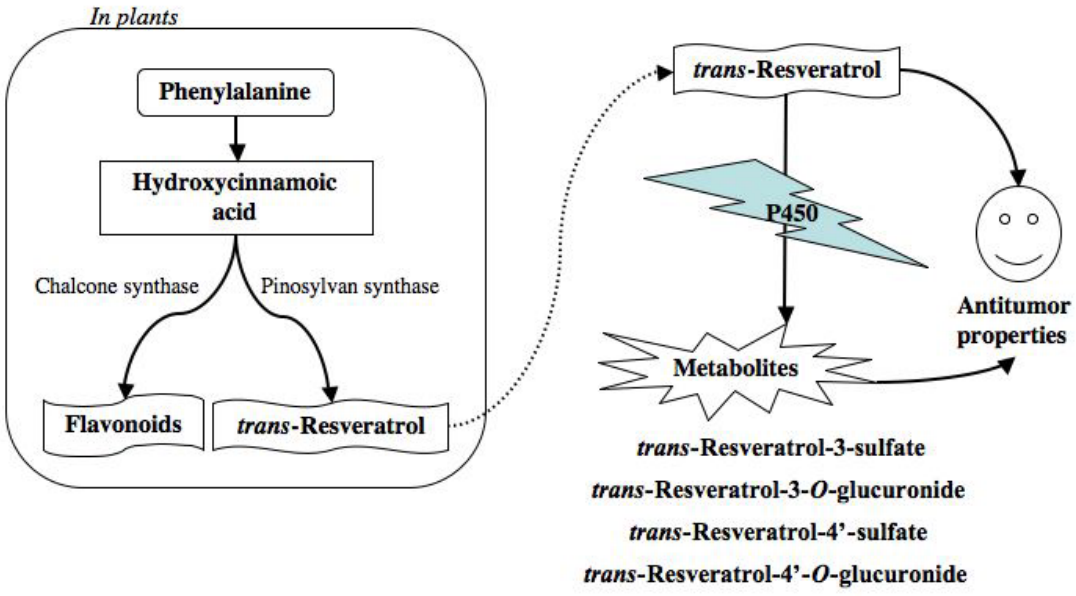

FIGURE 1.10: METABOLISM OF *trans*-RESVERATROL. Adapted from [58-59].

SELENIUM

Selenium is an essential nutrient for humans that can be found in cereal grains, meats, and seafood and is required for more than 13 human enzymes and proteins, in the form of L-selenocysteine [61]. Dietary supplementation of selenium beyond the recommended dietary allowance of 55 μg/day for women and 70 μg/day for men, at up to 200 μg/day, reduces the incidence of lung, colorectal, and prostate cancer in humans [61-64]. *Se*-(Methyl)selenocysteine (MSC) has been shown to be an effective suppressor of chemically induced mammary carcinogenesis in rats [61, 63-68]. Unfortunately it is not a good agent for use for *in vitro* studies because it requires conversion to methylselenol by β-lyase in the liver and kidney [63, 68]. Methylseleninic acid (MSA) is a better agent for *in vitro* studies because it easily undergoes reduction to methylselenol once taken up by the cells [62-63, 68] and has been shown to induce apoptosis in murine and human mammary cells [63-64, 68]. Also, MSC and MSA have been shown to have equal chemopreventive efficacy *in vivo* and are thus considered interchangeable [63, 68].

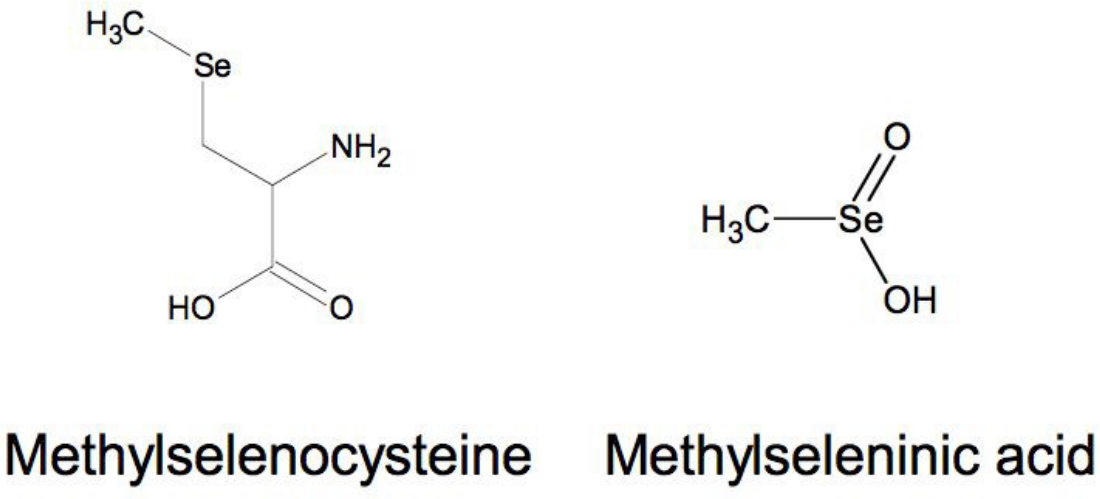

FIGURE 1.11: STRUCTURES OF MSA AND MSC. Adapted from [62, 69].

Function

Selenium is an essential trace mineral that is required for human health and is usually found in amino acids selenocysteine and selenomethionine. In humans it functions as a cofactor for reduction of antioxidant enzymes like glutathione peroxidase, which works together with vitamin E to prevent free radical formation, and thioredoxin reductase. Dietary sources include cereals, many meats, fish, and eggs [31].

Selenium toxicity, also called selenosis, generally occurs at daily intakes of greater than 1 mg per day but symptoms can be seen with doses as low as 400 μg per day. It causes a variety of symptoms including garlic odor on the breath, vomiting, diarrhea, hair loss, skin lesions, fatigue, irritability and nervous systems disorders. Extreme cases can lead to pulmonary edema, liver cirrhosis, and death [31].

Selenium deficiency is relatively rare in developed countries. Most cases occur when people have severely compromised intestinal function or where they rely on food grown in selenium-deficient soil. Deficiency can cause a predisposition to two types of heart disease called Keshan disease and Kashin-Beck disease. Keshan disease is characterized by an enlarged heart and myocardial necrosis. Kashin-Beck disease is characterized by atrophy, degeneration and necrosis of cartilage tissue. Both of these diseases are common to certain provinces of China where there are selenium-poor soils but symptoms can be reduced by taking selenium supplements. In other geographical locations with selenium-poor soil, selenium deficiency is associated with certain types of cancer, goiter, cretinism, and recurrent miscarriage [31].

Metabolism

Different forms of selenium can be metabolized *in vivo* in several ways depending on the structure. Ip *et al* [71-72] have previously shown that structures that can undergo conversion to a monomethylated form have the highest *in vivo* tumor efficacy. This is

mainly due to their point of entry into the selenium metabolic pathway. Entry of a selenium compound at a point below the hydrogen selenide pool produces large amounts of monomethylated metabolites that bypass the conventional assimilatory pathway for incorporation into selenoproteins and selenocysteine [62]. Se-methylselenocysteine is metabolized *in vivo* by β-lyase enzyme to methylselenol. This enzyme can be found in several tissues including liver, mammary gland, and intestine [72]. Likewise, methylselininic acid can also easily converted to methylselenol in cells either by enzymatic reduction through NADPH-linked reductases like glutathione reductase or nonenzymatic reduction through excess thiol [69].

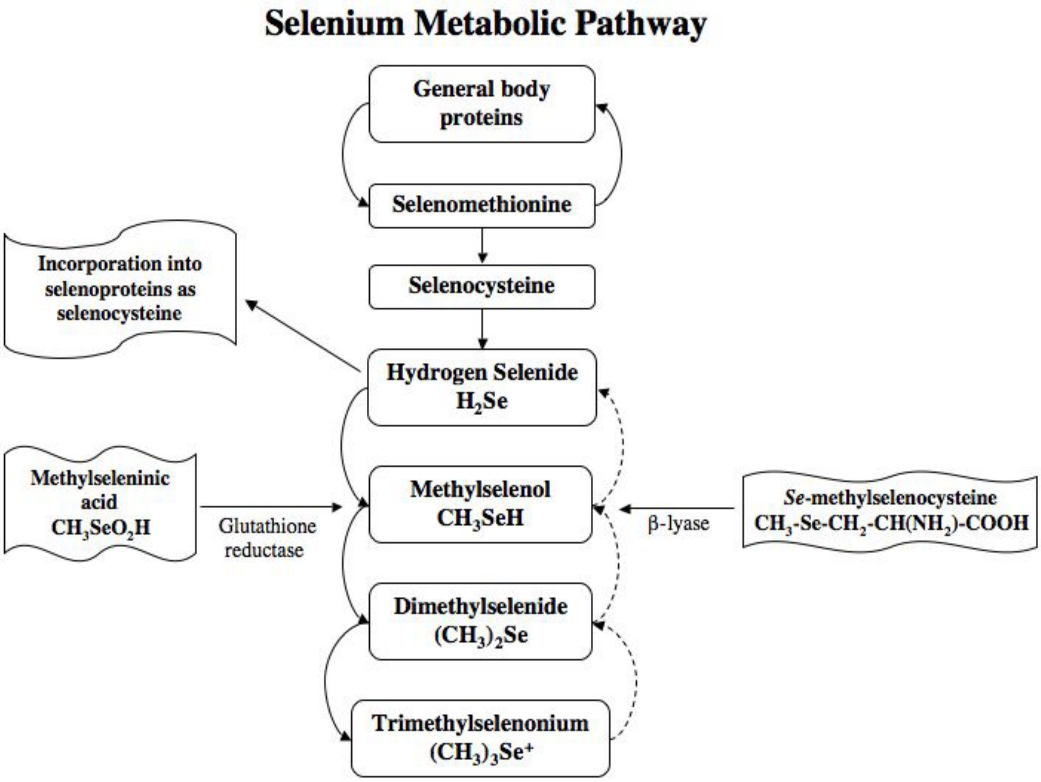

FIGURE 1.12: METABOLISM OF SELENIUM. Adapted from [62, 69, 72].

CELL LINES

The main cell line in our studies, MDA-MB-435-F-L, is a derivative of the parental MDA-MB-435 human breast carcinoma cell line first derived by Dr. Janet Price (MD Anderson, Houston, TX). Dr. LuZhe Sun (University of Texas Health Science Center, San Antonio, TX) derived this highly metastatic variant from a mouse lung metastasis after the parental MDA-MB-435 cell line was injected into the flank of an athymic nu/nu mouse. In addition to selecting for a highly metastatic variant, Dr. Sun's lab has stably transfected the cell line with green fluorescent protein (GFP) to allow for fluorescent detection of these cells within animal tissue [73].

XENOGRAFT NUDE MOUSE MODEL

Often what occurs *in vitro* does not mimic what occurs *in vivo*. Many times there are unforeseen interactions between drugs and systems in the body that are difficult if not impossible to predict. One method that is commonly used to test the efficacy of novel chemotherapy agents on human cancer cells is with an immunodeficient mouse model. There are three main types of immunodeficient mice commonly used: T lymphocyte deficient mice, T and B lymphocyte deficient mice, and T, B, and NK cell deficient mice [74-78]. T lymphocyte deficient mice have a spontaneous autosomal recessive Foxn1 (forkhead N1) gene mutation, which causes abnormal thymus development and no body hair. Normal and malignant tissues from xenograft and allograft donors are able to grow well in this model due to the deficient T cell function [74-75]. T and B lymphocyte deficient mice, also known as severe combined immuno-deficient (SCID) mice, lack both T and B cell function. This is due to a spontaneous Prkdc (protein kinase, DNA activated, catalytic polypeptide gene) mutation that causes defects in V(D)J recombination and allows mice to more easily accept foreign tissue transplants [76-77]. T, B, and NK cell deficient mice carry three separate gene mutations that result in T, B,

and NK cell deficiencies [78]. Besides the obvious advantage that human cells and tissues can be transplanted into these animal models, their lack of body hair allows for easy identification of growing tumors.

CHEMOPREVENTION

The definition of chemoprevention is the intervention in the tumorigenic process by a natural or synthetic compound. Specifically, it is an agent that can block the early stages of initiation, pre-malignant development, and/or arrest malignant cell progression [38]. Most chemically induced mammary chemoprevention animal models use either DMBA or MNU to induce lesions. There are several common features to DMBA and MNU induced lesions including organ specificity, reliable induction of mammary tumors, few metastases, and the examination of tumor initiation and promotion/progression. One major difference between MNU and DMBA is that MNU is a direct acting carcinogen and thus does not require metabolic activation, whereas DMBA is a proximate carcinogen that requires metabolic activation. Another difference is that MNU induces more aggressive carcinomas than DMBA, so that a higher proportion of MNU induced lesions are malignant compared to those induced by DMBA [79]. In our studies, DMBA was used to induce lesions in the mouse mammary organ culture (MMOC) model and MNU was used to induce lesions in the rat carcinogenesis model.

Mouse Mammary Organ Culture Model

The MMOC model is an *ex vivo* chemoprevention model that can be used to examine the effects of compounds on the very early stages of chemically induced lesion formation. Studies have shown that there is a high correlation between agents that show chemopreventive activity in this model with those that show activity in the two-stage skin carcinogenesis and the chemically induced rodent mammary carcinogenesis model. The

model can be adapted to target lesions to be either alveolar or ductal in origin and both methods consist of three main phases: pre-treatment, growth, and regression. In the pretreatment phase, female balb/c mice are treated with 1 μg 17β-estradiol (E) and 1 mg progesterone (Pg) daily for nine days in order to stimulate growth of the mammary glands. During the growth phase, animals are sacrificed and the glands are cultured in media containing different constituents depending on the desired type of lesion. These additions to the media induce mammary gland differentiation so that at the end of the 10-day phase, the glands morphologically resemble the gland of a pregnant animal, complete with lobulo-alveolar structures. Chemopreventive agents to be tested are given in the media starting at day 1 of the growth phase and continue throughout the growth phase. On the third day, 2 μg/ml DMBA is added to the growth media for 24 h and then replaced with fresh growth media. During the regression phase, the glands revert back to that of an involuted mammary gland. Glands that contain DMBA lesions do not fully regress at the location of the lesion and can be quantitated after the glands have been mounted and stained with alum carmine [80-82].

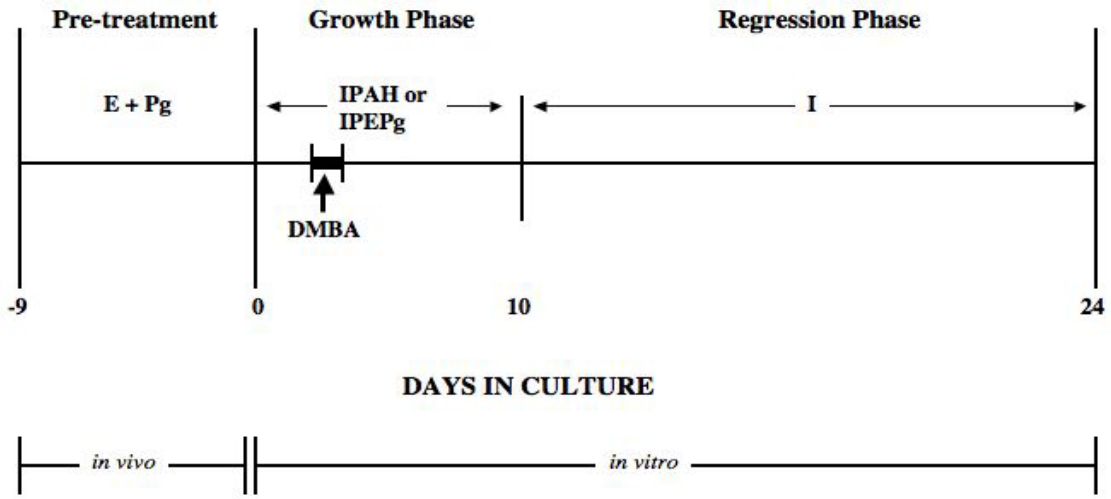

FIGURE 1.13: TIMELINE OF MOUSE MAMMARY ORGAN CULTURE MODEL. Adapted from [81]. I = insulin, P = prolactin , A = aldosterone, H = hydrocortisone, E = 17β-estradiol, Pg = progesterone

Rat Carcinogenesis Model

Most work on early lesion formation is done in mouse models despite that mouse models predominantly form alveolar lesions. MNU induced rat carcinogenesis models are another commonly used method to study chemically induced mammary gland lesions because the tumors in these animals typically show similar estrogen responsiveness and chromosomal abnormalities to that seen in humans, and therefore serve as a better model for human disease. Similar to human pathology, MNU-induced rat models show an 80% incidence of intraductal hyperplasia, 45% incidence of ductal carcinoma *in situ* (DCIS), and greater than 95% incidence of adenocarcinomas [83]. Recently, a short-term carcinogenesis model has been developed by Thompson *et al* [79, 83, 86] that allows for the rapid induction of premalignant and malignant stages of mammary carcinogenesis.

The main difference between this model and the conventional model is the age at which the rats are injected (21 d versus 50 d) which allows that the experiment be completed in 35 d compared to 6 months in the conventional model [79, 83-86]. In either model, the mammary glands are removed and mounted on glass slides at sacrifice. Lesions are quantitated and classified as adenocarcinoma (AC), ductal carcinoma *in situ* (DCIS), intraductal proliferation (IDP), or within normal limits [79, 83-86]. The short-term carcinogenesis model has several advantages over the conventional model in addition to a shorter latency to carcinoma occurrence. This model also shows a lower frequency of ovarian hormone-dependent tumors [86], and the relative simplicity of the gland in the younger rats allows for easier detection of IDP and DCIS in the gland [79].

Histological classification of the rat whole mount lesions is based on classification criteria published by Russo *et al* [115]. Lesions are classified as intraductal proliferation (IDP), ductal carcinoma *in situ* (DCIS), adenocarcinoma (AC), or "within normal limits." The criteria for diagnosing hyperplasia is primarily based on an increase in the epithelial cells lining the acini and ducts, which can range from 3-4 four cells thick in mild subtypes or completely full in florid hyperplasias. The individual cells that make up IDPs are not distinguishable and the nuclei are generally round to oval, haphazardly arranged, and lack nucleoli [86]. DCIS have at least one expanded ductal structure that is completely replaced by neoplastic cells that have uniform, monotonous, round, hyperchromatic and non-overlapping nuclei, and retain an intact ductal basement membrane. DCIS can be further classified as cribiform or comedo carcinoma *in situ*. Lesions that have only a single duct replaced are labeled atypical ductal hyperplasia (ADH). ACs are defined as the earliest breach of the ductal basement membrane and tend to invade as a broad front of several cells with clusters of neoplastic acini and like DCIS can be subdivided into cribiform and comedo [86].

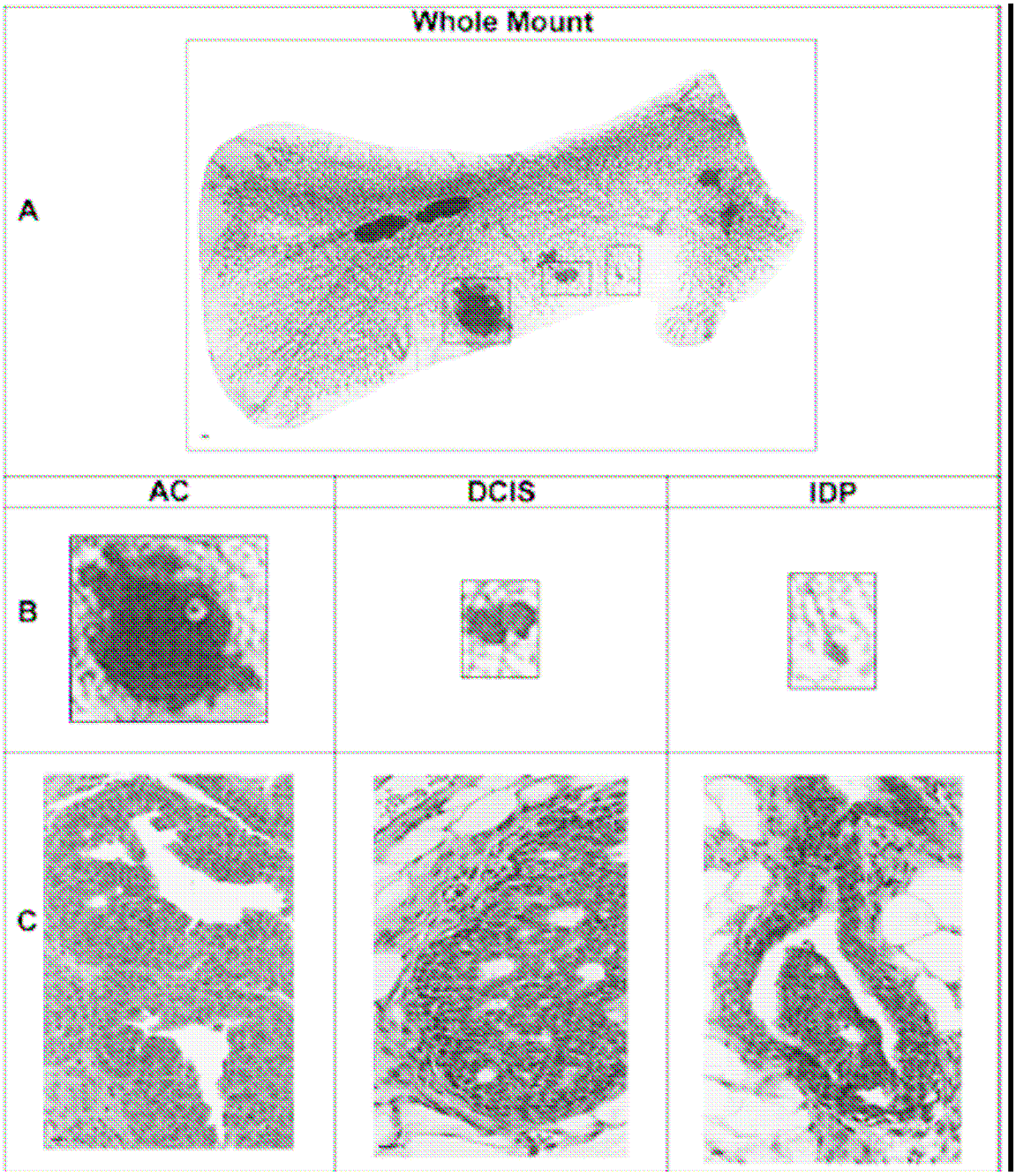

Figure 1.14: Mammary Gland While Mount. Adapted from [79]. A, fixed and stained mammary gland whole mount preparation showing premalignant and malignant mammary gland lesions. B, Subgross morphology of lesions identified in panel A. C, histology of lesions shown in Panel B.

SUMMARY

More than 90% of all cancer deaths can be attributed to distal secondary lesions [87]. These metastases arise from aggressive tumor cells that have escaped and survived earlier attempts at treatment, most likely due to the heterogeneity of cells within a tumor. As we continue to understand more about the nature of tumor cells and their signaling mechanisms, it becomes increasingly clear that treatment with a single agent or method will not eliminate all of the cells of a tumor, and that perhaps a cocktail of treatments would be more effective. Based on this hypothesis, and the ability to induce cell death via different mechanisms with little to no toxicity to normal cells, α-TEA, *t*-RES, and MSC/MSA were chosen to investigate the combined effects of these compounds on a highly metastatic human breast cancer cell line.

This dissertation focuses on studies of α-TEA, *t*-RES, and MSC/MSA, alone and together, as inhibitors of human breast cancer cells using both *in vitro* and *in vivo* methods. The aim of this chapter was to introduce methods of cancer cell death, specifically apoptosis and autophagocytosis, as well as to provide background information on the function and metabolism of α-TEA, *t*-RES, and MSC/MSA. Various animal models and the main cell line used in the investigations presented in this dissertation were also reviewed. Chapter 2 will focus on the initial studies that characterized how α-TEA, *t*-RES, and MSC/MSA synergize to inhibit proliferation and induce apoptosis in various breast and prostate cancer cell lines. Chapter 3 will build on these findings and show how a combination of the three agents used together is just as effective as α-TEA used alone to treat tumor cells in a murine xenograft model, but can inhibit more metastases than individual treatments. This chapter will also show that the diet that animals are fed is important to the overall tumor growth in the studies. Chapter 4 will focus on the use of α-TEA, *t*-RES, and MSA as chemopreventive agents and show

that α-TEA and *t*-RES together without MSA is the most effective combination for preventing DMBA-induced lesions in the mouse mammary organ culture model. Chapter 5 will report on studies designed to characterize the molecular signaling events that account for the synergistic ability of α-TEA and *t*-RES to induce cell death when used in combination, and will explore the role of apoptosis and autophagocytosis signaling proteins.

Taken together, these studies suggest that α-TEA, in combination with other pro-cell death agents such as *t*-RES and MSC/MSA, can reduce human breast cancer growth *in vitro* and *in vivo* more effectively than any of the agents alone. These studies add insight into the complex mechanisms that regulate cell death in human breast cancer cells and provide a basis for future breast cancer treatment and prevention regimens.

Chapter 2: RRR-α-tocopherol ether analog, α-TEA, methylseleninic acid (MSA), and *trans*-resveratrol (*t*-RES) in combination synergistically inhibit human breast cancer

ABSTRACT

Alpha-tocopherol ether analog (α-TEA) is a novel form of vitamin E that is effective at killing cancer cells but not normal cells. α-TEA alone and together with methylseleninic acid (MSA) and *trans*-resveratrol (*t*-RES) were investigated for ability to induce apoptosis, DNA synthesis arrest, and cellular differentiation, and inhibit colony formation in human MDA-MB-435-F-L breast cancer cells in culture. The three agents alone were effective in inhibiting cell growth by apoptosis, DNA synthesis arrest, cellular differentiation, and reducing colony formation. Combination treatments synergistically inhibited cell proliferation in the four different assays conducted, in comparison to individual treatments. For induction of apoptosis, enhanced levels of apoptosis were also found using human breast (MDA-MB-231, MCF7, and T47D) and human prostate (LNCaP, PC-3, and DU-145) cancer cell lines, as well as in immortalized but non tumorigenic MCF10A cells. No apoptosis was seen in primary cultures of human mammary epithelial cells (HMECs). Western immunoblotting confirmed that all three compounds individually and in combination induced poly(ADP-ribose) polymerase cleavage with more complete cleavage seen in the combination treatment. In studies of DNA synthesis arrest, clonegenic, and cell differentiation assays, all three compounds produced dose-dependent responses individually and enhanced responses in combination. In summary, the combination of α-TEA, MSA, and *t*-RES is more effective than single treatments for inhibiting cell proliferation, and inducing differentiation and apoptosis of human cancer cells in culture.

INTRODUCTION

Breast cancer is the most common cancer among US women and second only to lung cancer in deaths [1]. Despite intense studies, the incidence of breast cancer remains high. Toxicity and resistance to standard drug treatments limit the effectiveness of chemotherapy so there remains an urgent need for alternative strategies for prevention and treatment of cancers, specifically combinations of nutrient-based agents with low toxicities that act in a synergistic manner to enhance treatment efficacy.

α-TEA has been developed for potential use in chemoprevention and chemotherapy [38, 40]. α-TEA is capable of inducing human ovarian (A2780/cp-70), cervical (ME-180), breast (MCF-7, MDA-MB-231, MDA-MB-435), endometrial (RL-952), prostate (LNCaP, PC-3, DU-145), lung (A-549), colon (HT-29, DLD-1) and lymphoid (Raji, Ramos, Jurkat) cells to undergo apoptosis [38-40]. α-TEA does not induce apoptosis in normal human mammary epithelial cells or normal PrEC human prostate epithelial cells [38-40, 42]. Previous studies have also shown α-TEA to be effective at reducing tumor burden and metastasis *in vivo* [40-44].

trans-Resveratrol (3,5,4'-trihydroxy-*trans*-stilbene; *t*-RES) is a naturally occurring phytoalexin that can be found in a variety of foods such as grapes, wine, berries, and peanuts [46-53]. This phytoalexin is considered a promising chemotherapeutic agent based on its ability to inhibit free radical formation [46-48, 53], and to induce cellular differentiation and apoptosis in human promyelocytic leukemia cells [47-48], human colon cancer cells [48-49], and human breast cancer cells [48, 50] *in vitro*. *t*-RES has been shown to inhibit the development of 7,12-dimethylbenz(a)anthracene-induced hyperplastic and atypical preneoplastic lesions in the mouse mammary organ culture model [47-48, 53]. It also inhibits N-methyl-N-

nitrosourea induced mammary lesions in rats, and tumorigenesis in a two-stage mouse skin cancer model with no observed toxicity *in vitro* and *in vivo* [47, 49, 51, 53].

Selenium is an essential nutrient for humans that can be found in cereal grains, meats, and seafood and is required for more than 13 human enzymes and proteins, in the form of L-selenocysteine [61]. Dietary supplementation of selenium beyond the recommended dietary allowance of 55 μg/day for females and males 14 years of age or greater at up to 200 μg/day reduces the incidence of lung, colorectal, and prostate cancer in humans [61, 63, 65, 67-68]. Se-(Methyl)selenocysteine (MSC) has been shown to be an effective suppressor of chemically induced mammary carcinogenesis in rats [62, 64-68, 71]. Unfortunately MSC is not a good agent for use for *in vitro* studies because it requires conversion to methylselenol by the liver and kidney [62, 64, 66-68, 71]. Methylseleninic acid (MSA) is a better agent for *in vitro* studies because it easily undergoes reduction to methylselenol once taken up by the cells [63, 67, 71] and has been shown to induce apoptosis in murine and human mammary cells [67-68, 71]. MSC and MSA have been shown to have equal chemo-preventative efficacy *in vivo* and are considered interchangeable [67, 71].

Based on promising anticancer actions of the novel vitamin E analog, α-TEA, and that of *t*-RES and MSA, the combined effects of these compounds on the highly metastatic human breast MDA-MB-435-F-L cell line were investigated. In these studies the effects of α-TEA plus *t*-RES and MSA, alone and in combination on cell proliferation and the induction of apoptosis and differentiation were investigated. Combination treatments synergistically inhibited tumor cell growth by analyses of apoptosis, and greatly inhibited DNA synthesis arrest, colony formation, and cellular differentiation.

MATERIALS AND METHODS

Chemicals and Reagents

t-RES was purchased from Cayman Chemical Co. (Ann Arbor, MI), MSA was purchased from PharmaSe, Inc. (Lubbock, TX), and Vitamin E Succinate (VES) was purchased from Sigma-Aldrich (St. Louis, MO). All reagents for morphological analyses of apoptosis were purchased from Boehringer Mannheim (Indianapolis, IN). α-TEA was prepared and validated as previously described [40].

Cell Lines and Culture Conditions

MDA-MB-231, T47D, MCF10-A, LNCaP, PC-3, and DU-145 cell lines were obtained from the American Type Culture Collection (ATCC; Manassas, VA). The MCF-7 cell line was provided by Dr. Suzanne Fuqua (University of Texas Health Science Center, San Antonio, TX). HMECs are primary cultures of mammary cells derived from normal mammoplasty specimens and received from the cooperative human tissue network Southern Division (CHTN; Birmingham, AL). MDA-MB-435-F-L cells were a kind gift from Dr. LuZhe Sun (University of Texas Health Science Center, San Antonio, TX). These cells are derived from MDA-MB-435 cells and have been stably transfected with enhanced green fluorescence protein (GFP). They are more metastatic than the parental MDA-MB-435 cell line having been injected into the flank of a nude mouse and recovered from a lung metastasis [73].

MDA-MB-435-F-L, MDA-MB-231, MCF-7, T47D, MCF10A, HMECs, LNCaP, PC-3, and DU-145 cells were cultured as previously described [43, 88-89]. For apoptosis analysis, exponentially growing T47D, MCF10A, and HMEC cells were plated at 1.5 x 10^5 cells/well in 12-well plates while MDA-MB-435-F-L, MDA-MB-231, and MCF-7 cell lines were plated at 1.0 x 10^5 cells/well in 12-well plates (1 ml/well). MDA-MB-

435-F-L cells were plated at 1.67 x 10^5 cells/ml in T-25 flasks (10 ml per flask) for Western analysis, 1.0 x 10^5 cells/ml in 96-well plates (150 µl/well) for DNA synthesis arrest studies, and 1.5 x 10^5 cells/ml in 6-well plates (2 ml/well) for differentiation studies. Cells were allowed to attach overnight and the following day growth media were replaced with experimental media containing treatments. Stock solutions of *t*-RES and α-TEA were at 20 mg/ml in DMSO, and MSA was at 1 mg/ml in water. All solutions were stored at –20°C and diluted in experimental media to the desired final concentration. Vehicle controls consisted of 0.167 % DMSO, or 1.67 µl/ml media.

Apoptosis Analysis Using Morphology of 4', 6-Diamidino-2-Phenylindole Dihydrochloride (DAPI) Nuclear Stained Cells

All cell lines were plated and treated with α-TEA at 10.25 or 20.5 µM, *t*-RES at 44 or 88 µM, MSA at 5 or 10 µM, a combination of the above drugs, or vehicle. Treatments were for two or three days and then cells were collected and stained with DAPI as previously described [88]. Cells in each sample were counted a minimum of 3 times, with •100–200 cells/count. Cells where the nucleus contained clearly condensed chromatin or fragmented nuclei were scored as apoptotic. Apoptotic data are reported as percent apoptosis (number apoptotic/total number of cells counted). Data are mean ± S.D. of three independent experiments.

Western Immunoblot Detection of Poly(ADP-Ribose) Polymerase (PARP) cleavage

MDA-MB-435-F-L cells were plated and treated with 20 µM α-TEA, 88 µM *t*-RES, 10 µM MSA, a combination of the three at the same concentrations, or a vehicle and allowed to incubate for 6, 12, 24, or 48 h. Cells were detached by scraping and both adherent and floating cells were pelleted by centrifugation for 5 minutes at 350 × *g*. Whole cell lysates were prepared and western immunoblotting performed as previously described [88] with the exception that 50 µg of protein were loaded in each well of a 10%

polyacrylamide gel. Immunoblotting was performed using 1 μg of primary rabbit anti-human PARP antibody [PARP (H-250), Santa Cruz Biotechnology, CA], and horseradish peroxidase-conjugated goat anti-rabbit immunoglobulin (Ig) was used as the secondary antibody (Jackson Immunoresearch Laboratory, West Grove, PA) at a 1:2000 dilution; detection was carried out with enhanced chemiluminescense (ECL, Pierce, Rockford, IL). Glyceraldehyde-3-phosphate dehydrogenase (GAPDH, in house) was used to verify equal lane loading.

DNA Synthesis Arrest Assay

Detection of DNA synthesis arrest was measured by [^{3}H]-thymidine incorporation as previously described [90]. MDA-MB-435-F-L cells were plated and treated with different amounts of α-TEA, MSA, or *t*-RES to establish a dose response for each compound. After 24 hours, 0.5 μCi [^{3}H]-thymidine was added to media and allowed to incubate for another 8.5 hours. Cells were harvested and [^{3}H]-thymidine uptake was measured with a Beckman LS5000TD liquid scintillation counter. Following establishment of a dose response, data were entered into CalcuSyn 2.0 (Biosource, Ferguson, MO), a software program designed to determine drug interactions and ED_{50}. Next, cells were plated as previously described and followed by a variety of combination treatments based on the ED_{50} values on day 2. Pulsing and harvesting was performed as described previously. Data are mean ± S.D. of three independent experiments.

Clonegenic Assay

Inhibition of colony formation was performed as previously described with the exception that treatments were given for 3 instead of 10 days [41]. MDA-MB-435-F-L cells were plated at increasing cell numbers ranging from 5 x 10^2 to 1 x 10^5 cells/well in laminin (2 μg) coated 6-well plates and allowed to adhere overnight. The following day,

growth media was removed and replaced with experimental media containing different amounts of α-TEA, MSA, or *t*-RES to establish a dose response for each compound. On day 4, treatment media were replaced with fresh experimental media and the cells were allowed to grow for 9 days, after which the media was removed and the plates were stained for 30 minutes with 1% methylene blue. Plates were examined and colonies greater than 100 cells were counted manually in wells containing 50 to 300 colonies. Surviving fractions were calculated as number of colonies present divided by number of cells seeded x plating efficiency. The dose response data were entered into CalcuSyn and ED_{50} values were determined. Cells were plated as described above and treated with a variety of combination treatments based on the ED_{50} values. Plating efficiencies and surviving fractions were determined. Data are the mean ± S.D. of three independent experiments.

Differentiation with Oil Red O-Stain

Samples were prepared as previously described [91-92]. Cells were plated on cover slips and treated for 12, 24, or 48 h with experimental media containing various treatments. Cells were fixed in 4% paraformaldehyde overnight at 4˚C and washed three times with phosphate buffered saline (PBS) solution. Cells were stained with an Oil Red O working solution (6:4, saturated Oil Red O: distilled water) for 10 min and then washed three times with PBS. Cells were counterstained for 5 min with Mayer's hematoxylin solution and washed until the background was clean. Cover slips were mounted onto a glass slide and examined with a Zeiss microscope at 1000x. Cells containing 10 or more Oil Red O-stained lipid droplets were scored positive. Data are the mean ± S.D. of three independent experiments. Data was analyzed using ANOVA followed by a Newman-Keuls post-hoc test.

Statistical Analyses

Statistical analyses were conducted using Prism software version 4.0 (Graphpad, San Diego, CA) and a level of $p < 0.05$ was considered statistically significant. CalcuSyn 2.0 was used to determine ED_{50} values and synergy values.

RESULTS

α-TEA, *t*-RES, and MSA in combination act synergistically to induce apoptosis in MDA-MB-435-F-L cells

Prior to conducting combination studies, α-TEA, *t*-RES, and MSA at sub-optimal to optimal concentrations were analyzed for ability to induce apoptosis (Fig 1A). Based on these data, sub-optimal dosages of α-TEA at 10 and 20 μM, *t*-RES at 44 and 88 μM, and MSA at 5 and 10 μM were chosen for combination treatments. MDA-MB-435-F-L cells were treated with sub-optimal apoptotic levels of α-TEA, *t*-RES, and MSA, separately and in combination, for 2 (data not shown), and 3 days (Fig 1 A). Combination treatments for two days with each of the lower individual agents induced 28% apoptosis and a combination with the higher individual treatments induced 47% apoptosis, however, levels of apoptosis at 2 days treatment were not significantly different from single treatments (data not shown). Combination treatments for 3 days significantly enhanced apoptosis in comparison to single treatments. The low combination treatment induced 41% and the higher induced 82% apoptosis, respectively (Fig 1A). Analyses of the combination data using CalcuSyn software to determine a combination index value (CI) and synergy, showed the enhanced apoptosis to be synergistic at both concentrations of the three agents, CI for α-TEA (10 μM), *t*-RES (44 μM) and MSA (5 μM) = 0.682. CI for α-TEA (20 μM), *t*-RES (88 μM) and MSA (10 μM) = 0.465. Synergistic relationship is defined as $CI < 1$.

Evidence of apoptosis induced by treatments was also confirmed using PARP cleavage (p84). VES, a known inducer of apoptosis [88] was used as a positive control for PARP cleavage. Combination treatments, in comparison to single treatments, cleave PARP at an earlier time point and more completely than individual treatments (Fig 1B). At 12 h, a p84 cleavage band was seen in the combination treatment. At 24 h, α-TEA and the combination treatments both show PARP cleavage with the combination showing a 2.7-fold stronger cleavage band in comparison to the α-TEA band. α-TEA, MSA, *t*-RES, and the combination treatments all have cleavage bands at 48 h with the combination treatment showing a 5.9, 2.8, and 2.4 fold increase over individual treatments (Fig. 1B).

α-TEA, *t*-RES, and MSA in combination act synergistically to induce apoptosis in breast and prostate cancer cells and immortalized but non-tumorigenic breast cells, but not normal mammary epithelial cells.

To determine if the enhanced effect of the combination treatment was applicable to other cell lines, breast (MDA-MB-231, MCF-7, and T47D); prostate (PC-3, LnCaP, and DU-145), immortalized but non-tumorigenic MCF-10A cells, and normal epithelial mammary cells (HMECs) were examined. All cell lines were treated at the same concentrations of the three agents separately and in combination and durations as used to treat MDA-MB-435-F-L cells in Fig 1A. Combination treatments for 2 and 3 days significantly enhanced apoptosis, in comparison to single treatments, in all tumorigenic cell lines and the immortalized cell line, but not HMECs (Table 1).

α-TEA, *t*-RES, and MSA in combination act synergistically to enhance DNA synthesis arrest in MDA-MB-435-F-L cells

Prior to conducting combination treatments, the EC_{50} values for α-TEA, *t*-RES, and MSA treatments alone for induction of DNA synthesis arrest were established. MDA-MB-435-F-L cells showed a dose-dependent arrest of DNA synthesis after 30 h of

single treatments with several levels of α-TEA, *t*-RES, and MSA (Fig 2). ED_{50} values generated by CalcuSyn were 14.23, 19.8, and 1.16 μM for α-TEA, *t*-RES, and MSA respectively (Fig 2). For combination studies, α-TEA, *t*-RES, and MSA treatments were made using either the ED_{50} or half of the ED_{50} concentrations derived from Fig 2A. The combination treatments induced percent DNA synthesis arrest in the range of 53-92% (Table 2). Two of the combination treatments significantly induced DNA synthesis arrest at 92 and 90% respectively. (Table 2, CI values of 0.93 and 0.95 respectively). One combination treatment additively enhanced DNA synthesis arrest (CI value of 1.04). The most effective combination was 14.23 μM α-TEA + 19.8 μM *t*-RES + 1.16 μM MSA (Table 2, CI value of 0.93).

α-TEA, *t*-RES, and MSA in combination act synergistically to inhibit colony formation in MDA-MB-435-F-L cells

Prior to conducting combination treatments, the EC_{50} values for α-TEA, *t*-RES, and MSA treatments alone for inhibition of colony formation were established. Using CalcuSyn, ED_{50} values were calculated to be 4.73, 13.2, and 6.9 μM for α-TEA, *t*-RES, and MSA, respectively (Fig 3). Using these values, combinations were made using either the ED_{50} concentration or concentrations half of the ED_{50}. The combination treatments induced percent cell death in the range of 62 to 92% (Table 3). Three of the combination treatments synergistically inhibited colony formation (CI values of 0.54, 0.88, and 0.94, respectively). One combination treatment additively inhibited colony formation (CI value of 1.03). The most effective combination was 4.73 μM α-TEA + 13.2 μM *t*-RES + MSA at 3.45 μM (Table 3).

α-TEA, *t*-RES, and MSA in combination act synergistically to induce cellular differentiation in MDA-MB-435-F-L cells

Incorporation of Oil Red O-stain was used to assess cell differentiation. MDA-MB-435-F-L cells were treated with vehicle control, VES (40 μM), *t*-RES (88 μM), α-TEA (20.5 μM), MSA (10 μM), or a combination of *t*-RES, α-TEA and MSA for 12, 24, and 48 h. VES, a compound known to induce differentiation in MDA-MB-435 cells [91-92] was used as a positive control. All single treatments significantly induced cellular differentiation at the three time points in comparison to vehicle control (Fig 4). Combination treatments were significantly different from individual treatments at all time points (Fig 4).

DISCUSSION

In the studies reported here, we show that α-TEA alone and together with *t*-RES and MSA, can prevent the formation of colonies, inhibit DNA synthesis, increase cell death by apoptosis and induce cell differentiation in human MDA-MB-435 cells in culture. These studies demonstrate that the administration of α-TEA together with *t*-RES and MSA induces synergistic levels of apoptosis, DNA synthesis arrest, inhibition of colony formation, and enhanced levels of cellular differentiation in comparison to individual treatments in MDA-MB-435-F-L human breast cancer cells. Combination treatments enhanced apoptosis in a variety of epithelial prostate and breast cancer cell lines. These data show that the combination effects are not limited to a single cancer cell line, supporting broad-spectrum use in humans.

Perhaps significant to the potential use of these compounds in human chemotherapy is not only the observation that individually these compounds do not induce apoptosis in normal human mammary epithelial cells, but neither do combination treatments. These data suggest that these agents in combination selectively target

tumorigenic and not normal cells, suggesting potential synergistic anti-cancer potential in humans with perhaps limited to no toxicity when used as a chemotherapeutic treatment. To a lesser extent, combination treatments selectively target immortalized but non-tumorigenic cells, suggesting potential use as a long-term chemoprevention regimen. Data in the literature using these three agents singly as anticancer agents is supportive of the data reported here. α-TEA [39-40, 42] is nontoxic to normal human prostate epithelial cells *in vitro* [38-40, 42] and exhibits no visible signs of toxicity to mice *in vivo* [40-44]. *t*-RES does not have toxic effects *in vitro* or *in vivo* [46-53]. Although selenium toxicity can occur, the levels that were used here were below the threshold for toxicity and within the range of concentrations reported in the literature [63, 67, 71]. Additionally, several forms of selenium are commonly used in long-term chemoprevention models [64-66, 68, 71], re-enforcing the relevance of its use.

Combination treatments showed an enhanced ability to inhibit tumor cell growth at lower concentrations when compared to individual treatments. Using DNA synthesis as an example, the most effective combination (14.23 μM α-TEA + 19.8 μM *t*-RES + 1.16 μM MSA) inhibited DNA synthesis arrest by 92%. In order to obtain similar results with individual agents, treatments would require 2.4 fold more α-TEA, 2.89 fold more *t*-RES, or 6.5 fold more MSA than what was used in the combination treatment. These combination treatments have the potential to maximize anticancer efficacy with reduced levels of potentially toxic agents.

Unlike the DNA synthesis arrest data, MSA appears to play an inhibitory role in combination treatments when *t*-RES is at high concentrations. For example, the combination of 4.73 μM α-TEA + 13.2 μM *t*-RES + 3.45 μM MSA had a much greater inhibition on colony formation than with the same concentration of α-TEA and *t*-RES but with twice as much MSA (92 vs. 70 % inhibition of colony formation). By adding more

MSA to the combination, the effectiveness decreased by 24%. This inhibitory effect is also reflected in the CI value (0.54 v 1.66, CI > 1 is antagonistic). However, when *t*-RES is at low concentrations, MSA does not seem to affect the results. For example, the combination of 4.73 μM α-TEA + 6.6 μM *t*-RES + 6.9 μM MSA is nearly identical to that with half as much MSA (74 vs. 75%). Likewise, the combination of 2.36 μM α-TEA + 6.6 μM *t*-RES + 6.9 μM MSA is very similar to that with half the MSA (67 vs. 62%).

Differentiation is another mechanism by which cancer therapeutic and chemopreventive agents can work. The data for the individual treatments is consistent with that found in the literature. Previous reports by our lab have shown that several forms of vitamin E, including α-TEA can induce cellular differentiation in human MDA-MB-435 and MCF-7 breast cancer cell lines [91-92]. *t*-RES has been shown to induce differentiation in medulloblastoma cells and promyelocytic leukemia cells [47, 93]. Results with the differentiation assay were similar to that for apoptosis (PARP cleavage) in that the combination showed both a quantitative and kinetic advantage over all the individual treatments.

It seems highly plausible that these unique combinations of compounds could be extremely effective if used either as a chemotherapy or chemoprevention cocktail *in vivo*. If successful, this combination could be a very attractive alternative to traditional chemotherapy due both to the absence of toxicity and the effectiveness of treatment. However, the combination data point out a challenging problem, the need to obtain different levels of each agent in order to maximize anticancer efficacy. Data show that α-TEA can be effectively paired with more traditional and toxic chemotherapeutic agents (celecoxib, 9-nitro-camptothecin, and cisplatin) to significantly reduce tumor burden, while using reduced levels of toxic chemotherapeutic agents [42-44].

Based on data reported in this paper, and the effectiveness of α-TEA *in vivo*, preclinical animal studies were conducted using α-TEA, *t*-RES and MSC separately and in combination. Unfortunately synergisms found in cell culture did not occur in the animal study. MSC, *t*-RES, and α-TEA alone decreased tumor volume by 0.1, 23.5, and 59.7%, respectively, and only a 52.6% decrease in the combination treatment (*Chapter 3*). One possible explanation is that MSC was inhibitory to the combination of *t*-RES and α-TEA, as was found in the colony assay. The combination of MSC + α-TEA showed a 51.4% reduction in tumor volume, which was less effective than α-TEA alone. A group containing only *t*-RES + α-TEA was not present in this study that could have supported the theory that MSA inhibited the combination. A second possible explanation is that synergistic combinations of the three agents were not obtained *in vivo*. Thirdly, cell culture data may not be predictive of *in vivo* outcome.

ACKNOWLEDGEMENTS AND NOTES

We would like to thank Jessica Lee for her assistance with the clonegenic assay. This work was supported by Public Health Service Grant CA59739 awarded by the National Cancer Institute, the Foundation for Research (KK & BGS), the National Institute of Environmental Health Sciences Center Grant ES 07784 (KK & BGS are members), and Toxicology Training Grant T32 ES 07247 (predoctoral support for RMS).

Table 2.1. Apoptosis induced in human breast cancer, immortalized, and normal mammary cells treated with α-TEA, MSA, and *t*-RES[a]

	Breast					Prostate		
Tumorigenic	+	+	+	-	-	+	+	+
Immortalized	-	-	-	+	-	-	-	-
Normal	-	-	-	-	+	-	-	-
	MDA-MB-231	MCF-7	T47D	MCF-10A	HMEC	PC-3	LNCAP	DU-145
Treatment (μM)- 2 Day								
VEH	4 ± 1	3 ± 1	3 ± 1	5 ± 2	3 ± 1	4 ± 1	4 ± 1	4 ± 1
α-TEA 20	17 ± 2 *(3)*	7 ± 2 *(4)*	4 ± 1 *(1.5)*	8 ± 2 *(3)*	2 ± 1	12 ± 2 *(5.8)*	20 ± 3 *(1.5)*	10 ± 2 *(4.9)*
RES 88	7 ± 1 *(7.3)*	9 ± 3 *(3.1)*	3 ± 1 *(2)*	7 ± 2 *(3.4)*	2 ± 1	14 ± 4 *(4.9)*	7 ± 2 *(4.3)*	12 ± 2 *(4.1)*
MSA 10	14 ± 2 *(3.6)*	7 ± 2 *(4)*	2 ± 1 *(3)*	5 ± 2 *(4.8)*	2 ± 1	31 ± 6 *(2.2)*	6 ± 1 *(5)*	19 ± 3 *(2.6)*
α-TEA 20 + RES 88 + MSA 10	51 ± 3 *	28 ± 2 *	6 ± 2 *	24 ± 5 *	2 ± 1	69 ± 3 *	30 ± 2 *	49 ± 3 *
Treatment (μM)- 3 Day								
VEH	3 ± 1	3 ± 1	3 ± 1	3 ± 1	3 ± 1	3 ± 1	4 ± 1	5 ± 2
α-TEA 20	51 ± 3 *(1.7)*	17 ± 2 *(2.7)*	5 ± 2 *(3.4)*	11 ± 3 *(2.9)*	3 ± 1	15 ± 3 *(5.8)*	60 ± 5 *(1.2)*	9 ± 3 *(8.1)*
RES 88	13 ± 1 *(6.6)*	13 ± 2 *(3.5)*	4 ± 2 *(4.3)*	6 ± 8 *(5.3)*	3 ± 1	15 ± 2 *(5.8)*	12 ± 1 *(6.2)*	16 ± 3 *(4.6)*
MSA 10	34 ± 3 *(2.5)*	20 ± 3 *(2.3)*	5 ± 1 *(3.4)*	4 ± 2 *(8)*	2 ± 1	44 ± 5 *(2)*	7 ± 1 *(10.6)*	30 ± 3 *(2.4)*
α-TEA 20 + RES 88 + MSA 10	86 ± 4 *	46 ± 4 *	17 ± 2 *	32 ± 8 *	2 ± 1	87 ± 2 *	74 ± 4 *	73 ± 3 *

a: Cells were treated with α-TEA, MSA, *t*-RES, or a combination, and analyzed after 48 and 72 h treatment. Treatments are given in μM concentrations. Data reflect an average of three experiments +/- S.D. Percentages have been rounded to the nearest integer.
(#): Represents fold increase of combination over individual treatment
* $p<0.05$ compared to the individual treatments for that cell line. Data was analyzed using a one-way analysis of variance followed by a Tukey post-hoc test.

Table 2.2. Combination Treatments with α-TEA, *t*-RES, and MSA Synergistically Reduce DNA Synthesis[a]

α-TEA (μM)	***t*-RES (μM)**	**MSA (μM)**	**Ratio**	**% DNA Synthesis Arrest**	**Fold Increase**	**CI value**
14.23	19.8	1.16	2:2:2	92	1.8	0.93**
14.23	19.8	0.58	2:2:1	90	1.8	0.95**
7.11	19.8	1.16	1:2:2	80	1.6	1.18
7.11	19.8	0.58	1:2:1	79	1.6	1.04*
14.23	9.9	1.16	2:1:2	82	1.6	1.19
14.23	9.9	0.58	2:1:1	73	1.5	1.32
7.11	9.9	1.16	1:1:2	68	1.4	1.31
7.11	9.9	0.58	1:1:1	53	1.1	1.42

a: Data represent an average of three experiments. The ED_{50} values were 14.23, 19.8, and 1.16 μM for α -TEA, *t*-RES, and MSA, respectively. These values were designated as a 2:2:2 ratio. Other ratios were made with respect to the ED_{50} values. % DNA Synthesis Arrest was rounded to the nearest integer.

**: Data represent synergistic effect

*: Data represent additive effect

Table 2.3. Combination Treatments with α-TEA, *t*-RES, and MSA Synergistically Inhibit Colony Formation[a]

α-TEA (μM)	*t*-RES (μM)	MSA (μM)	Ratio	Survival Fraction	% Death	Fold Increase	CI Value
4.73	13.2	6.9	2:2:2	30	70	1.4	1.66
4.73	13.2	3.45	2:1:2	8	92	1.8	0.54**
2.36	13.2	6.9	1:2:2	20	80	1.6	0.88**
2.36	13.2	3.45	1:1:2	27	73	1.5	0.94**
4.73	6.6	6.9	2:2:1	26	74	1.5	1.28
4.73	6.6	3.45	2:1:1	25	75	1.5	1.03*
2.36	6.6	6.9	1:2:1	33	67	1.3	1.20
2.36	6.6	3.45	1:1:1	38	62	1.2	1.37

a: Data are representative of three experiments. The ED_{50} values were 4.73, 13.2, and 6.9 μM for ⟨-TEA, *t*-RES, and MSA, respectively. These values were treated as a 2:2:2 ratio. Other ratios were made with respect to the ED_{50} values.

**: Data represent synergistic effect

*: Data represent additive effect

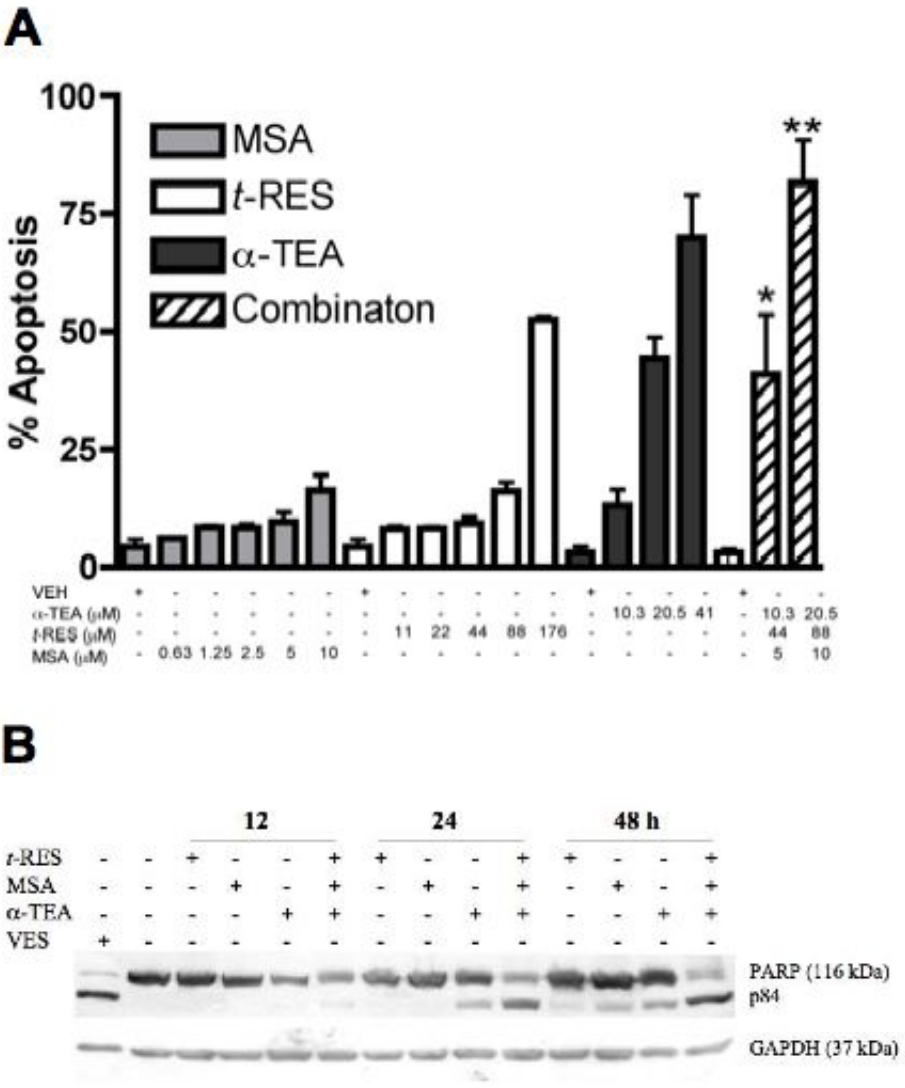

Figure 2.1. α-TEA, *t*-RES, and MSA induce apoptosis. A: MDA-MB-435-F-L cells were treated with various individual or combined treatments of α-TEA, *t*-RES, and MSA for 72 h. Cells were collected, DAPI stained, and analyzed for apoptosis. Data are the mean ± S.D. of three independent experiments. * (CI = 0.682) and ** (CI = 0.465) indicates synergy in comparison to vehicle and individual treatments. B: MDA-MB-435-F-L cells were treated for 6, 12, 24, and 48 h with α-TEA, *t*-RES, and MSA, alone or in combination. Western immunoblotting was performed to evaluate PARP cleavage (p84) in response to treatments. GAPDH was used to verify lane loading and to perform densitometric analyses. Numerical value represents fold increase of combination over respective individual treatment. Data are representative of 3 or more experiments.

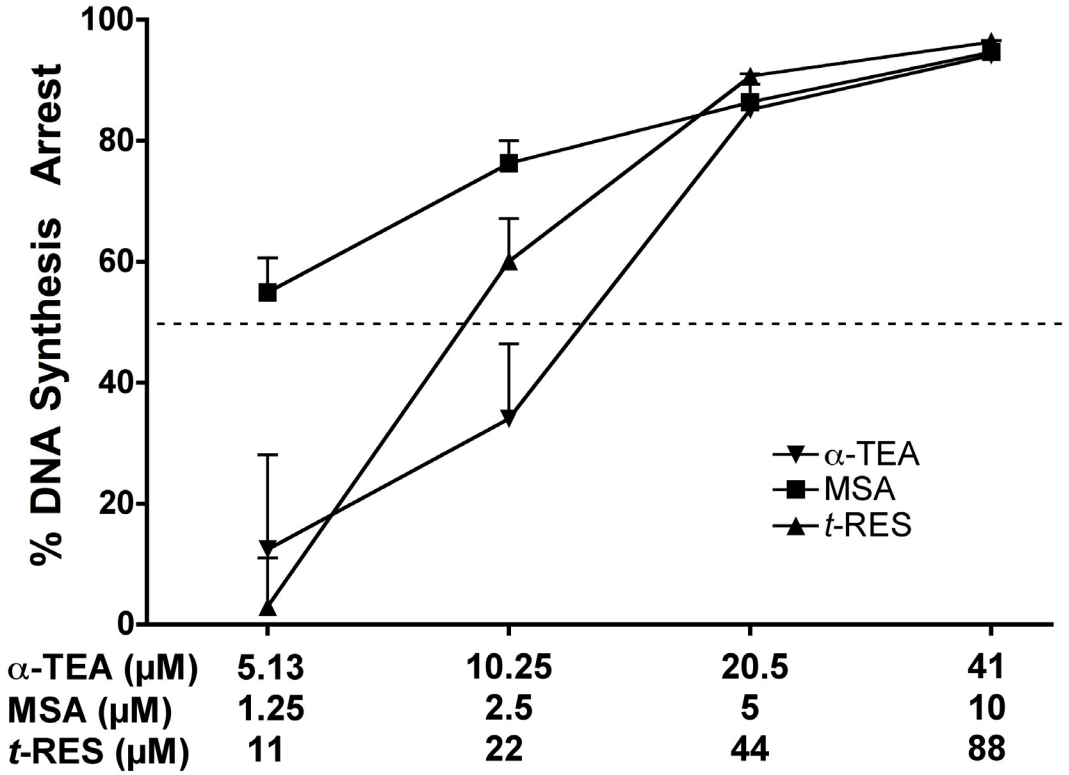

Figure 2.2. Dose-dependent DNA synthesis arrest. Uptake of [^{3}H]-thymidine was used as a measure of DNA synthesis arrest. MDA-MB-435-F-L cells were treated for 30 h with various concentrations of α-TEA, *t*-RES, and MSA to determine a dose response for each compound to induce DNA synthesis arrest. ED_{50} values were 14.23, 19.8 and 1.16 μM for α-TEA, *t*-RES, and MSA, respectively (indicated by the dashed line). Data are mean ± S.D. of three independent experiments.

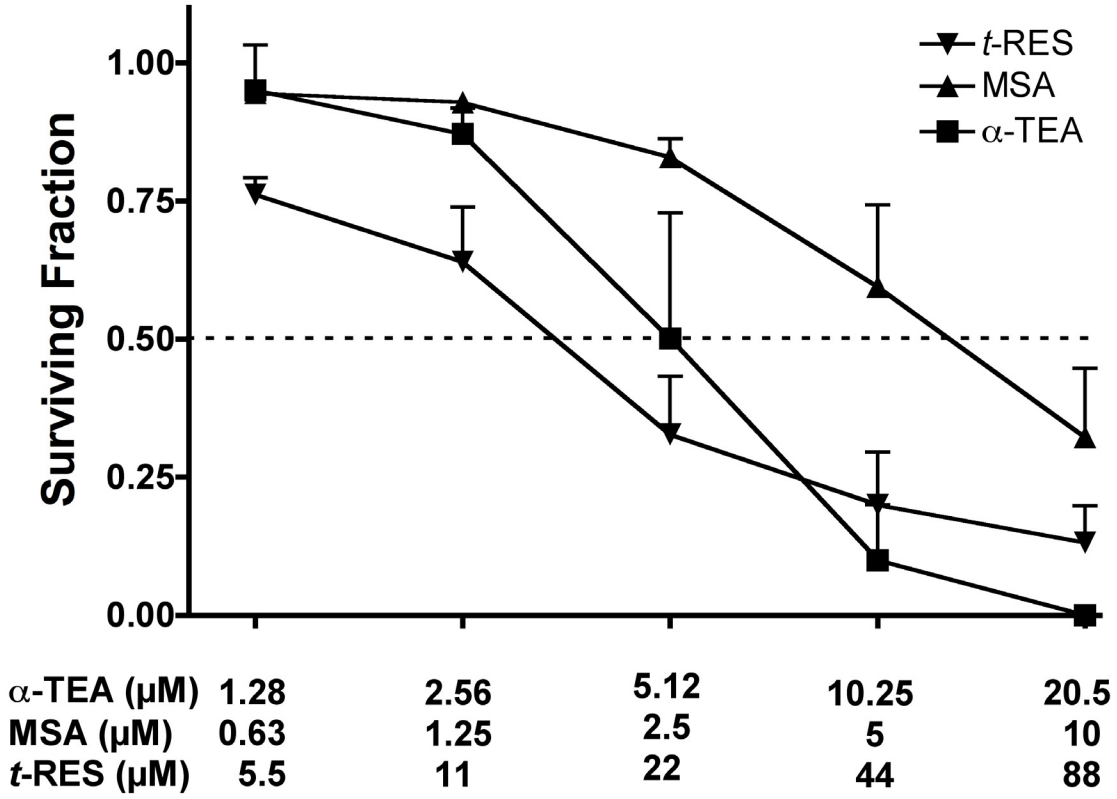

Figure 2.3. Dose-dependent inhibition of colony formation. MDA-MB-435-F-L cells were seeded at varying concentrations per well in laminin-coated wells and treated with varying concentrations of α-TEA, *t*-RES, and MSA for 72 h. Treatment media was replaced with fresh media and cells were allowed to grow for nine days. Surviving fractions were calculated as number of colonies present divided by number of cells seeded x plating efficiency. ED_{50} values were 4.73, 13.2 and 6.9 μM for α-TEA, *t*-RES, and MSA, respectively (indicated by the dashed line). Data are mean ± S.D of three independent experiments.

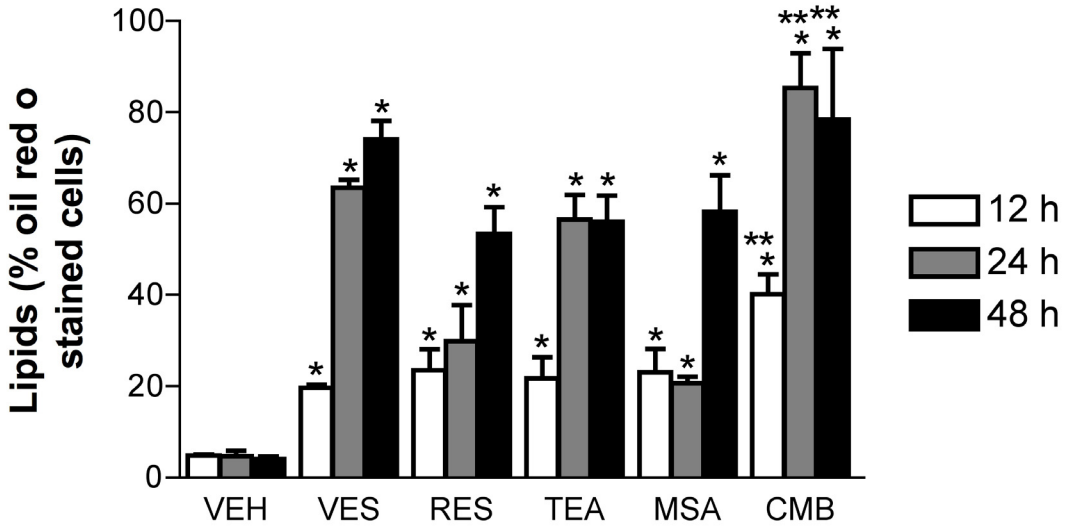

Figure 4. Cell differentiation by α-TEA, *t*-RES, and MSA. MDA-MB-435-F-L cells were treated with VEH, VES (40 μM), *t*-RES (88 μM), α-TEA (20.5 μM), MSA (10 μM), or a combination of *t*-RES + MSA + α-TEA for 12, 24, and 48 h. Cells were analyzed for expression of neutral oil droplets using Oil Red O-stain. Results are expressed as mean percentage of Oil Red O-stained cells ± S.D. of three independent experiments. * $p < 0.05$ compared with VEH for that time point, ** $p < 0.05$ compared to individual treatments.

Chapter 3: α-TEA, *trans*-resveratrol, and selenium, alone and together, reduce human MDA-MB-435 tumor burden and metastases in a human MDA-MB-435 breast cancer xenograft model

ABSTRACT

α-TEA, methylselenocysteine (MSC) and *trans*-resveratrol (*t*-RES) alone were shown to be effective in inducing human MDA-MB-435 breast cancer cells to undergo cell death by apoptosis. Combinations of the three agents significantly enhanced DNA synthesis arrest and apoptosis (Chapter 2). Studies reported here investigated the ability of α-TEA, MSC, and *t*-RES (low dose, 10 mg/kg bw; and high dose, 100 mg/kg bw) alone and in combination to reduce tumor burden and inhibit lung and lymph node metastases using human MDA-MB-435-F-L breast cancer cells transplanted into nude mice. Two animal studies were conducted. In study #1 all treatments significantly reduced tumor burden, in comparison to control, with the exception of high dose *t*-RES. High dose *t*-RES alone and in combination enhanced tumor growth in comparison to control and other treatments. MSC was less effective than α-TEA or low dose *t*-RES in reducing tumor burden, and α-TEA alone was as effective as combination treatments in reducing tumor burden. Analyses of tumor sections show α-TEA alone and in a two-way combination with MSC, as well as in three-way combinations to significantly enhance TUNEL positive cells. α-TEA and both doses of *t*-RES alone significantly reduced Ki-67 positive cells. Treatments had no effect on CD31 positive cells. α-TEA alone and in combination with MSA significantly reduced the average number of visible lung metastases. All treatments significantly reduced the total number of lung micrometastatic lesions, and with the exception of low dose *t*-RES, lymph node metastases. Study #2 was

conducted to determine if the ability of high dose *t*-RES to enhance tumor growth was repeatable. The tumor burden data was not repeatable in that both low and high dose *t*-RES significantly reduced tumor burden. Both doses of *t*-RES significantly reduced average number of visible lung metastases, as well as micrometastatic lung and lymph node lesions. In summary, these data do not support the use of α-TEA with MSA or *t*-RES over α-TEA alone in treatment of human breast cancer.

INTRODUCTION

Cancer is the most common cause of death for women under the age of 85 in the U.S. It is estimated that breast cancer specifically will have the highest incidence of reported new cases in 2006 (32%) and will be responsible for about 15 percent of cancer deaths in women [1]. Without question, it is necessary to find ways to treat and prevent breast cancer, preferably via methods that involve little to no toxicity.

A novel, non-hydrolyzable ether analog of RRR-α-tocopherol, 2,5,7,8-tetramethyl-2R-(4R, 8R-12-trimethyltridecyl)chroman-6-yloxyacetic acid (called RRR-α-tocopheryloxyacetic acid or RRR-α-tocopherol ether-linked acetic acid analog and abbreviated α-TEA) was synthesized based on a desire to develop a clinically useful vitamin E-based chemotherapeutic agent. α-TEA is capable of inducing human ovarian (A2780/cp-70), cervical (ME-180), breast (MCF-7, MDA-MB-231, MDA-MB-435), endometrial (RL-952), prostate (LNCaP, PC-3, DU-145), lung (A-549), colon (HT-29, DLD-1) and lymphoid (Raji, Ramos, Jurkat) cells to undergo apoptosis [38]. α-TEA does not induce apoptosis in normal human mammary epithelial cells or normal PrEC human prostate epithelial cells [38-40, 42]. Preclinical animal studies show α-TEA to be effective at reducing tumor burden and metastasis [39-44].

trans-Resveratrol (3,5,4'-trihydroxy-*trans*-stilbene; *t*-RES) is a naturally occurring phytoalexin that can be found in a variety of foods such as red grapes, wine,

berries, medicinal plants and peanuts [46-53]. This antioxidant is considered a promising chemotherapeutic agent based on its ability to inhibit free radical formation [46-49], and to induce differentiation and apoptosis in promyelocytic leukemia cells [47-48], colon cancer cells [48-49], and breast cancer cells [48, 50] *in vitro*. *t*-RES has been shown to inhibit the development of 7,12-dimethylbenz(a)anthracene (DMBA) induced hyperplastic and atypical preneoplastic lesions in the mouse mammary organ culture model, (MMOC) [47-48, 53] and N-methyl-N-nitrosourea (NMU) induced mammary lesions in rats with no observed toxicity *in vitro* and *in vivo* [47-49, 51, 53].

Selenium is an essential nutrient for humans that can be found in cereal grains, meats, and seafood and is required for more than 13 human enzymes and proteins, in the form of L-selenocysteine [61]. Dietary supplementation of selenium beyond the recommended dietary allowance of 55 μg/day for women and 70 μg/day for men, at up to 200 μg/day reduces the incidence of lung, colorectal, and prostate cancer in humans [61, 63-65, 68]. One particularly active form, Se-(Methyl)selenocysteine (MSC), has been shown to be an effective suppressor of chemically induced mammary carcinogenesis in rats [62, 64-68, 71]. *In vivo*, MSC is converted to methylselenol by β-lyase in the kidney and liver [64, 71].

Due to the chemotherapeutic actions of α-TEA, *t*-RES and MSC, alone, and cell culture data showing that a combination of these three agents synergistically enhanced apoptosis in human MDA-MB-435 breast cancer cells, preclinical animal studies were conducted to evaluate the combination effects of the three agents in the highly metastatic human breast MDA-MB-435-F-L cell line growing in immune compromised nude mice. Study #1 evaluated the three agents separately and in combination for ability to inhibit human MDA-MB-435 breast cancer tumor growth and metastases. An unexpected finding from Study #1 was that high dose *t*-RES (100 mg/kg/bw) enhanced tumor growth.

Study #2 was conducted, using two doses of *t*-RES, to determine if high-dose *t*-RES enhanced tumor growth found in Study #1 was repeatable.

MATERIALS AND METHODS

Chemicals and Reagents

Se-(methyl)selenocysteine hydrochloride (MSC) was purchased from Sigma Chemical Co. (St. Louis, MO). *trans*-Resveratrol (*t*-RES) was purchased from Cayman Chemical Co. (Ann Arbor, MI). Neobee oil was purchased from Stepan (Anaheim, CA). α-TEA was synthesized, purified, and characterized in house. For scaled-up production, α-TEA was prepared as previously described [40].

Cell Lines and Culture Conditions

MDA-MB-435-F-L (a kind gift from Dr. LuZhe Sun, University of Texas Health Science Center, San Antonio, TX) cells are an estrogen-receptor-negative human breast cancer cell line. MDA-MB-435-F-L cells are MDA-MB-435 cells that have been stably transfected with enhanced green fluorescent protein (GFP) by Dr. LuZhe Sun. These cells were then injected into the flank of a nude mouse and removed from a metastasis to the lung. Prior to use in the nude mouse studies, cells were sent to the University of Missouri Research Animal Diagnostic and Investigative Laboratory (RADIL; Columbia, MO) and were certified to be pathogen free.

MDA-MB-435-F-L cells were cultured in McCoys's 5A medium (Life Technologies, Inc., Grand Island, NY) supplemented with 10% FBS plus 100 μg/ml streptomycin, 100 IU/ml penicillin, 1X (v/v) nonessential amino acids, 1X (v/v) MEM vitamins, 1.5 mM sodium pyruvate, and 50 μg/ml gentamycin (Sigma). Cell lines were routinely examined to verify absence of mycoplasma contamination.

Nude Mice

Female NU/NU homozygous mice (approximate 23 g in weight) were purchased from Charles River Laboratories (Wilmington, MA) at 6 weeks of age and were allowed to acclimate for one week. Animals were housed in the Transgenic Suite at the Animal Resource Center at the University of Texas at Austin at 74 ± 2°F with 30-70% humidity and a 12 hour alternating light-dark cycle. Animals were housed 5/cage and given water and diet *ad libitum*. The diets for study # 1 and #2 were Teklad 2018 and Teklad 7012, respectively. Guidelines for the humane treatment of animals were followed as approved by the University of Texas Institutional Animal Care and Use Committee.

Tumor Cell Inoculation and Treatment Groups

MDA-MB-435-F-L cells were harvested by trypsinization, centrifuged, and resuspended in McCoy's media containing no supplements and at a density of 1 x 10^6/100µl. Mice were injected subcutaneously in the inguinal area at a point equal distance between the 4th and 5th nipples in the right side using a 23-gauge needle.

Study 1: Twenty-one days after tumor inoculation, 80 mice were assigned (10 per group) to one of the following eight groups: control, α-TEA, MSC, low *t*-RES (10 mg/kg bw), high *t*-RES (100 mg/kg bw), α-TEA+MSC, low combination (α-TEA + MSC + low *t*-RES), or high combination (α-TEA + MSC + high *t*-RES). *Study 2*: mice were assigned 18 days post inoculation as described above to one of three groups: control, low *t*-RES (10 mg/kg bw), or high *t*-RES (100 mg/kg bw). The average tumor volumes for all groups were closely matched and the average tumor volume was 18.94 and 21.07 mm^3 in studies 1 and 2, respectively. Animals in groups receiving α-TEA were given α-TEA formulated in liposomes and delivered via aerosol, depositing approximately 36 µg/α-TEA into the respiratory tract/mouse daily; those receiving MSC were gavaged daily at 3 ppm MSC dissolved in sterile filtered milli-Q water, and those receiving *t*-RES were

gavaged daily with either 10 or 100 mg/kg bw dissolved in 6.5% EtOH and 93.5% Neobee oil. The control group was given aerosolized liposome, sterile-filtered milli-Q water, and the *t*-RES solvent. Treatments were given 7 days per week and tumors were palpated using calipers every other day. Tumor volumes were calculated using the formula: volume (mm^3) = [width $(mm)^2$ x 1ength (mm)]/2 [94]. Body weights were determined weekly.

Preparation of MSC for Delivery by Gavage

It was determined that each mouse would be gavaged a volume of 100 µl daily and receive 3 ppm MSC [66-67]. This was determined to be equal to 12 µg MSC based on an estimate that an average mouse eats four grams of food per day. A stock solution was made by dissolving MSC in sterile filtered milli-Q water at a concentration of 120 µg/ml. The solution was aliquoted into sterile eppendorf tubes and stored at –20°C until needed. Control treatments consisted of sterile filtered milli-Q water. Prior to delivery, aliquots were brought to room temperature

Preparation of *t*-RES for Delivery by Gavage.

It was determined that each mouse would receive 10 or 100 mg/kg bw [53]. Treatments of *t*-RES were made weekly and amounts of *t*-RES were adjusted based on the weight of the animals. *t*-RES was dissolved in 100% EtOH and then mixed with Neobee oil to give a final solution of 6.5% EtOH and 93.5% Neobee oil. Control treatments consisted of 6.5% EtOH and 93.5% Neobee oil, as contained in the *t*-RES treatments [53]. Solutions were aliquoted into sterile eppendorf tubes and stored at –20°C until needed. Prior to delivery, aliquots were brought to room temperature.

Preparation of α-TEA Liposomes for Delivery by Aerosol.

Preparations of α-TEA liposomes were made as previously described [40-44]. An α-TEA/liposome ratio of 1:3 (w/w) was determined empirically to be optimal by methods previously described [96]. To prepare the α-TEA/lipid combination, the components were first brought to room temperature. The lipid [1,2-dilauroyl-sn-glycero-3-phosphocholine (DLPC); Avanti Polar-Lipids, Inc., Alabaster, AL], at a concentration of 120 mg/ml, was dissolved in *t*-butanol (Fisher Scientific, Houston, TX) then sonicated to obtain a clear solution. α -TEA at 40 mg/ml was also dissolved in tertiary-butanol and vortexed until all solids were dissolved. The two solutions were then combined in equal amounts (v:v) to achieve the desired ratio of 1:3 α -TEA/liposome, mixed by vortexing, frozen at -80° C for 1-2 h, and lyophilized overnight to a dry powder prior to storing at -20°C until needed. Each treatment vial contained 75 mg α -TEA.

Aerosol Delivery.

Aerosol was administered to mice as previously described [40-44]. Briefly, an air compressor (Easy Air 15 Air Compressor; Precision Medical, Northapton, PA) producing a 10 L/min airflow was used with an Aero Tech II nebulizer (CIS-US, Inc. Bedford, MA) to generate aerosol. The particle size of α-TEA liposome aerosol discharged from the AeroTech II nebulizer was determined by the Anderson Cascade Impactor to be 2.01-μm mass median aerodynamic diameter (NMAD), with a geometric standard deviation of 2.04. About 30% of such particles when inhaled will deposit in the respiratory tract of the mouse and the remaining 70% will be exhaled [96]. Prior to nebulization, the α-TEA/lipid powder (75 mg/vial) was brought up to room temperature then reconstituted by adding 3.75 ml sterile filtered milli-Q water to achieve the final desired concentration of 20 mg/ml α-TEA. The mixture was allowed to swell at room temperature for 30 min with periodic inversion and vortexing, and then transferred to the reservoir of a nebulizer.

Mice were placed in clear plastic cages (7 x 11 x 5 in.) with a sealed top in a safety hood. Aerosol entered the cage via a 1 cm (i.d.) accordion tube at one end and discharged at the opposite end, using a one-way pressure release valve. Animals were exposed to aerosol until all α-TEA/liposome was aerosolized (approximately 20 min).

Aerosol Characteristics of α-TEA Incorporated into Liposomes.

HPLC analyses were conducted on α-TEA liposomes recovered from aerosol in the All Glass Impinger (Ace Glass Co., Vineland, NJ). The delivered dosage = concentration (μg/L) x mouse minute volume (1-min/kg) x duration of delivery (min) x estimated deposited fraction (30%; [96]). Based on this formula, we estimate that 36 μg of α-TEA was deposited in the respiratory tract of each mouse each day. Thus, for the 43-day treatment period, we estimate that each mouse received 1548 μg of α-TEA from liposomal delivery. For this same period, animals in the MSC group received 516 μg MSC (12 μg/day), and those in the *t*-RES group, were given 9.23 and 92.3 mg *t*-RES for the low and high dose groups, respectively.

Lung and Lymph Node Metastases.

Metastatic lesions in the five lung lobes were counted visually at time of sacrifice. Fluorescent green micro-metastatic cancer cell colonies in the left lung lobe and lymph nodes were counted using a Nikon fluorescence microscope (TE-200) with a 20X objective (200X magnification) as previously described [40-44]. Prior to counting, lungs were flattened and both sides (top and bottom) were counted. Lymph nodes were flattened and one side was counted. Fluorescent lesions were separated into four sizes: <20 μm, 20-50 μm, 50-100 μm, and >100 μm. The size of a MDA-MB-435-F-L cell is 10-20 μm in diameter so it is thought that the <20 μm group represents single cells and larger groups involve larger and larger clusters of cells.

H&E Staining of Tumor Tissue.

Tumors were fixed with 10% neutral buffered formalin, and embedded in paraffin according to standard histological procedures. H&E stained 5 μm thick sections were used to examine tumor morphology.

Terminal Deoxynucleotidyl Transferase-mediated Nick End Labeling (TUNEL) Assay for Detection of Apoptosis *in Vivo*.

Deparaffinized sections (5 μm) of tumor tissue were processed as previously described [40] using reagents supplied in the ApopTag *In Situ* Apoptosis Detection Kit (Intergen, Purchase, NY) according to the manufacture's instructions. Nuclei that stained brown were scored as positive for apoptosis and those that stained blue were scored as negative. At least sixteen 400X microscopic fields were scored per tumor. Data are presented as the mean ± S. E. number of apoptotic cells counted (n = 4).

Ki-67 Staining for Detection of Proliferation *in Vivo*.

Deparaffinized sections (5μm) of tumor tissue were processed as previously described [40]. Briefly, endogenous peroxidase activity was blocked using a 3% H_2O_2 solution for 10 min followed by washing with PBS. Ten-percent rabbit serum in PBS was applied to sections in order to clock non-specific antibody binding. Sections were incubated with Ki-67 antibody (1:200) dilution overnight at 4°C. After primary antibody incubation, slides were incubated with biotinylated rabbit-anti-rat IgG (Vector Laboratories, Burlingame, CA) at a 1:200 dilution for 30 min at room temperature. Sections were then incubated with avidin-biotin complex (ABC-HRP, Vector Laboratories) for 30 min at room temperature. Immunoreactivity was visualized via incubation with Di-aminobenzidine Dihydrochloride (DAB). Slides were lightly counterstained with hematoxylin. Nuclei that stained brown were scored as positive for apoptosis and those that stained blue were scored as negative. At least sixteen 400X

microscopic fields were scored per tumor. Data are presented as the mean ± S. E. number of apoptotic cells counted (n= 4).

CD31 Staining for Determination of Blood Vessel Formation *in Vivo*.

Deparaffinized sections (5μm) of tumor tissue were processed as previously described [40, 43] to detect the intratumoral microvessel density based on the "hot spot" method [97]. Areas of highest microvascularization were found by scanning tumor sections at low magnification (200X) with a light microscope. Areas with the greatest density staining were selected and microvessel counts were made using a 400X field. Ten fields were counted for each tumor section. Data are presented as mean ± S. E. (n=4).

Statistical Analyses.

Animal numbers for experiments were determined to be adequate based on power calculations. Tumor growth was evaluated by transforming volumes using a logarithmic transform (base 10) and analyzed using a nested two-factor ANOVA using SPSS (SPSS, Inc., Chicago, IL). Statistical significance for macroscopic and microscopic metastases, TUNEL, Ki-67 and CD31 were determined using a two-tailed Mann-Whitney rank test in Prism software version 4.0 (Graphpad, San Diego, CA). A level of $p < 0.05$ was considered statistically significant.

RESULTS

Treatment Effects on Tumor Growth.

Study 1. All treatment groups significantly reduced tumor burden in comparison to control ($P < 0.001$ for all) with the exception of high-dose *t*-RES and combination treatment with high-dose *t*-RES. Tumor volume of mice receiving the combination of α-

TEA + MSC + high dose *t*-RES were slightly larger than tumor volume of control (Fig 1). Average tumor volumes of the MSC and α-TEA groups, compared to the control group at sacrifice, were reduced 0.13 and 59.7%, respectively (Fig. 1). The low *t*-RES and the low combination groups reduced average tumor volumes 23.5 and 52.6%, respectively (Fig. 1). Average tumor volumes were enhanced 15.1 and 108.2% by the high combination, and high *t*-RES groups, respectively, and reduced 51.4% by α-TEA + MSC treatment (Fig 1). *Study 2*. This animal study, utilizing low and high dose *t*-RES, was conducted to determine if the unexpected finding that high-dose *t*-RES to enhance tumor burden was repeatable. Both doses of *t*-RES significantly reduced tumor volume in comparison to control (low-dose *t*-RES, $P< 0.0001$; and high-dose *t*-RES, $P < 0.0001$; Fig 2). Average tumor volumes at the low- and high-dose *t*-RES, in comparison to control, at sacrifice were reduced 25.6 and 42 %, respectively (Fig 2). No differences in mean body weight among any of the groups for study 1 and study 2 were observed (data not shown).

Treatment Effects on Visible Lung Metastases.

Study 1. At sacrifice, all lung lobes were examined for visible metastasis. The average number of visible lung tumors was significantly reduced by treatments with α-TEA ($P <0.0147$) and α-TEA + MSC ($P < 0.0185$) (Table 1). *Study 2*. The average number of visible lung tumors were significantly reduced by both low- and high-dose *t*-RES (low dose, $P < 0.0119$; high-dose, $P < 0.0013$), respectively Table 1). Percent inhibition of multiplicity was reduced 45 and 67 percent in low *t*-RES and high *t*-RES groups, respectively (Table 1).

Treatment Effects on Apoptosis, Cell Proliferation, and Blood Vessel Density.

TUNEL assay was used to detect apoptosis, Ki-67 assay to detect cell proliferation, and CD31 to detect an increase in blood vessel density as an indicator of angiogenesis in tumor tissue sections from control and treatment groups. α-TEA, α-TEA + MSC, α-TEA + MSC + low-dose *t*-RES, and α-TEA + MSC + high-dose *t*-RES significantly enhanced apoptosis in comparison to control ($P < 0.0286$ for all; Fig. 3A). The average number of Ki-67 positive nuclei was significantly reduced by treatments with α-TEA, low-dose *t*-RES, and high-dose *t*-RES ($P < 0.0286$ for all treatments). Combination treatments did not significantly reduce Ki-67 positive cells (Fig 3B). Blood vessel density was not significantly different among control and treatment groups (Fig 3C).

Treatment Effects on Lung and Lymph Node micrometastatic lesions.

Study 1. Total number of lung micrometastatic lesions were significantly reduced in all treatment groups with the exception of low-levels of *t*-RES [α-TEA, $P < 0.023$; MSC $P < 0.0052$, high *t*-RES $P < 0.0185$, α-TEA + MSC $P < 0.0011$, α-TEA + MSC + low-*t*-RES $P < 0.0355$, and α-TEA+ MSC + high *t*-RES $P < 0.0003$, respectively (Table 2)]. Likewise, the total number of axillary and brachial lymph node metastatic lesions were significantly reduced in all treatment groups with the exception of low-level *t*-RES treatment [α-TEA, $P < 0.0066$; MSC $P < 0.0023$, high *t*-RES $P < 0.003$, α-TEA + MSC $P < 0.0019$, α-TEA + MSC + low-*t*-RES $P < 0.0002$, and α-TEA+ MSC + high *t*-RES $P < 0.0002$, respectively (Table 2)]. *Study 2.* Lung micrometastatic lesions were significantly reduced by both low-and high-dose *t*-RES treatments in comparison to control. (low-*t*-RES, $P < 0.0094$; high-*t*-RES, $P < 0.0266$). Likewise, lymph node micrometastatic lesions were significantly reduced by both treatments (low and high *t*-RES, $P < 0.0001$).

DISCUSSION

The focus of our lab has been on the development of α-TEA as a stand alone as well as companion drug for treatment and prevention of cancers. Rationale for conducting preclinical animal studies using combinations of α-TEA, MSC, and *t*-RES came from encouraging data from cell culture studies showing that combinations of these three compounds induced apoptosis in human MDA-MB-435 breast cancer cells in a synergistic manner (Chapter 2). Two animal studies were conducted. In study #1, with the exception of high-dose *t*-RES and the combination containing high-dose *t*-RES, all treatments significantly reduced tumor burden. Surprisingly, high-dose *t*-RES significantly enhanced tumor growth in comparison to control and all treatment groups. Synergisms obtained with combination treatments in cell culture were not obtained in these animal studies, α-TEA was more effective than both combination treatments in reducing tumor burden. All treatments, except low-dose *t*-RES, were effective in reducing lung and lymph node metastases; however, there were no significant differences among single and combination treatment groups. Although MSC was the less effective than α-TEA or low-dose *t*-RES in reducing tumor burden, MSC was equally effective in reducing metastases. High-dose *t*-RES in a second animal study significantly reduced tumor burden rather than enhanced tumor growth.

The anticancer effects of individual treatments on tumor volume reported here are consistent with reports in the literature, with the exception of high-dose *t*-RES. α-TEA decreases tumor burden and metastases significantly from control in ovarian [44], breast [38, 40-43], and prostate cancer models (Jia*, Manuscript in Preparation*). *t*-RES reduces metastases [98], induces apoptosis [99] and reduces tumor burden *in vivo* [99]. Consistent with cell culture studies (Chapter 2), *in vitro* data show *t*-RES to inhibit cell proliferation [48-50, 52-53]. In study #2, high and low dose *t*-RES reduced tumor burden

in a manner consistent with the literature. MSC has been shown to be an effective suppressor of chemically induced mammary carcinogenesis in rats [61, 63-68].

The ability of high-dose *t*-RES to enhance tumor growth, with one exception, is not consistent with the literature. Sato *et al* reported a similar differential response to *t*-RES in prepubescent rats [100]. In their study, rats were given control, 10mg/kg bw or 100 mg/kg bw *t*-RES for 5 consecutive days prior to an injection of 50mg/kg MNU. Control and treated mice were evaluated for tumor incidence and tumor volume for 33 weeks. Prior treatment with high-dose *t*-RES, in comparison to low-dose *t*-RES and control, significantly increased the incidence of mammary carcinomas greater than 1 cm in diameter [100]. The ability of high-dose *t*-RES to increase tumor growth reported in this paper, and the literature showing that pretreatment with high-dose *t*-RES prior to carcinogen treatment accelerates mammary cancer occurrence are not understood but have important implications that require further study.

Inhibition of metastases is perhaps just as important as the effect an agent has on primary tumors since the majority of cancer deaths result from metastases [87]. The mechanisms whereby high-dose *t*-RES increases tumor growth, but reduces lung and lymph node metastases are also not understood. Likewise, it is not understood how MSC was more effective in inhibiting metastasis than tumor burden. Perhaps *t*-RES and MSC are more effective in inhibiting smaller tumors or are inhibiting tumor cell migration. Mechanistically, α-TEA alone and in combination with MSC or the three agents kill tumor cells by induction of apoptosis.

Growth rates of tumors in control mice in study #2 were much slower than control tumors in study #1, even though the tumor sizes in the two studies were equal at the start of treatments. Also, tumor sizes in studies #1 and 2 were smaller when compared to published data from our lab using the same MDA-MB-435-F-L cell line, mice from the

same source and age and housed in the same environment [43]. Control tumors in experiment 1 were 52% smaller (101 mm^3) and those in experiment 2 were 60% smaller (84 mm^3) after 31 days compared to those seen by Zhang *et al* (212 mm^3) [43]. The only discernable difference between these studies was the diets. Animals treated by Zhang *et al* were fed gamma-irradiated AIN-76A diet, those in experiment 1 an autoclavable Teklad 2018 diet, and those in experiment 2 were fed Teklad 7012 diet. The general content of the three diets is very similar. All three have similar percentages of protein (19, 19, and 20% for 7012, 2018, and AIN-76A, respectively) and fat (5, 4, and 5%, respectively). The largest difference between these diets is the concentration of isoflavones, a class of phytoestrogens called isoflavonoids [101]. The 7012 diet has nearly twice as many isoflavones as the 2018 diet (400 ppm v 207 ppm), and both have more than the AIN-76A diet, which has undetectable levels of isoflavones because the protein source is casein [101-102]. Previous studies have shown that diets containing isoflavones can reduce mammary tumors in animal models [101-104], in some cases by as much as 40% [101-103]. This is consistent with the trend in our data showing smaller tumors with higher levels of isoflavones in the diet. Many reports accredit the reduction in tumor volume to genistein and daidzein [87, 103], the main isoflavones in soy [102]. Genistein has been shown to significantly reduce the latency, incidence, and tumor number in DMBA treated rats [102] and to inhibit the proliferation of human tumor cell lines *in vitro* [102]. There are also reports that genistein's effect on mammary cancers is diet dependent [105]. In one study, animals fed the AIN-76A diet showed no protection from MNU-induced breast cancer, but those fed Teklad 4% diet (containing genistein) had 44-61% fewer lesions [105]. The levels of genistein and daidzein in rodent chow are in the same range for that found in human soy products like tofu and soy flour. Species differences in uptake, distribution, and elimination could affect the potency, but

correlation from human epidemiology studies find that phytoestrogens, specifically from soy, can decrease human cancer risk [106], suggesting a similar relationship between tumor volume and phytoestrogen intake in rodents and humans. The difference in isoflavone content might also account for the difference in *t*-RES tumor response. These isoflavones could act as antagonists to *t*-RES, preventing the uptake and decreasing the bioavailability of *t*-RES or yield effects of their own that affect tumor growth in addition to those arising from *t*-RES administration.

Another difference between studies 1 and 2 was that the 7012E diet in experiment 2 was autoclaved, but not the 2018 diet in study #1. Despite containing extra vitamins to account for nutrient loss during autoclaving, it has been shown that irradiated diets maintain higher levels of intact nutritional components when compared to autoclaved diets [107]. Susceptible targets of autoclave breakdown are essential fatty acids (EFAs), which are known to drive tumor growth [108-111]. If these were destroyed during autoclaving, then their absence could be responsible for the slower tumor growth rates in control and treatment mice in study #2. Irradiated diets do not increase temperature significantly (5˚c at 2.4 Mrad) nor do they significantly alter proteins, amino acids, or PUFAs [107], which may make them a more ideal choice for future animal studies.

Upon analysis of the diets pre-autoclave using information provided by the manufacturer, both diets contained similar levels of EFA (7012 diet had 33.8 and 3.5 g/kg linoleic and linolenic acids, while the 2018 had 31.4 and 2.8 g/kg linoleic and linolenic acids [107]). If EFA were destroyed in autoclaving, then perhaps there were more EFA in the 2018 diet. Several studies have shown that linoleic acid can drive MDA-MB-435 tumor growth, incidence and multiplicity [108, 110-111], metastases [108, 110-111] and tumor cell invasion *in vitro* in MDA-MB-435 and MDA-MB-231 cell lines [109]. In all

of these studies, irradiated diets were used to minimize the risk or nutrient deterioration [108-111].

If differences in the results of *in vivo* studies can be diet-dependent, it is important to note that the nutritional value of any diet can change over time. Nutritional values and sources for components will vary by plant source, species differences, geographical location grown, season grown, time of harvest, and method used to process the ingredients [101, 106, 112]. Differences in isoflavone content alone can vary greatly between varieties of soybeans (116-309 mg/g between species) and 46-195 mg/g within the same variety grown in different locations [101, 113]. Because these studies were performed far apart in time, actual diet samples were not taken and analyzed at the time of the study that could have allowed insight into the actual nutritional content of our diets.

Further work into the mechanism of action for α-TEA alone and in combination with MSA and *t*-RES are needed. Perhaps the knowledge gained from these studies can help to explain the apparent differences that we have seen *in vitro* and *in vivo*. Future work will also investigate the effects of α-TEA in combination with *t*-RES, without MSC. Another reason to look into the α-TEA and *t*-RES combination is that both compounds appear to be effective chemopreventive agents so one could hope that their combination would prove more beneficial than either of the two alone.

ACKNOWLEDGEMENTS

We would like to thank the Histology Core Facility for preparation of H&E and immunohistochemically stained tissues and Dr. Howard Thames for his help with statistical analyses (NIEHS Center Grant ES 07784; University of Texas, M.D. Anderson). We thank Dr. John Richburg for the use of his microscope to evaluate metastatic lesions and Dr. Vernon Knight's laboratory at Baylor College of Medicine,

Houston, TX, for the method of aerosol preparation, particle size determination and output studies.

Table 3.1: α-TEA, MSC, and *t*-RES treatments alone or together reduce visible lung metastases

	Study 1		Study 2	
Treatments[a]	# Animals/ group with macroscopic lung metastases[b]	Average # macroscopic lung tumor foci[c]	# Animals/ group with macroscopic lung metastases[b]	Average # macroscopic lung tumor foci[c]
Control	8/10	4.4 ± 1.0	12/12	5.8 ± 0.9
α-TEA	5/10	1.0 ± 0.4[*]		
MSC	6/10	1.3 ± 0.4[*]		
t-RES (low)	10/10	5.8 ± 0.8	12/12	3.2 ± 0.5[*]
t-RES (high)	8/10	2.6 ± 0.8	8/12	1.9 ± 0.6[*]
α-TEA + MSC	6/10	1.1 ± 0.4[*]		
α-TEA + MSC + *t*-RES (low)	6/10	2.6 ± 0.8		
α-TEA + MSC + *t*-RES (high)	6/10	1.9 ± 0.8		

[*] Designates significant difference from control. Study #1:Average # macroscopic lung tumor foci (α-TEA $P < 0.0147$; MSC, $P < 0.023$; α-TEA + MSC, $P < 0.0185$. Study #2: Average # macroscopic lung tumor foci *t*-RES low, $P < 0.0119$; *t*-RES high, $P < 0.0013$).

[a] α-TEA was formulated into liposomes and delivered daily (7 days/week) by aerosol, MSC and *t*-RES were fed daily (7 days/week) by gavage

[b] Macroscopic lesions in all lung lobes in control and treatment groups were counted visually at the time of sacrifice

[c] Data are expressed as the average number of macroscopic lung tumor foci observed in tumor bearing mice in control and treatment groups.

Table 3.2: Comparison of Microscopic Metastatic Lesions After Treatment with α-TEA, MSA, and *t*-RES Separately and Together

		Size Classification					
		<20 μM	20-50 μM	50–100 μM	>100 μM	Total	*(p value)*
Lung Microscopic Metastases	Control	**56**	**41**	**12**	**4**	**113**	
	α -TEA	**40***	**22***	**12**	**3**	**78***	***(0.0232)***
	MSC	**40**	**24***	**8***	**3**	**75***	***(0.0052)***
	Low *t*-RES	**32***	**28**	**11**	**4**	**76**	
	High *t*-RES	**42**	**24***	**5***	**2**	**73***	***(0.0185)***
	α -TEA + MSC	**32***	**21***	**7**	**2**	**62***	***(0.0011)***
	Low Combination	**42**	**26***	**10**	**4**	**82***	***(0.0355)***
	High Combination	**29***	**20***	**7***	**1***	**58***	***(0.0003)***
Axillary and Brachial Microscopic Lymph Node Metastases	Control	**9**	**7**	**0**	**0**	**16**	
	α -TEA	**5***	**4***	**0***	**0**	**9***	***(0.0066)***
	MSC	**5***	**3***	**0**	**0**	**8***	***(0.0023)***
	Low *t*-RES	**7**	**5**	**0**	**0**	**13**	
	High *t*-RES	**3***	**3***	**0**	**0**	**7***	***(0.0003)***
	α -TEA + MSC	**5***	**3***	**0**	**0**	**8***	***(0.0019)***
	Low Combination	**4***	**4***	**0**	**0**	**8***	***(0.0002)***
	High Combination	**4***	**3***	**0**	**0**	**7***	***(0.0002)***

Lungs and lymph nodes removed at sacrifice were evaluated under fluorescent microscopy for microscopic metastases. Metastases were grouped into four size classifications. Values were rounded to the nearest integer. * indicates significance ($p < 0.05$)

Table 3.3. Comparison of Microscopic Metastatic Lesions After Treatment with *t*-RES

		Size Classification					
		<20 µM	20-50 µM	50–100 µM	>100 µM	Total	*(p value)*
Lung Microscopic Metastases	Control	**101**	**40**	**6**	**3**	**151**	
	Low *t*-RES	**53**	**20***	**5**	**2**	**80***	***(0.0094)***
	High *t*-RES	**48***	**22**	**7**	**2**	**78***	***(0.0226)***
Axillary and Brachial Microscopic Lymph Node Metastases	Control	**24**	**13**	**5**	**1**	**43**	
	Low *t*-RES	**8***	**4***	**1***	**0***	**12***	***(0.0001)***
	High *t*-RES	**8***	**3***	**1***	**0**	**11***	***(0.0001)***

Lungs and lymph nodes removed at sacrifice were evaluated under fluorescent microscopy for microscopic metastases. Metastases were grouped into four size classifications. Values were rounded to the nearest integer. * indicates significance ($p < 0.05$)

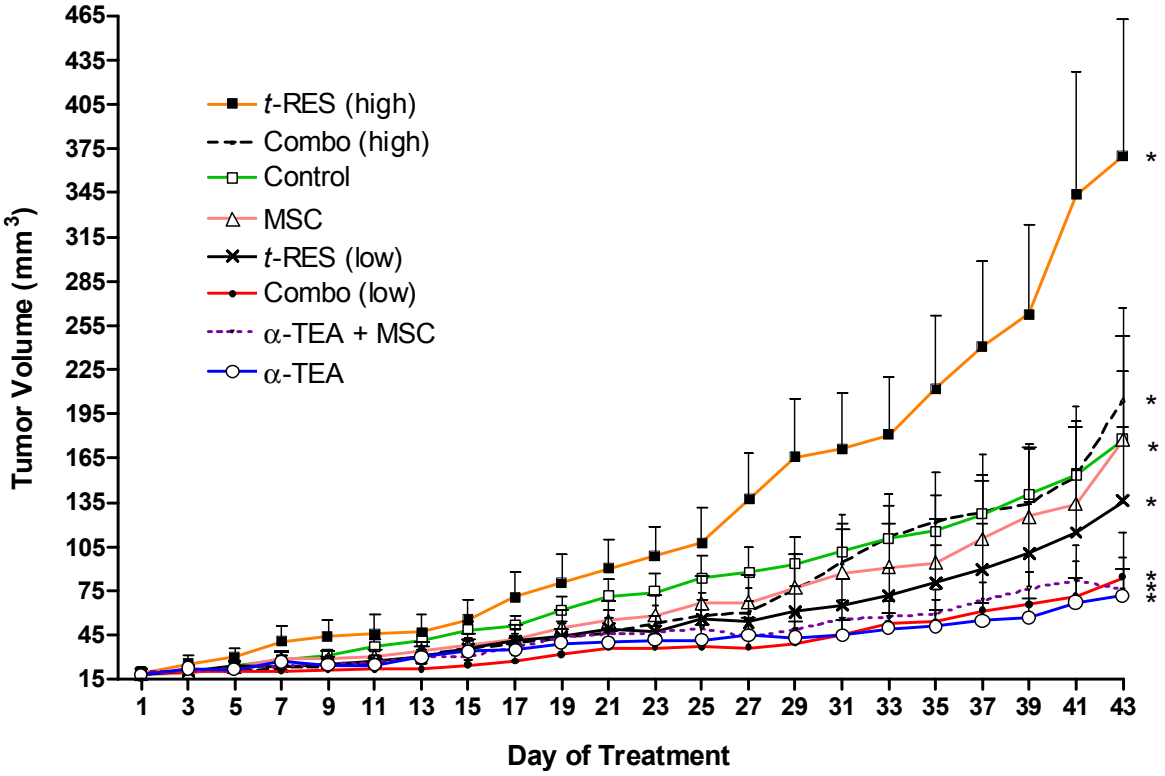

Figure 3.1. Study 1: MDA-MB-435-F-L Tumor Volume. Athymic nu/nu mice were injected with 1 x 10^6 MDA-MB-435 GFP FL cells. Following establishment of tumors, treatments were given daily for 43 days. □ = control, △ = MSC, ○= α-TEA, ✕ = low *t*-RES, ● = low combination, ■ = high *t*-RES, ◆ = high combination, ▽ = α-TEA + MSC. Statistical analyses compared treatment groups to the control group in SPSS. Volumes reflect mean tumor volume +/- S.E. * $p < 0.05$ was considered significant.

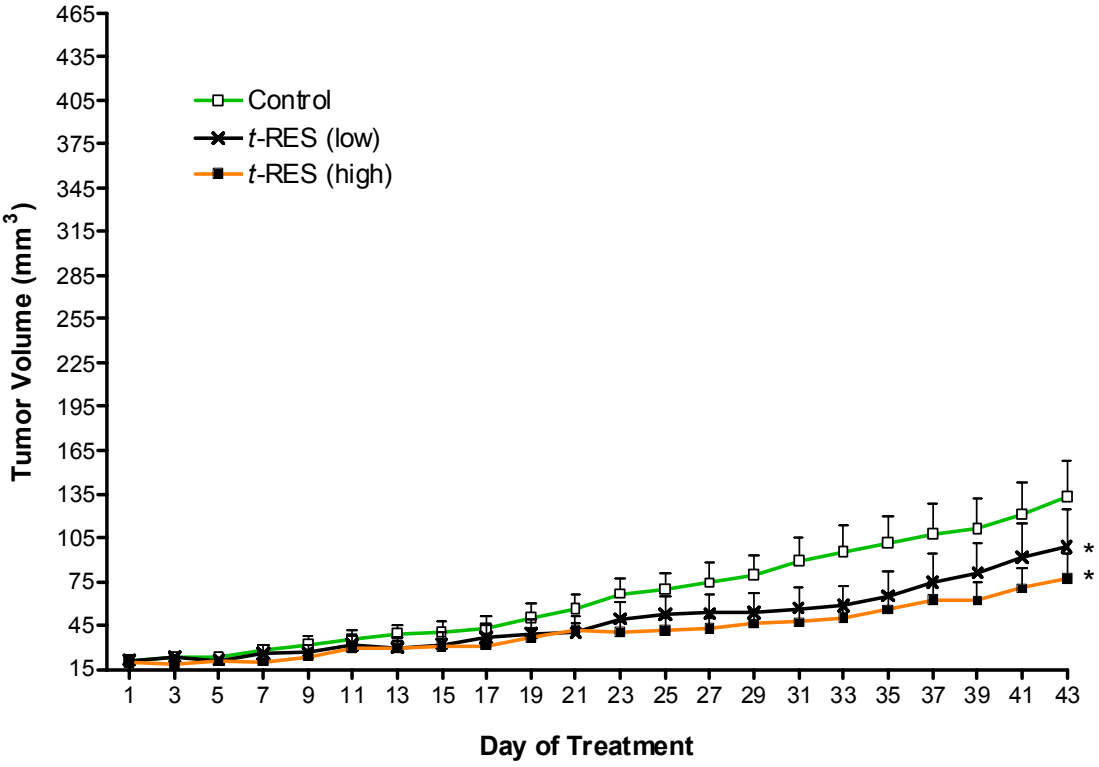

Figure 3.2. Study 2: MDA-MB-435-F-L Tumor Volume. Athymic nu/nu mice were injected with 1 x 10^6 MDA-MB-435 GFP FL cells. Following establishment of tumors, treatments were given daily for 43 days. □ = control, ✕ = low *t*-RES, ■ = high *t*-RES. Statistical analyses compared treatment groups to the control group in SPSS. Volumes reflect mean tumor volume +/- S.E. * $p < 0.05$ was considered significant.

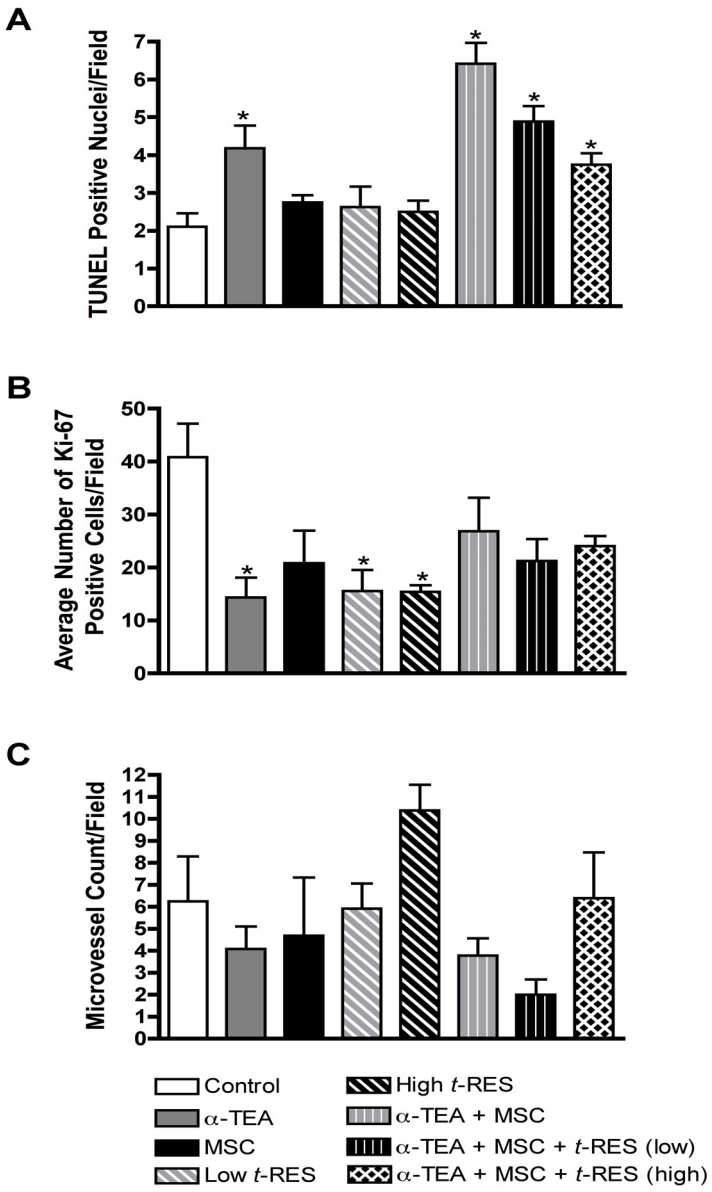

Figure 3.3 Study 1: Effects of α-TEA, MSA, *t*-RES on MDA-MB-435-F-L tumors. Immunohistochemistry for increased apoptosis, reduced cell proliferation and reduced blood vessel density was performed on 5 μm sections of tumors taken from animals in all groups (n = 4). *A and B,* The number of positive nuclei were scored in 16 separate microscopic fields (x400) of each slide/tumor. The data are depicted as mean +/- S.E. of number of TUNEL and Ki-67 positive nuclei per field. *C.* The number of CD31 positive staining blood vessels was scored for each slide/tumor using the 'hotspot' method for 10 separate microscopic fields. * designates a significant increase in positive cells compared to control ($p < 0.05$).

Chapter 4: α-TEA, methylselininic acid, and *trans*-resveratrol: potential chemopreventive agents when given in combination

ABSTRACT

Epidemiological studies suggest that diet can account for as much as 30% of cancers. Since diet is a relatively easy risk to reduce in humans and because tumors take years to develop, there are many opportunities for intervention in this process. Here we evaluate the effectiveness of several natural compounds, α-TEA, MSA and *t*-RES, to inhibit the formation of DMBA-induced lesions in the MMOC model and to prevent MNU-induced lesions in a rat mammary carcinogenesis model. In the MMOC model, α-TEA, MSA and *t*-RES were each effective at inhibiting the incidence and multiplicity of alveolar lesions and the multiplicity of ductal lesions. Four combinations of co-treatments were also made and analyzed for increased efficacy over individual treatments. A combination of α-TEA + *t*-RES was most effective against alveolar and ductal lesions. Based on these results, α-TEA + *t*-RES were combined in the MNU-induced rat mammary carcinogenesis model. Treatments lasted for 39 days at which time there were 45, 55 and 65% fewer tumors in the α-TEA, *t*-RES and Co-tx groups compared to the control. Even though a statistical difference was not seen between Co-tx, α-TEA and *t*-RES, the co-treatment group had 36% fewer tumors than α-TEA and 22% fewer than *t*-RES. Weight loss was also looked at in this study as a measure of toxicity. Neither α-TEA nor *t*-RES caused significant weight loss, nor did α-TEA cause significant loss in tissue weight for spleen, heart, ovaries/uterus, lungs or kidneys. Together, these results suggest that α-TEA and *t*-RES may be an effective chemopreventive regimen.

INTRODUCTION

Cancer is a major public health problem in the U.S. and in developed countries. Currently, one in four deaths in the U.S. are due to cancer [1]. The precise number of cancer cases diagnosed each year in the U.S. is unknown since complete cancer registration has not been achieved [1]. However, based on data available, estimates are that 1.4 million new cases of invasive cancer will occur this year, of which over 214,000 will be new cases of breast cancer [1]. Prevention of new cases of cancer is a major challenge, and the failure to reduce the trend in cancer incidence from year to year point to the urgent need for new agents with low toxicity that can be used by high risk individuals for several years to a life time.

Chemoprevention can be defined as an intervention in the tumorigenic process by a natural or synthetic compound. Specifically, it is an agent that can block the early stages of initiation, pre-malignant development, and/or arrest malignant cell progression [38]. Transgenic murine models and chemically induced cancers in mice and rats serve as useful models for studying potential chemoprevention agents. Most chemically induced mammary chemoprevention animal models use either DMBA or MNU to induce lesions *in vivo* or in mouse mammary organ culture (MMOC).

The MMOC model is an *ex vivo* chemoprevention model that can be used to screen potential preventive agents on the very early stages of chemically induced lesion formation [114]. Studies have shown that there is a high correlation between agents that show chemopreventive activity in this model with those that show activity in the two-stage skin carcinogenesis and the chemically induced rodent mammary carcinogenesis model [114]. MMOC can be adapted to target lesions to be either alveolar or ductal in origin and both methods consist of three main phases: pre-treatment, growth, and regression [80-82, 114].

A short-term rat carcinogenesis model has been developed by Thompson *et al* [79, 83, 86] that allows for rapid induction of premalignant and malignant stages of mammary carcinogenesis using 50 mg/kg bw MNU [79, 83]. The main difference between this model and the conventional rat model is the age at which the rats are injected (21 d versus 50 d), which allows for the experiment to be completed in 35 d compared to 6 months in the conventional model [79, 83]. In this short-term model, greater than 90% of animals injected with MNU have a spectrum of premalignant and malignant lesions greater than 1 mm^2 in their abdominal-inguinal mammary glands 35 d post-carcinogen [79].

Histological classification of the rat whole mount lesions is based on classification criteria published by Russo *et al* [115]. Lesions are classified as intraductal proliferation (IDP), ductal carcinoma *in situ* (DCIS), adenocarcinoma (AC), or "within normal limits." In rats, IDPs are equivalent to ductal hyperplasias in human breast carcinogenesis. The criteria for diagnosing hyperplasia is primarily based on an increase in the epithelial cells lining the acini and ducts, which can be further categorized as mild, moderate, or florid. Mild hyperplasias are generally three to four cells thick while moderate lesions have four or more cells with an occasional bridge across the lumen. Florid hyperplasias have ducts, which are packed with cells and lumen that are identifiable but displaced. The individual cells that make up IDPs are not distinguishable and the nuclei are generally round to oval, haphazardly arranged, and lack nucleoli [86].

To meet the criteria of a DCIS at least one expanded ductal structure must be completely replaced by neoplastic cells that have uniform, monotonous, round, hyperchromatic and non-overlapping nuclei, and retain an intact ductal basement membrane. The two main DCIS subtypes are cribiform and comedo carcinoma *in situ*. In the cribiform subtype there is at least one expanded ductal lumen that has been

completely replaced by a monotonous population of cells with round, hyperchromatic, and non-overlapping nuclei with no remnants of the primary lumen. Comedo subtypes are centrally necrotic and have a high-grade anaplastic nuclei and nucleoli. Lesions that have only a single duct replaced are labeled atypical ductal hyperplasia (ADH) []. ACs are defined as the earliest breach of the ductal basement membrane and tend to invade as a broad front of several cells with clusters of neoplastic acini. Like DCIS, there are two main subtypes observed in the rat model, cribiform and comedo [86].

trans-Resveratrol (3,5,4'-trihydroxy-*trans*-stilbene; *t*-RES) is a naturally occurring antioxidant that can be found in a variety of foods such as grapes, wine, berries, and peanuts [46-53]. This phytoalexin is considered a promising chemopreventive agent based on its ability to inhibit the development of DMBA induced hyperplastic and atypical preneoplastic lesions in the mouse mammary organ culture model [47-48, 53], MNU induced mammary lesions in rats, and tumorigenesis in a two-stage mouse skin cancer model [47, 49, 51, 53].

Selenium is an essential nutrient for humans that can be found in cereal grains, meats, and seafood and is required for more than 13 human enzymes and proteins, in the form of L-selenocysteine [61]. Dietary supplementation of selenium beyond the recommended dietary allowance of 55 μg/day for females and males 14 years of age or greater at up to 200 μg/day has been shown to reduce the incidence of lung, colorectal, and prostate cancer in humans [61, 63, 65, 67-68]. Methylseleninic acid (MSA), a form of selenium that easily undergoes reduction to methylselenol by cells [61, 63, 65, 67-68], has been shown to be an effective suppressor of chemically induced mammary carcinogenesis in rats [62, 64-68, 71].

α-TEA has been shown to be an effective chemotherapeutic agent, inhibiting human ovarian, cervical, breast, endometrial, prostate, lung, colon and lymphoid cells to

undergo apoptosis [38-40], and reducing tumor burden and metastases in breast, ovarian, and prostate cancer [39-44]. Furthermore, α-TEA does not induce apoptosis in normal human mammary epithelial cells or normal PrEC human prostate epithelial cells nor show overt toxicity in animal studies [38-40, 42], suggesting potential as a chemopreventive agent. α-TEA has not been studied extensively as a preventative agent, but has been shown to prevent papilloma development in a UV-B mouse skin model (Best, *Manuscript in Preparation*).

In the studies reported here, DMBA was used to induce lesions in the mouse mammary organ culture (MMOC) model and MNU was used to induce lesions in the rat carcinogenesis model. In the MMOC model, α-TEA, *t*-RES and MSA, separately and in combination, were screened for ability to prevent DMBA-induced alveolar and ductal lesions. In the NMU Sprague Dawley rat model, α-TEA and *t*-RES, separately and together, were evaluated for ability to prevent NMU-induced mammary lesions.

MATERIALS AND METHODS

Chemicals and Reagents

α-TEA was prepared and characterized as previously described [40]. *trans*-Resveratrol (*t*-RES) was purchased from Cayman Chemical Co. (Ann Arbor, MI). Neobee oil was purchased from Stepan (Anaheim, CA). HPLC grade methanol, hexane, 10 % neutral buffered formalin, 10% A/OT solution, xylene and ethanol were purchased from Fischer Scientific (Pittsburgh, PA). Sodium dodecyl sulfate (SDS), RRR-δ-tocopherol, estradiol-17β, progesterone, insulin, prolactin, aldosterone, hydrocortisone, DMBA, gum arabic, aluminum potassium sulfate, carmine, methyl salicylate, Scott's water, and saline were purchased from Sigma (St. Louis, MO). Waymouth's MB 152/1

medium, and streptomycin and penicillin antibiotics were purchased from Gibco (Grand Island, NY).

Mouse Mammary Organ Culture (MMOC) Model

DMBA-induced mammary gland lesions were induced and analyzed according to procedures previously published [80-82]. Female balb/c mice were purchased from Charles River (Wilmington, MA) at 3-4 weeks of age and separated into groups of 10. Stock solutions of 1 μg/ml estradiol-17β, 1 mg/ml progesterone, 1 mg/ml aldosterone and 1 mg/ml hydrocortisone were prepared in 100% ethanol. Insulin was dissolved at 1 mg/ml in 0.3 ml 0.001 N HCl and 0.7 ml saline and sterile filtered. Prolactin was dissolved at 1 mg/ml in 0.25 ml 0.001N HCl and 0.75 ml medium and then sterile filtered. DMBA was dissolved at 2 mg/ml in DMSO and used at 2 μg/ml final concentration (5 μl into 5 ml medium). Media for the glands was prepared using Waymouth's media supplemented with 290 μg glutamine/ml media, and (0.5 ml insulin, 0.5 ml prolactin, 0.1 ml estradiol-17β, 0.1 ml progesterone, and streptomycin (100 μg/ml) and penicillin (100 U/ml) per 100 ml media. Mammary alveolar lesions and ductal lesions were induced as described below. To use this model for chemoprevention studies, potential agents are added to the media during the growth phase. Following a dose-response experiment, the following concentrations were chosen for combination studies: α-TEA at 1 μg/ml, MSA at 1 μg/ml, and *t*-RES at 2.5 μg/ml. In order to test α-TEA, MSA, and *t*-RES for their effectiveness at preventing these types of lesions, mammary glands were divided evenly into one of eight treatment groups: α-TEA, MSA, *t*-RES, α-TEA + MSA, α-TEA + *t*-RES, MSA + *t*-RES, α-TEA + MSA + *t*-RES, and DMBA control.

Hormone Pretreatment

A working solution of 10 μg estradiol-17β and 10 mg progesterone per ml of suspension was prepared as previously described [81-82]. Estradiol was prepared at 5 mg/ml in ethanol. Progesterone was prepared by adding 1 g progesterone to 10 mg gum arabic into 10 ml physiological saline. To this suspension, 90 ml saline and 0.2 ml estradiol-17β (5 mg/ml stock) were added to make the working solution above. Mice were injected daily with 0.1 ml of the suspension in order to yield a final concentration of 1 μg estradiol and 1 mg progesterone per mouse per day for 9 days.

Mammary Gland Preparation

Stencil silk (Nazdar, Elk Grove Village, IL) was cut into 7 mm squares, put into group labeled tissue culture dishes (Fischer Scientific) and autoclaved. Dishes were then filled with 5 ml prepared Waymouth's media containing the appropriate hormones for the protocol (see below). Mice were sacrificed by CO_2 asphyxiation and disinfected with 70% ethanol. Following incision, the thoracic mammary glands were removed and placed onto the floating silk rafts (five glands/dish). Dishes were placed on a tray and placed into a controlled atmosphere chamber for 10 min at 10 psi, 95% O_2 and 5% CO_2. Following removal, dishes were transferred to an incubator kept at 37˚C. Media was changed as required by the protocol 3 times per week and the chamber gassed after each change.

Alveolar Lesion Induction (MAL)

Mammary alveolar lesions (MAL) were induced according to previously published procedures [81-82]. Glands were incubated for 10 days in Waymouth's media containing 5 μg/ml insulin, 5 μg/ml prolactin, 1 μg/ml aldosterone, and 1 μg/ml hydrocortisone (growth phase). On day 3, DMBA (2 μg/ml) was added to the culture

dishes. After 24 h, medium was replaced with fresh growth media and incubated for 6 more days (changing media as needed). After the 10 d growth phase, growth media was replaced with fresh media containing only insulin (5 μg/ml) and incubated for an additional 14 d, changing media 3 times/week (regression phase). Glands were then fixed in 10% buffered formalin for whole mount preparation.

Ductal Lesion Induction

Mammary ductal lesions were induced according to previously published procedures [81-82] and identical to the procedures for MAL induction with one exception. Glands were incubated for 10 days in Waymouth's media containing 0.001 μg/ml estradiol-17β and 1 μg/ml progesterone in place of aldosterone and hydrocortisone during the growth phase.

MMOC whole mounts

Whole mounts were prepared as described previously [81]. A working solution of alum carmine stain was prepared by suspending 1 g alum carmine and 2.5 g potassium sulfate into 500 ml water, then it was boiled for 20 min, and filtered. Formalin fixed glands were washed in water for 5 min and then stained with alum carmine overnight. Glands were then washed in a series of increasing ethanol concentrations (50, 70, 95 and 100%) for 15 min. Glands were transferred to xylene for 72 h and then analyzed for lesions.

Rat Chemoprevention Model

Female Sprague-Dawley rats were purchased from Harlan (Madison, WI) at 21 days of age. Following injection (see below), rats were assigned to one of four treatment groups (30 rats/group): α-TEA, *t*-RES, α-TEA + *t*-RES, and a vehicle control. Rats were treated daily for 39 days beginning on the day of MNU injection and weighed weekly.

Animals were housed at the Animal Resource Center at the University of Texas at Austin at 74 +/- 2˚F with 30-70% humidity and a 12-h alternating light-dark cycle. Rats were housed 3/cage and given water and AIN-76A (Dyets Inc., Bethlehem, PA) purified diet *ad libitum*. Guidelines for the humane treatment of animals were followed as approved by the University of Texas Institutional Animal Care and Use Committee.

MNU Preparation and Injection

MNU was purchased from the Midwest Research Institute Chemical Carcinogen Reference Standard Repository (Kansas City, MO) and prepared according to the procedures published by Thompson *et al* [84]. Safety procedures and training for safe use of NMU and disposal of animal waste were provided by the U.T. Environmental Health and Safety Office, and were followed throughout the study. MNU was added into pre-weighed glass injection vials (Wheaton Inc, Wheaton, IL), sealed and re-weighed to determine weight of MNU inside of vials, and returned to ice. After weighing, vials were kept over a desiccant at -80˚C, and wrapped in aluminum foil until use to prevent decomposition from light and moisture sensitivity. Vials were carried to the animal room on ice and MNU was dissolved in acidified 0.9% NaCl solution (pH 4.0 using acetic acid) immediately prior to use and used within 20 minutes. Saline was added to bring a final working solution of 1.4% w/v MNU. To completely dissolve MNU, vials were heated under tap water and shaken vigorously one at a time as needed. Rats were weighed and injected intraperitoneally (ip) along the ventral midline, halfway between the third and fourth pairs of nipples with 50 mg/kg body weight MNU using 26-guage 3/8-inch-long needles.

Preparation of *t*-RES for Delivery by Gavage

Based on the literature, it was determined that each rat would receive 10 mg/kg bw *t*-RES [53]. Treatments of *t*-RES were made weekly and amounts of *t*-RES were adjusted based on the weight of the animals. The stock solution was based on the average weight of rats receiving the *t*-RES and *t*-RES control treatments. *t*-RES was dissolved in 100% EtOH and then mixed with Neobee oil to give a final solution of 6.5% EtOH and 93.5% Neobee oil. Control treatments consisted of 6.5% EtOH and 93.5% Neobee oil, as contained in the *t*-RES treatments [53]. Solutions were aliquoted into sterile eppendorf tubes and stored at –20°C until needed. Prior to delivery, aliquots were brought to room temperature.

Preparation of α-TEA Liposomes for Delivery by Aerosol

Preparations of α-TEA liposomes were made as previously described [40-44]. An α-TEA/liposome ratio of 1:3 (w/w) was determined empirically to be optimal by methods previously described [96]. To prepare the α -TEA/lipid combination, the components were first brought to room temperature. The lipid [1,2-dilauroyl-sn-glycero-3-phosphocholine (DLPC); Avanti Polar-Lipids, Inc., Alabaster, AL] at a concentration of 120 mg/ml was dissolved in tertiary butanol (*t*-butanol) from Fisher Scientific (Houston, TX) then sonicated to obtain a clear solution. α -TEA at 40 mg/ml was also dissolved in tertiary-butanol and vortexed until all solids were dissolved. The two solutions were then combined in equal amounts (v:v) to achieve the desired ratio of 1:3 α -TEA/liposome, mixed by vortexing, frozen at -80° C for 1-2 h, and lyophilized overnight to a dry powder prior to storing at -20°C until needed.

Aerosol Delivery

Aerosol was administered to rats as previously described [40-44]. Briefly, an air compressor (Easy Air 15 Air Compressor; Precision Medical, Northapton, PA) producing a 10 L/min airflow was used with an Aero Tech II nebulizer (CIS-US, Inc. Bedford, MA) to generate aerosol. The particle size of α-TEA liposome aerosol discharged from the AeroTech II nebulizer was determined by the Anderson Cascade Impactor to be 2.01 μm mass median aerodynamic diameter (NMAD), with a geometric standard deviation of 2.04. About 30% of such particles when inhaled will deposit in the respiratory tract of the rat and the remaining 70% will be exhaled [96]. Prior to nebulization, the α-TEA/lipid powder (75 mg/vial) was brought up to room temperature then reconstituted by adding 3.75 ml sterile filtered milli-Q water to achieve the final desired concentration of 20 mg/ml α-TEA. The mixture was allowed to swell at room temperature for 30 min with periodic inversion and vortexing, and then transferred to the reservoir of a nebulizer. Rats were placed in clear plastic cages (6.5 x 26.1 x 15.6 in) with a sealed top in a safety hood. Aerosol entered the cage via a 1 cm (i.d.) accordion tube at one end and discharged at the opposite end, using a one-way pressure release valve. Animals were exposed to aerosol until all α-TEA/liposome was aerosolized (approximately 20 min).

Aerosol Characteristics of α-TEA Incorporated into Liposomes

HPLC analyses were conducted on α-TEA liposomes recovered from aerosol in the All Glass Impinger (Ace Glass Co., Vineland, NJ). The delivered dosage = concentration (μg/L) x rat minute volume (1-min/kg) x duration of delivery (min) x estimated deposited fraction (30%; [96]). Based on this formula, we estimate that 1327 μg/kg bw of α-TEA was deposited in the respiratory tract of each rat each day. Thus, for the 39 day treatment period, we estimate that each rat received 5.02 mg α-TEA. For this same period, animals treated with *t*-RES were given 37.8 mg *t*-RES.

Rat Mammary Gland Whole Mounts

Mammary glands were removed and processed as previously described [83, 85-86]. At necropsy, 40 rats were killed by $C0_2$ inhalation each day (10 from each group) at 41, 42, and 43 days post-carcinogen. Rats were skinned and the skin was examined under translucent light. Both the cervical-thoracic and abdominal-inguinal mammary glands were evaluated for visual lesions and then the abdominal-inguinal mammary glands were carefully excised and spread onto clean 50 x 70 mm pre-labeled microscope slides. These whole mounts were processed and photographed as previously described [83, 86]. The whole mounts were fixed in 10% neutral buffered formalin for 12-18 h and then rinsed in distilled water for 15 min. Whole mounts were then dehydrated with a series of ethanol washes, 1 h each (70, 95 and 100%), and then cleared in two changes of toluene for 1 h each. The process was then reversed to rehydrate the glands to water followed by immersion in alum carmine stain for 5-7 d. Once staining was complete, the whole mounts were dehydrated using ethanol as described above and cleared once in xylene for 2 h. One at a time whole mounts were removed and placed in 4 x 6 in 4.5 ml clear heat seal pouches filled with 20 ml methyl salicylate and sealed. The following day air bubbles were removed and then the mounts were photographed at a uniform magnification (2X). Photographs were kept as a permanent record of the mammary glands to identify the location and gross morphology of the lesions. Lesions were identified on the photograph using a scanned image of the photograph overlaid with a sheet of transparent 18 X 24 cm graph paper (each square is 2 X 2 mm to the cm) where a 2 mm^2 lesion on the photograph is analogous to a 1 mm^2 lesion (lower size limit for histological analyses) and removed. Dissected lesions were individually placed into tissue processing cassettes and processed through three changes of toluene to remove residual methyl salicylate and two changes of molten paraffin. The embedded lesions

were then rough cut to expose the surface of the lesion and then overlaid with a surfactant, 10% A/OT solution for 30 min to soften the tissue and reduce 'Venetian blind' effect during microtomy. Four-micron sections were cut and placed onto glass microscope slides pre-coated with homogenized rat tail collagen. Sections were heat immobilized in an 80˚C oven for 2 h and allowed to cool. Sections were then stained using a standard H&E protocol with the following exceptions: sections were destained using a 0.1% Li_2CO_3 solution prior to staining with modified Harris hematoxylin and then blued with Scotts water in lieu of 0.25% ammonia water in order to prevent detachment of the tissue sections. All removed lesions were histologically classified according to published criteria for the rat [115].

Lipid Extraction from Serum Samples

Lipid extraction was performed using previously published procedures [39-116] with slight modifications on serum removed from rats treated with α-TEA or untreated to measure the concentration of α-TEA in serum. Fifty µl of internal standard, RRR-δ-tocopherol (10 mg/ml in ethanol) were added to each sample in disposable 5-ml centrifuge tubes (Sarstedt Inc, Newton, NC). Serum was resuspended in 0.1 M SDS as described previously [39, 116-117] and two ml of ethanol were added to each vial and mixed by vortexing. Lipids were extracted using 1 ml of hexane, followed by vortexing for 60 s, centrifugation for 5 min at 1000 X *g*, and organic layer removed. Extraction was repeated twice for each sample and the hexane extracts combined and evaporated under nitrogen. Samples were resuspended in 200 µl of methanol before HPLC analyses. Stock standard solutions were prepared fresh prior to use by dissolving 10 mg of standards in 10 ml of methanol.

HPLC Analyses of α-TEA Concentration in Rat Serum

α-TEA levels were measured by an internal standard method using reverse-phase HPLC with fluorometric detection as previously described [39, 116]. Forty µl of each sample in methanol were injected into a Waters 717 HPLC equipped with an autosampler. The mobile phase consisted of 96% HPLC grade methanol, 4% water, and 0.001% glacial acetic acid. Samples were separated on a Waters spherisorb ODS-2 5u (250 X 4.6-mm) column (Alltech, Deerfield, IL). Excitation and emission wavelengths of 210 and 300 nm, respectively, and a flow-rate of 1.5 ml/min were used for all determinations. Quantitation of the separated compounds was performed based on the internal standard method using RRR-δ-tocopherol as the internal standard and Millennium-32 chromatography manager software for data analyses (Waters Corp., Milford, MA). To prevent possible degradation of α-TEA, samples were run within one week of being resuspended in methanol.

Rat tissue collection

Six female rats were cared for and fed as described above, four were treated for 39 consecutive days with aerosolized α-TEA and two served as controls. Following the final treatment, food was withdrawn and animals were sacrificed 18 h later. Animals were anesthetized with diethyl ether and tissues were removed for weighing.

Statistical Analyses

Animal numbers for experiments were determined to be adequate based on power calculations. Statistical test were performed using Prism software version 4.0 (Graphpad, San Diego, CA). Tissue weights and animal weights were compared using a two-tailed t-test. Palpable tumors were compared using a one-way analysis of variance followed by a Neuman-Keul's post-hoc test. A level of $p < 0.05$ was considered statistically significant.

RESULTS

α-TEA, MSA and *t*-RES inhibit DMBA-induced alveolar lesions in the MMOC.

After the regression phase of the MMOC, mammary glands were removed from mice and analyzed for alveolar lesions. α-TEA, *t*-RES, and MSA were each effective at inhibiting lesions individually showing a 63, 63, and 38 percent inhibition of incidence compared to control glands (Table 1). Each of the compounds was also able to inhibit the number of lesions per gland showing a 64, 79, and 29 percent inhibition of multiplicity compared to the control glands. Four combinations of co-treatments were also made and analyzed including α-TEA + *t*-RES, α-TEA + MSA, *t*-RES + MSA, and α-TEA + *t*-RES + MSA. The most effective combination was α-TEA + *t*-RES which showed a 75% inhibition of incidence and a 79% inhibition of multiplicity compared to control and was more effective than α-TEA or *t*-RES alone. This combination was 19% more effective than either treatment alone in terms of incidence and 23% more effective than α-TEA alone and the same as *t*-RES alone in terms of multiplicity. The least effective combination was α-TEA + *t*-RES + MSA which showed a 38% inhibition of incidence and a 32% inhibition of multiplicity, values that were less effective than α-TEA and *t*-RES alone but very similar to MSA alone. This combination was 40% less effective than α-TEA and *t*-RES alone in terms of incidence, and the same as MSA alone. It was also 50 and 59% less effective than α-TEA and *t*-RES in terms of multiplicity, and was 10% more effective than MSA alone. Combinations of α-TEA+ MSA and *t*-RES + MSA both showed a 63% inhibition of incidence which is the same as α-TEA or *t*-RES alone but more effective than MSA alone, and a 54 and 64% inhibition of multiplicity, which is less effective than α-TEA or *t*-RES alone but more effective than MSA alone (Table 1).

α-TEA, MSA and *t*-RES inhibit DMBA-induced ductal lesions in the MMOC.

After the hormone treated regression phase of the MMOC, mammary glands were removed from mice and analyzed for ductal lesions. α-TEA, *t*-RES and MSA were each able to inhibit the number of lesions per gland showing a 61, 65, and 49 percent inhibition of multiplicity compared to the control glands (Table 2). Four combinations of co-treatments were also made and analyzed including α-TEA + *t*-RES, α-TEA+ MSA, *t*-RES + MSA, and α-TEA + *t*-RES + MSA. The most effective combination was α-TEA + *t*-RES which showed a 73% inhibition of multiplicity compared to control and was more effective than α-TEA or *t*-RES alone. This combination was 20% more effective than α-TEA alone and 12% more effective than *t*-RES alone. The least effective combination was α-TEA + MSA which showed only a 34% inhibition of multiplicity, which was less effective than α-TEA or MSA alone. This combination was 44% less effective than α-TEA alone and 31% less for MSA alone. A combination of *t*-RES + MSA showed 38% inhibition of multiplicity which was less effective than either *t*-RES or MSA alone. The combination containing all three agents showed a 55% inhibition of multiplicity, which was less effective than α-TEA or *t*-RES alone but more effective than MSA alone.

Rats treated with α-TEA and *t*-RES maintain weight.

Animals were fed AIN-76A lab chow *ad libitum* over the course of the study and were weighed weekly starting on day 1 and on the last day (Fig 1). There was no observed weight loss in any of the treatment groups and no statistical difference between control and treatments.

α-TEA does not cause a loss in tissue organ weight.

Spleen, heart, ovary/uterus, lungs, and kidneys were removed from two rats that were untreated or 4 rats treated with α-TEA for 39 days. Tissues were weighed and no statistical difference in tissue weights was seen between control and α-TEA treated tissues (Fig 2).

α-TEA and *t*-RES reduce palpable tumors in MNU-injected rats.

Twenty-one day old rats were i.p. injected with 50 mg/kg bw MNU to induce mammary gland tumors. Animals were palpated every other day beginning at day 31 of treatment for their presence of palpable tumors (Fig 3). At each of the days observed, control animals had more palpable tumors than α-TEA, *t*-RES, or co-treated groups. Control animals had an incidence rate of 20, 30, 47, 57 and 67% for 31, 33, 35, 37, and 39 post-carcinogen, respectively. α -TEA animals had an incidence rate of 0, 13, 23, 30 and 37% for 31, 33, 35, 37, and 39 post-carcinogen, respectively. *t*-RES animals had an incidence rate of 7, 10, 23, 23 and 30% for 31, 33, 35, 37, and 39 post-carcinogen, respectively. Co-treated animals had an incidence rate of 7, 7, 10, 17 and 23% for 31, 33, 35, 37, and 39 post-carcinogen, respectively, which made it the most effective treatment. Starting at day 35, the difference between the control and co-treated animals was statistically significant and beginning at day 37 all three treatment groups were statistically significant from control.

Analyses of NMU-induced lesions using rat mammary gland whole mounts

At this time, data analyses are still in progress for mammary whole gland mounts.

Serum levels of α-TEA

Lipid fractions were extracted from serum collected from control and α-TEA treated rats and analyzed by HPLC. Delta-tocopherol and α-TEA standards were run at

the same time as samples to identify sample peaks. Analyses of samples did not show detectable levels of α-TEA in samples from α-TEA treated animals (data not shown).

Blood Chemistry Profile

Rat serum was also used for a full serum chemistry profile (Fig 4). Creatine and BUN were as indicators of renal toxicity. ALT, ALK, total bilirubin, albumin, and total protein were used as indicators of hepatic toxicity. No statistical difference was seen between control and α-TEA treated serum for any of these assays. Additional assays that were performed included: cholesterol, triglyceride, glucose, globulin, calcium, phosphorous, sodium, potassium, chloride, $C0_2$, anion gap, and osmolarity. Statistical differences were seen in phosphorous ($p < 0.0372$) and $C0_2$ ($p < 0.0047$) assays.

DISCUSSION

The ideal chemopreventive agent would either restore normal growth to preneoplastic or cancerous cell populations or selectively kill these cells. Characteristics of an ideal chemopreventive agent would include selectivity for transformed cells, good bioavailability, and more than one mechanism of action to avoid cross-talk and redundancy in signaling pathways. Epidemiology studies suggest that dietary intake can account for as many as 30% of cancers. This reflects that there are a number of dietary components that can induce cancer, but there are also an increasing number of compounds in nutrients being discovered that may be protective. Because the carcinogenic process involves many steps over a long time period, there are many opportunities for intervention in the process by dietary constituents or nutrient-based agents. There are also an increasing number of reports that show combinations of two or more chemopreventive agents to be highly effective at doses where single administration is less effective or where single administration has no effect. One example of this in

humans is the ongoing chemoprevention trial (SELECT) using selenium and vitamin E individually and in combination to prevent prostate cancer [42]. For these reasons, we have chosen three compounds that show potential as chemopreventive agents, α-TEA, *t*-RES and MSA [12-14, 16, 18, 21-27, 29-33]. There are five main *in vitro* models used to predict *in vivo* efficacy for mammary models: MMOC, human lung tumor A427 cell assay, JBC epidermal cell assay, human foreskin epithelial (HFE) cell assay, and rat tracheal epithelial (RTE) cell transformation assay. If the results from these assays are positive, then 83% of the time there is a similar positive result *in vivo*, and a positive in at least one assay is an accurate predictor at least 70% of the time. Of these, the MMOC model has the highest positive predictive value to predict success of a chemopreventive agent for mammary cancer *in vivo*. It has the highest sensitivity; the highest specificity, the highest positive and negative predictive value, and the highest overall accuracy in predicting positive efficacy of chemopreventive agents in mammary models. (A positive result in the MMOC is defined when an agent can inhibit 60-100% of lesions at nontoxic doses [3].

In studies presented here, α-TEA, *t*-RES, and MSA were evaluated in the MMOC to predict which agents would be best to use in the *in vivo* rat mammary carcinogenesis model. Data show that α-TEA and *t*-RES are effective at inhibiting both the incidence and multiplicity of DMBA-induced alveolar lesions and the multiplicity of DBMA-induced ductal lesions. MSA also reduced the incidence and multiplicity of these lesions but to a smaller degree, less than the 60% considered to be the cutoff as a positive predictor of *in vivo* efficacy.

Results for α-TEA in the MMOC model are consistent for those previously seen for other forms of vitamin E, vitamin E acetate and Vitamin E succinate, both of which have shown positive results in the MMOC [3]. Results for *t*-RES alone is also consistent

with studies showing *t*-RES to be effective in a dose-dependent manner when used alone with IC_{50} values ranging from 3.0-3.2 μM [12, 18]. Though MSA has not previously been tested in the MMOC model, predictions were that it would be effective since MSC reduces tumorigenesis by as much as 54% in rat mammary carcinogenesis models [21, 23-25, 27] and because studies have shown MSA and MSC to be interchangeable *in vivo* [22-24].

Interestingly the most effective combination to inhibit alveolar lesions was α-TEA + *t*-RES and not the combination with all three compounds. This combination produced a 75% inhibition of incidence and a 79% inhibition of multiplicity, better than α-TEA alone and equal to *t*-RES alone in terms of inhibition of multiplicity. The addition of MSA to the combination cut both inhibition rates by approximately half (75% vs 38% and 79% vs 32%). Combinations of MSA + α-TEA were equally as effective as α-TEA alone in terms of inhibition of incidence (63%) and were slightly less than α-TEA alone to inhibit multiplicity (64% vs 54%). Combinations of MSA + *t*-RES were also as effective as *t*-RES alone in terms of inhibition of incidence (63%) and were slightly less than *t*-RES alone to inhibit multiplicity (79% v 64%). The results of the DMBA-induced ductal lesion assay showed similar results. The most effective combination was again α-TEA + *t*-RES without MSA (73%), which was more effective than α-TEA or *t*-RES alone. In this assay the addition of MSA was not the least effective combination, but it did decrease the effectiveness to levels less than that seen for α-TEA and *t*-RES alone, negating the advantage given by the combination. In this assay, α-TEA + MSA was the least effective combination (34%) but the combination of *t*-RES + MSA was slightly higher (38%). Together, these results suggest that MSA is antagonistic when in the presence of α-TEA and *t*-RES together, and that it does not contribute to the combination effect when used with only one of the other agents.

The incidence of palpable tumors after *t*-RES treatment is consistent with previous studies reporting a delay to onset of MNU-induced tumors and a decrease in the total number of tumors in rats treated with 100 mg/kg bw t-RES compared to control animals in the traditional rat carcinogenesis model [18]. Starting at day 35, a statistical difference was seen between the control and co-treated animals and beginning at day 37 reduced tumors in all three treatment groups were statistically significant from control. On day 39, there were 45, 55 and 65% fewer tumors in the α-TEA, *t*-RES and α-TEA + t-RES groups compared to the control. Overall, the co-treated group was the most effective, followed by *t*-RES and then α-TEA. Even though a statistical difference was not seen between the co-treated, α-TEA and *t*-RES groups, the co-treatment group had 36% fewer tumors than α-TEA and 22% fewer than *t*-RES. At this time the histological data from the rat carcinogenesis model is incomplete and analyses are currently in progress.

Serum analyses of α-TEA and control treated animals were performed using HPLC. Levels of α-TEA in rat serum were undetectable. One possible explanation for this is that since the rats were fasted for overnight before euthanasia, the circulating α-TEA may have been metabolized. Previous studies have shown the presence of serum α-TEA 24 h post-treatment to be approximately 4 μg/ml in unfasted mice (unpublished). Another possible explanation for the difference between this study and previous studies by our lab could be due to species differences in uptake and metabolism. In support of the argument that these results are due to fasting is the triglyceride assay data. Due to errors in the test, only one animal from each treatment was tested. α-TEA treated animals showed a decrease in triglyceride levels compared to control animals which is consistent with fasted status [43].

Neither α-TEA nor *t*-RES caused weight loss in rats treated with individual treatments or combinations. Also, animals treated with α-TEA did not appear to have any significant loss in tissue weight for spleen, heart, ovaries/uterus, lungs or kidneys. Additionally, serum profile analyses for total bilirubin, ALT, ALK, BUN, creatine, total protein, and albumin did not show a statistical difference between control and α-TEA treated animals indicating no renal or hepatic toxicity. There was however a statistical difference between these two groups in phosphorous and $C0_2$ assays. Animals treated with α-TEA showed a statistical increase in phosphorous levels. Increased levels of inorganic phosphorous may be indicative of myeloma, Paget's disease of bone, osseous metastases, and a variety of other conditions in addition to drug-related causes [43]. Since these animals were i.p. injected with MNU and control animals were not, it is possible that the increase could be due to osseous metastases or perhaps some other MNU-related cause and not a direct result from α-TEA treatment. α-TEA treated animals showed a decrease in $C0_2$ levels which could be indicative of metabolic acidosis or compensated respiratory alkalosis [43]. More probable is that the serum samples were not collected under anaerobic conditions, which could have allowed for interaction of blood and atmosphere and may have varied enough between animals to cause a statistical difference [43]. Further work will need to be done to determine if these differences between α-TEA and control treated animals are due to α-TEA treatment. Overall, the anti-cancer efficacy of α-TEA and *t*-RES separately and together, and the lack of overt toxicity provide further support for the use of these compounds for prevention of breast cancer.

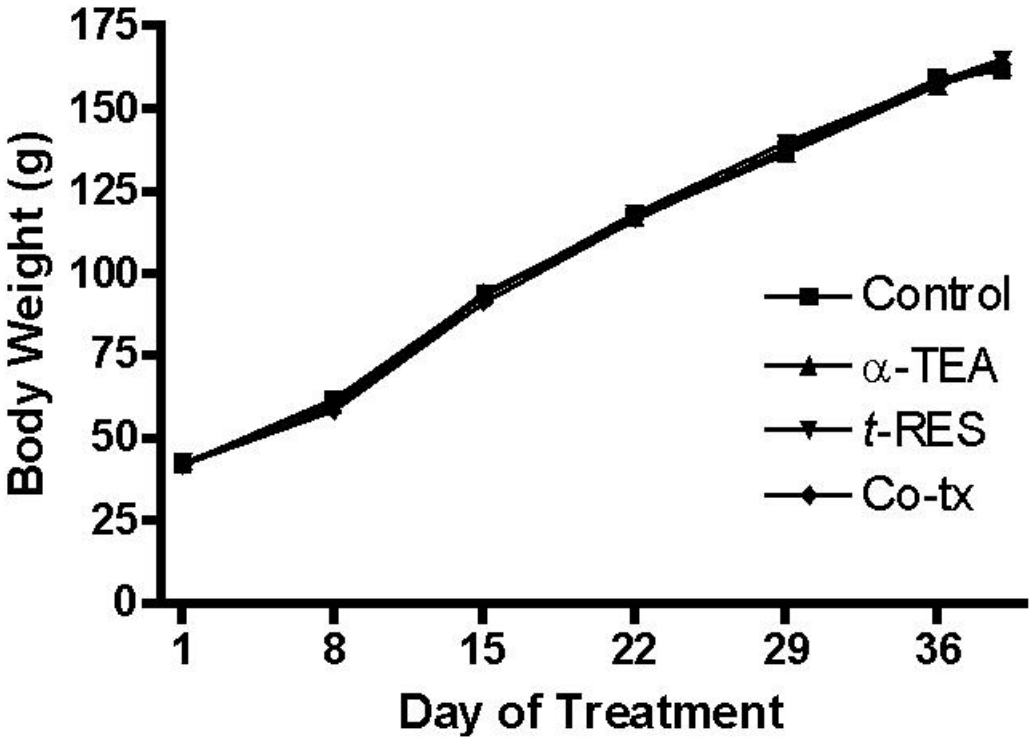

Figure 4.1. Rat Weights Over Time. Twenty-one day old rats were injected with 50 mg/kg bw. MNU to induce mammary gland tumors. Animals were fed AIN-76A lab chow *ad libitum* over the course of the study and were weighed weekly. Graph shows mean animal weight ± SE. No statistical difference was seen between any of the groups.

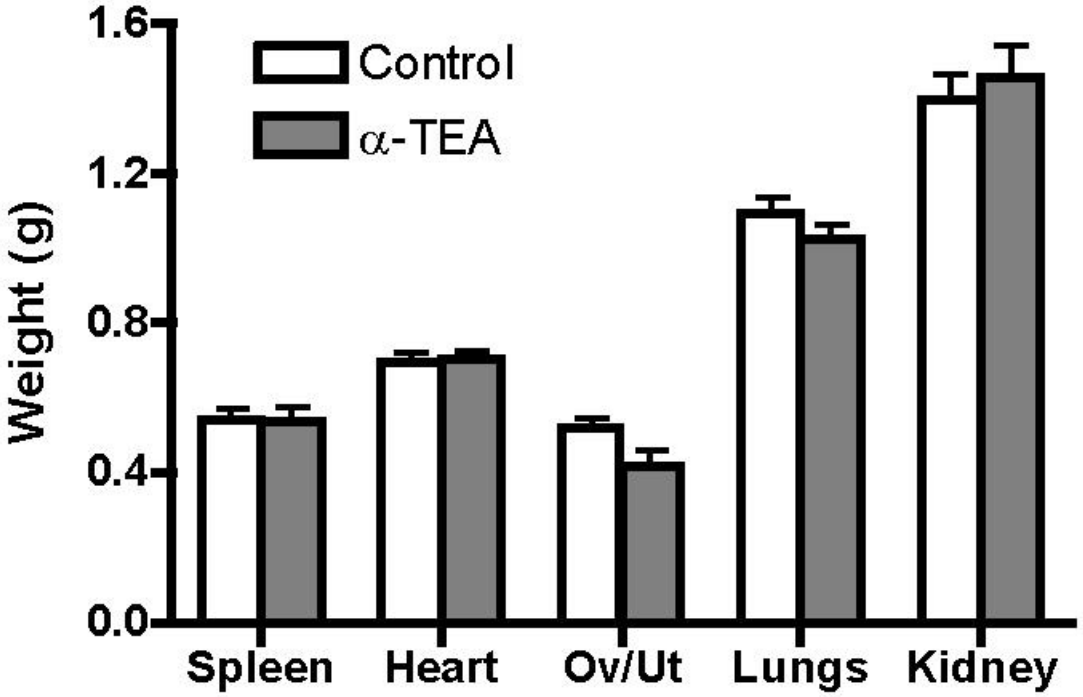

Figure 4.2. Tissue Weights from Rats Treated with α-TEA. Spleen, heart, ovary/uterus, lungs, and kidneys were removed from rats that were untreated or treated with alpha-TEA for 39 days. Graph shows tissue weights after removal. There was no statistical difference between control and alpha-TEA treated tissues using a two-tailed unpaired t-test. (n=2 for control, n=4 for α-TEA treated)

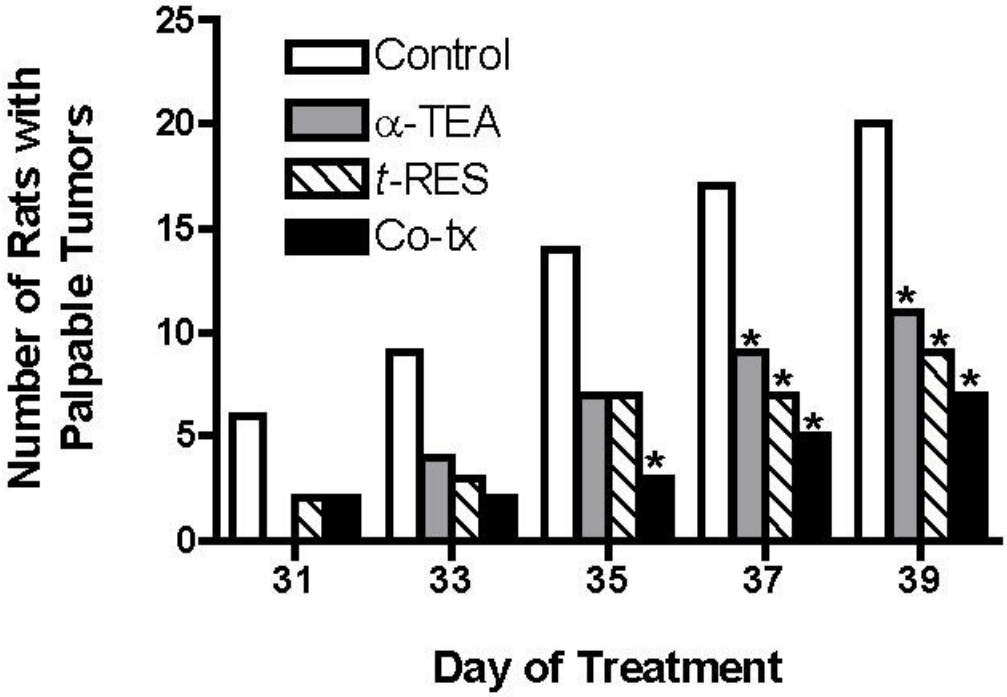

Figure 4.3. Palpable Tumors in Rat Carcinogenesis Model. Twenty-one day old rats were i.p. injected with 50 mg/kg bw. MNU to induce mammary gland tumors. Treatments were initiated on day 1 and animals were palpated every other day beginning at day 31 of treatment for their presence or absence. Graph shows the number of animals each day with palpable tumors. Number of rats for control and treatment groups = 30. * indicates $p < 0.05$ compared to control.

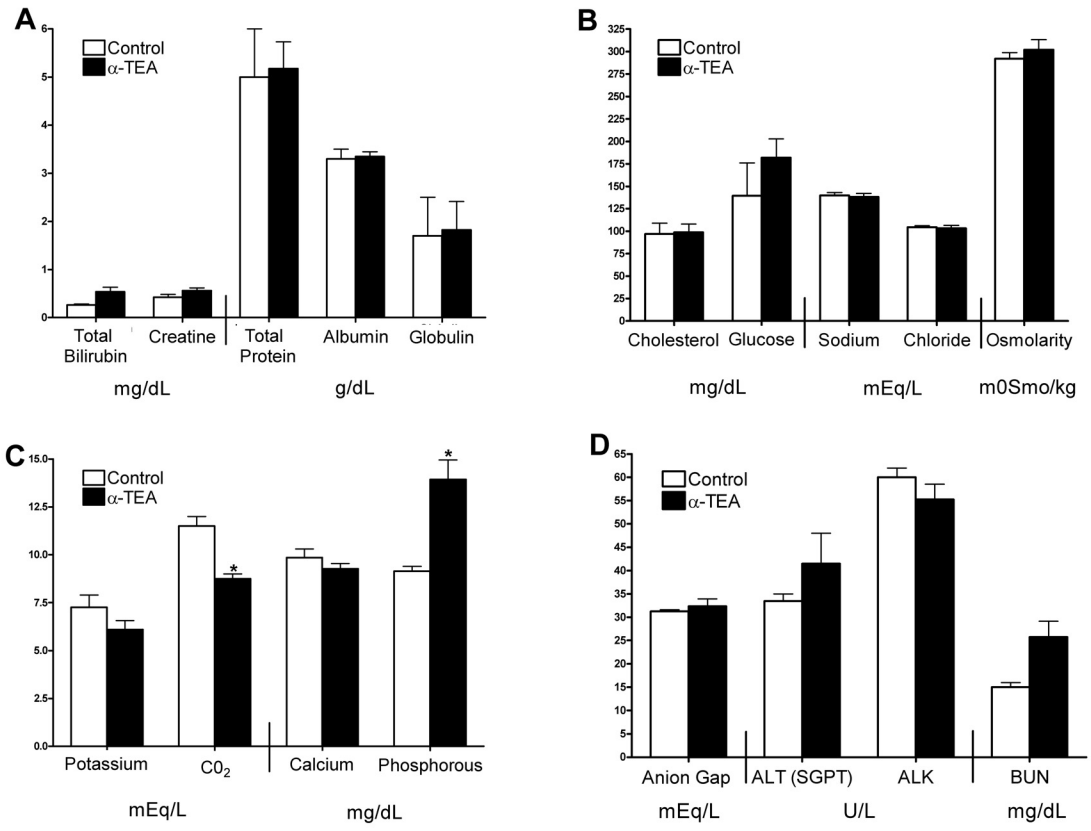

Figure 4.4 Blood Chemistry Profile. Serum from fasted rats was analyzed using a full serum chemistry profile. Statistical analyses was done using a two-tailed unpaired test. ($p < 0.05$) ($n = 2$ for control, $n = 4$ for α-TEA treated)

Table 4.1: Comparison of DMBA-induced alveolar lesions in the mouse mammary organ culture model (MMOC)

Group	Treatment	Conc.	Glands w/ Lesions	% Inc	% Inh (Inc)	Lesions/ gland	% inh mult
1	**DMBA**	2 μg/ml	8 of 10	80	--	28	--
2	**α-TEA**	1 μg/ml	3 of 10	30*	63	10	64
3	***t*-RES**	2.5 μg/ml	3 of 10	30*	63	6	79
4	**MSA**	1 μg/ml	5 of 10	50	38	20	29
5	**α-TEA + *t*-RES**	1 μg/ml 2.5 μg/ml	2 of 10	20*	75	6	79
6	**α-TEA + MSA**	1 μg/ml 1 μg/ml	3 of 10	30*	63	13	54
7	***t*-RES + MSA**	2.5 μg/ml 1 μg/ml	3 of 10	30*	63	10	64
8	**α-TEA + *t*-RES + MSA**	1 μg/ml 2.5 μg/ml 1 μg/ml	5 of 10	50	38	19	32

Mammary glands were removed from mice and analyzed for lesions. ⟨-TEA, MSA, *t*-RES and combinations were scored for their ability to prevent lesion formation after treatment with DMBA.

Table 4.2: Comparison of DMBA-induced ductal lesions in the mouse mammary organ culture model (MMOC)

Group	Treatment	Conc.	Multiplicity	% inh mult
1	**DMBA**	2 µg/ml	80	--
2	**α-TEA**	1 µg/ml	31	61
3	***t*-RES**	2.5 µg/ml	28	65
4	**MSA**	1 µg/ml	41	49
5	**α-TEA** + ***t*-RES**	1 µg/ml 2.5 µg/ml	22	73
6	**α-TEA** + **MSA**	1 µg/ml 1 µg/ml	53	34
7	***t*-RES** + **MSA**	2.5 µg/ml 1 µg/ml	50	38
8	**α-TEA** + ***t*-RES** + **MSA**	1 µg/ml 2.5 µg/ml 1 µg/ml	36	55

Mammary glands were removed from mice and analyzed for lesions. ⟨-TEA, MSA, *t*-RES and combinations were scored for their ability to prevent lesion formation after treatment with DMBA.

Chapter 5: α-TEA and *trans*-Resveratrol induce synergistic levels of apoptosis in human MDA-MB-435 breast cancer cells by caspase-dependent and -independent mechanisms

ABSTRACT

Combinations of *t*-RES and α-TEA synergize to produce increased levels of cell death in MDA-MB-435-F-L human breast cancer cells *in vitro*. Data reported here elucidates α-TEA and *t*-RES treatment, separately and in combination, mediated signaling events leading to cell death by apoptosis. Pretreatment with *t*-RES and α-TEA alone and together sensitizes the cells to Fas and TRAIL mediated apoptosis. Treatment with *t*-RES and α-TEA, separately and together, increases levels of DR5, TRAIL, and Fas, but decreases FasL. α-TEA and α-TEA + *t*-RES induced cell death was dependent on activation of caspases-2, -3, -8, and -9 while that for *t*-RES was not. Both *t*-RES and α-TEA decreased survivin and c-FLIP levels, and in combination decreased survivin and c-FLIP proteins to undetectable levels. To further evaluate whether DR5, Fas, c-FLIP and survivin are important to α-TEA + *t*-RES synergy, levels of these proteins were knocked down using siRNA. A significant decrease in apoptosis, in comparison to control siRNA treated cells, was seen in co-treated cells where Fas and DR5 were knocked down, and a statistical increase in apoptosis was seen in *t*-RES and α-TEA treated cells following knock down of survivin and c-FLIP. *t*-RES-induced cell death was also investigated. Autophagocytosis was evaluated in the MDA-MB-435 cells in an effort to explain *t*-RES-induced cell death. Using TEM, low levels of autophagic vacuoles (AV) were detected in cells treated with *t*-RES and the co-treatment but not in α-TEA treated cells. We were unable to confirm autophagocytosis using western

immunoblotting or flow cytometry. Based on the results reported here, we propose a signaling model where the synergy between α-TEA and *t*-RES is due to a combination of apoptosis and caspase-independent cell death (CICD).

INTRODUCTION

One specific type of cell death commonly studied in cancer is apoptosis, a highly regulated form of programmed cell death (PCD) commonly referred to as Type 1 PCD [4]. Apoptosis is initiated by the binding of ligands to one of several cell membrane death receptors, resulting in mitochondria-dependent or -independent mediated cell death. Apoptotic morphological characteristics include cell shrinkage, DNA fragmentation, chromatin condensation, blebbing of the nucleus and cytosolic cellular fractions into apoptotic bodies [4-5, 7-10], Type 1 PCD involves activation of caspases [4, 7-8, 11]. Some cancer therapeutic agents sensitize cells to apoptosis by down-regulating inhibitor of apoptosis proteins (IAPs) such as cIAP1, cIAP2, livin, XIAP and survivin, which are usually expressed at high levels in tumor cells. IAPs exert their anti-apoptotic activity by binding to the active form of caspases-3 and -9 [4, 11, 16]. To counteract the activity of IAPs, Smac/DIABLO and Omi/HtrA2 can bind to and inhibit their activity [8]. Cellular FLICE-inhibitory protein (c-FLIP), though not an IAP, is another anti-apoptotic protein that functions by competing with pro-caspase-8 for binding to FADD. c-FLIP is able to bind to FADD because it shares high sequence homology to caspase-8, however it cannot signal as caspase-8 because c-FLIP lacks a proteolytic domain required for downstream signaling [12, 15].

In contrast to apoptosis, some therapeutic agents can induce cancer cells to undergo type II PCD, or commonly referred to as autophagocytosis. Autophagocytic characteristics include the formation of autophagic vacuoles (AV), dilation of the endoplasmic reticulum (ER), and enlargement of the Golgi [4-5, 7, 9, 19-20]. Once

formed, AVs fuse with lysosomes to sequester cytoplasmic contents and degrade them via lysosomal hydrolases [4-5, 7, 19-22]. While the signaling events for autophagy are known in yeast, many of the mammalian homologs are yet to be found, so the exact signaling pathways are unknown [19, 21-23]. The general pathway begins with a signaling event that leads to the formation of a double membrane structure called an autophagosome, which fuses with cellular lysosomes to form an autolysosome [9, 19, 21-22, 24]. Often in autophagocytosis, caspases are not activated and DNA fragmentation does not occur. Three mammalian proteins are associated with autophagocytosis, beclin-1, MAP-LC3, and LAMP-1. Beclin-1 is involved in the early steps of autophagic vesicle formation and can be inhibited by bcl-2 [7, 10, 21, 25-26]. MAP-LC3 has been found to be recruited to the pre-autophagosome membranes [19, 21, 24, 28] where it remains associated with the inner and outer phagosomal membrane [24]. LAMP-1 is a highly N-glycosylated lysosomal protein that is critical for transport to lysosomes in cells. LAMP-1 is ubiquitously expressed in cells and has been shown to be localized in late endosomes and lysosomes [29-30] and to serve as a receptor for the import and degradation of cytosolic proteins in the lysosome during autophagy [30].

Caspase-independent cell death (CICD) is a third form of cell death that occurs under pro-apoptotic conditions but which proceeds without the activation of caspases [6, 119]. There are generally low levels of chromatin condensation, DNA fragmentation, cellular blebbing, and loss of mitochondrial permeability [6, 119]. The exact signaling is poorly understood but it is thought that signaling begins by the binding of FasL to either Fas or TNFα receptors. This binding leads to the recruitment of TRADD and RIP to the receptor. The chaperone protein Hsp90 can play an inhibitory role in this pathway by controlling RIP through the proteosome pathway [12]. RIP may activate cathepsins B and D via JNK, which may lead to the mitochondrial release of AIF, Omi/HtrA2 and

SMAC/DIABLO from the mitochondria [120]. Upon release, Omi/HtrA2 and SMAC/DIABLO can directly bind to and inhibit IAPs leading to apoptosis [10, 119]. The release of AIF can lead to DNA fragmentation [10] and cytochrome c release [119]. Another protein that may be involved and is released from the mitochondria is Endonuclease G (EndoG), which translocates into the nucleus and can induce DNA degradation [119].

trans-Resveratrol (3,5,4'-trihydroxy-*trans*-stilbene; *t*-RES) is a naturally occurring phytoalexin found in a variety of foods such as grapes and red wine [46-53]. *t*-RES has previously been shown to induce cellular differentiation and apoptosis in human promyelocytic leukemia cells [47-48], human colon cancer cells [48-49], and human breast cancer cells [48, 50]. It is not toxic *in vitro* and *in vivo* which makes it attractive as a chemotherapeutic agent [47-49, 51, 53].

α-TEA is a derivative of natural vitamin E, RRR-α-tocopherol, and is capable of inducing human ovarian (A2780/cp-70), cervical (ME-180), breast (MCF-7, MDA-MB-231, MDA-MB-435), endometrial (RL-952), prostate (LNCaP, PC-3, DU-145), lung (A-549), colon (HT-29, DLD-1) and lymphoid (Raji, Ramos, Jurkat) cells to undergo apoptosis [38, 40] and is nontoxic to normal epithelial cells [38-40, 42]. α-TEA induces apoptosis via the Fas [121] and DR5 receptor pathways [*unpublished*]. α-TEA and *t*-RES in combination prevent chemically induced lesions in the MMOC model [Chapter 4] and can synergize with MSA to induce cell death in vitro [Chapter 2].

Here we show that α-TEA + *t*-RES synergize *in vitro* to induce high levels of cell death in a highly aggressive human breast cancer cell line, MDA-MB-435-F-L. α-TEA and α-TEA + *t*-RES in combination, but not *t*-RES alone, sensitize the cells to both Fas and TRAIL induced apoptosis, involving caspases 8, 2, 9, and 3. Both agents, alone and in combination, reduce pro-survival c-FLIP and survivin proteins. Autophagy was

investigated in an effort to better understand how *t*-RES was inhibiting cell growth independent of caspases.

MATERIALS AND METHODS

Chemicals and Reagents

α-TEA was prepared as previously described [40]. *trans*-Resveratrol (*t*-RES) was purchased from Cayman Chemical Co. (Ann Arbor, MI). Acridine orange was purchased from Sigma Co. (St. Louis, MO). Caspase-3 inhibitor (Z-DEVD-FMK), caspase-9 inhibitor (Z-LEHD-FMK), caspase-8 inhibitor (Z-IETD-FMK), and a pan caspase inhibitor (Z-VAD-FMK) were purchased from BioVision Research Products (Palo Alto, CA), All reagents for the morphological analyses of apoptosis were purchased from Boehringer Mannheim (Indianapolis, IN). The following antibodies were used: Fas (sc-8009, Santa Cruz Biotechnology, Inc., Santa Cruz, CA), FasL (sc-959, Santa Cruz), DR5 (PX063A, Cell Sciences Inc., Canton, MA), TRAIL (sc-8440, Santa Cruz), pro- and cleaved caspase-8 (#9476, Cell Signaling Technology, Beverly, MA), pro- and cleaved caspase-9 (sc-8355, Santa Cruz), pro- and cleaved caspase-2 (clone 11B4, Axxora, San Diego, CA), pro- and cleaved caspase-3 (sc-7148, Santa Cruz), PARP (sc-7150, Santa Cruz), c-FLIP (sc-5276, Santa Cruz), survivin (sc-17799, Santa Cruz), beclin-1 (sc-10086, Santa Cruz), MAP-LC3 (sc-16756, Santa Cruz), lamp-1 (sc-17768, Santa Cruz), GAPDH (made in-house), antihuman Fas mouse monoclonal IgM antibody (clone CH-11; Upstate Biotechnology, Inc., Lake Placid, NY), antihuman DR5 mouse monoclonal IgM antibody (Upstate Biotechnology), and irrelevant control antibody (mouse IgM, Sigma). siRNA to Fas, DR5, c-FLIP, survivin, caspase-2 or silencer negative control were purchased from Ambion's Silencer Predesigned siRNA listing (Austin, TX). The wild type survivin, Myc-tagged pcDNA3.plasmid, was a kind gift from Dr. J. Q. Chen

(College of Medicine, University of South Florida [122]). The wild type HA-tagged c-FLIP$_L$ expression construct was kindly provided by Dr. John C. Reed (The Burnham Inst. La Jolla, CA; [123]). The empty pcDNA3 vector was purchased from Invitrogen (Carlsbad, CA).

Cell Culture and Treatment

MDA-MB-435-F-L cells, recovered from a metastatic tumor in the lung of a nude mouse and stably transfected with enhanced green fluorescence protein, were a kind gift from Dr. LuZhe Sun (University of Texas Health Science Center, San Antonio, TX. [73]). MDA-MB-435-F-L cells were cultured as previously described [43]. Stock solutions of *t*-RES and α-TEA were at 20 mg/ml in DMSO. All solutions were stored at –20°C and diluted in experimental media to the desired final concentration. Vehicle controls consisted of 0.167 % DMSO, or 1.67 μl/ml media.

Apoptosis Analysis Using Morphology of 4', 6-Diamidino-2-Phenylindole Dihydrochloride (DAPI) Nuclear Stained Cells

Cells were plated and treated with VEH, *t*-RES, α-TEA or a co-treatment at various concentrations. Treatments were for three days and then cells were collected and stained with DAPI for determination of apoptosis as previously described [88, 124]. Cells in each sample were counted a minimum of 3 times, with •100–200 cells/count. Cells where the nucleus contained clearly condensed chromatin or fragmented nuclei were scored as apoptotic. Apoptotic data are reported as percent apoptosis (number apoptotic/total number of cells counted). Data are mean ± S.D. of three independent experiments.

Western Immunoblot Analyses

Whole cell lysates were prepared as described by Yu *et al* [88, 124] from cells treated for 6, 12, 24, and 48 hrs with vehicle or 88 μM *t*-RES and 20.5 μM α-TEA alone

and in combination. Cells were washed with PBS and lysed with lysis buffer (13 PBS, 1% NP40, 0.5% sodium deoxyxholate, and 0.1% SDS) plus 1 μg/ml of aprotinin and leupeptin, 1 mM DTT, and 2 mM sodium orthovandate and incubated on ice for 30 min. Lysates were centrifuged at 15,000 x g for 15 min at 4˚C and protein concentrations determined with Bio-Rad Dye Binding protein assay. Western immunoblot analyses, using 50 μg protein per lane, were conducted as previously described [41, 42]. Proteins were separated using 10, 12 or 15% SDS-page under reducing conditions. Immunoblotting was performed using the primary antibodies listed above and peroxidase-conjugated goat anti-rabbit, goat anti-mouse, rabbit-anti-goat, or goat anti-rat secondary antibodies (Jackson Immunoresearch Laboratory, West Grove, PA), followed by detection with ECL (Pierce, Rockford, IL). Densitometry was performed using Scion Image Software (Scion Corporation, Frederick, MD). Glyceraldehyde-3-phosphate dehydrogenase (GAPDH, in house) was used to verify equal lane loading and for densitometric determinations.

Fas and DR5 Death Receptor Sensitivity Assays

MDA-MB-435-F-L ells were plated at 1.5 x 10^5 cells/ml overnight, followed by pretreatment for 6 h with VEH, 88 μM *t*-RES, 20.5 μM α-TEA alone and in combination, and vehicle. Cells were washed in medium to remove treatments and then treated with 0.5 μg/ml antihuman Fas mouse monoclonal IgM antibody, 5 ng/ml antihuman DR5 mouse monoclonal IgM antibody, or 0.5 μg/ml irrelevant control antibody for 42 h, DAPI stained and analyzed for apoptosis.

Caspase Inhibitors

MDA-MB-435-F-L cells were plated at 1.5 X 10^5 cells/well in 12-well plates overnight. Next, cells were pretreated for 2 h with media containing the following

caspase inhibitors: caspase-3 inhibitor (Z-DEVD-FMK), caspase-9 inhibitor (Z-LEHD-FMK), caspase-8 inhibitor (Z-IETD-FMK), a pan caspase inhibitor (Z-VAD-FMK) (each at 2 μM), or a vehicle control (0.1% DMSO). Following pre-treatment, cells were treated with 88 μM *t*-RES, 20.5 μM α-TEA, alone and in combination or vehicle, for 48 h, and analyzed for apoptosis using DAPI staining [124].

Functional knock down of Fas, DR5, c-FLIP, survivin, and caspase-2.

siRNA/siPORT NeoFX reagent complex was made by first mixing 3.6 μl siPORT NeoFX reagent with 0.2 ml serum-free media and incubated for 10 min with siRNA to Fas, DR5, c-FLIP, survivin, caspase-2, or silencer negative control. siRNA was added to the siPORT NeoFX mixture so that the final concentration of siRNA in 0.6 ml was 30 nM, and then incubated for 10 min. During the preparation of the reagent complex, MDA-MB-435-F-L cells were collected by trypsinization and resuspended in serum free medium at 3.75 x 10^5 cells/ml. Next, 0.2ml of the reagent mix plus 0.4 ml of the cell suspension were added to each well of a 12-well plate and allowed to incubate overnight. The following day the transfection media was replaced with normal culture media and cells were incubated for 24 h. Cells were then treated with 88 μM *t*-RES and 20.5 μM α-TEA), alone or in combination, and vehicle for 24 h. The cells from vehicle and treatment groups were sub-divided into two groups, one group was analyzed for apoptosis using DAPI staining, and lysates from the other group were analyzed by western immunoblotting to confirm knockdown of Fas, DR5, survivin, c-FLIP, and caspase-2.

Over-expression of wild-type survivin and c-FLIP$_L$

MDA-MB-435-F-L cells were plated at 1.5 X 10^5 cells/ml, and then transfected with plasmids encoding Myc-tagged wild-type survivin, HA-tagged wild-type c-FLIP$_L$, or

vector control using published procedures [124]. DNA/LipofectAMINE/Plus reagent complex was made by mixing 0.7 μg of DNA/50 μl of serum-free medium with 4 μl of Plus (Invitrogen, Carlsbad, CA) reagent and incubated for 15 min. This solution was then added to a second solution containing 2 μl of LipofectAMINE reagent/50 μl of serum-free medium and incubated for 15-min. We generally obtain about 50% transfected cells using this method in MDA-MB-435 cells [124]. After 8 h transfection, the cells were incubated with culture media overnight. . Next, the cells were treated with 88 μM *t*-RES and 20.5 μM α-TEA, alone or in combination, or vehicle for 48 h. The cells from vehicle and treatment groups were sub-divided into two groups, one group was analyzed for apoptosis using DAPI staining, and lysates from the other group were analyzed by western immunoblotting to confirm overexpression of survivin and c-FLIP$_L$.

Transmission electron microscopy

Transmission electron microscope (TEM) analyses were used to determine if treatments, especially treatments with *t*-RES, were causing the cells to undergo cell death by autophagocytosis. Cells were prepared according to the procedures of Opipari *et al* [43] and were evaluated at the Microscopy and Imaging Facility of the Institute for Cellular and Molecular Biology at The University of Texas at Austin. MDA-MB-435-F-L cells were treated with VEH, *t*-RES (88 μM), α-TEA (20.5 μM), or both. Human cisplatin sensitive A2780 ovarian cancer cells treated with cisplatin or *t*-RES served as positive controls for apoptosis and autophagocytosis. Cells were treated for 24 h at the concentrations indicated and then floating cells were collected into 15 ml centrifuge tubes and pelleted at 1,500 g for 3 min. Both floating and adherent cells were treated with the same reagents and combined after fixing. Cells were rinsed twice in warm serum free media and then fixed for 30 min at 4°C with 2.5% glutaraldehyde in 0.1 M Sorensen's buffer (pH 7.4). Cells were rinsed twice in 0.1 M Sorensen's buffer and then fixed for 15

min at 4°C in 1% osmium tetroxide in 0.1 M Sorensen's buffer. Samples were rinsed two more times with 0.1 M Sorensen's buffer and then adherent cells were scraped and added to the cell suspension from that sample. The new suspensions were rinsed with double distilled water to remove phosphate and then stained with 3% uranyl acetate in double distilled water for 15 min. Cells were rinsed once in double distilled water and then dehydrated in a series of ethanol incubations, 5 min each in 50, 70, 90, and 100 % ethanol. Samples were then infiltrated with Spurrs resin as follows: 3:1 (ethanol: resin) for 20 min, 1:1 (ethanol : resin) for 20 min, 3:1 (ethanol: resin) for 1 h, full strength resin for 1 h, fresh full strength resin for 1 h. Samples were then allowed to polymerize at 60°C for 24 h, after which they were given to the Microscopy facility for staining and sectioning. For each sample, cells were quantitated according to the classifications of Opipari *et al* [54]. Cells that showed at least 3 autophagic vacuoles, no nuclear condensation, and intact plasma membrane were scored autophagic. Cells that showed nuclear condensation and irregular plasma membranes were scored apoptotic. All other cells were scored normal.

Measurement of Red:Green Fluorescence Ratio in Acridine Orange-stained Cells Using Flow Cytometry

The cytoplasm and nucleoli of acridine orange-stained cells fluoresce bright green and dim red while acidic compartments fluoresce bright red. The intensity of the red fluorescence is therefore proportional to the degree of acidity and the volume of the cellular acidic compartment and so by measuring the change in mean red:green fluorescence ratio within different populations of cells, one can measure the change in the acidity or fractional volume of the acidic compartments. MDA-MB-435 cells were plated at 1.5 x 10^5 cells/ml in T-25 flasks. The following day cells were treated with VEH, *t*-RES (88 μM), α-TEA (20.5 μM), or both for 24 h. MDA-MB-435 cells were

prepared for flow cytometry according to the procedures published by Paglin *et al* [29]. A stock solution of 1 mg/ml acridine orange was made and cells were incubated for 17 min at a working concentration of 1 μg/ml at 37˚C. Adherent cells were removed from the plate using trypsin-EDTA and collected in phenol red-free growth medium. Green (510-530 nm) and red (>650 nm) fluorescence emission from 10^4 cells illuminated with blue (488 nm) excitation light was measured with a FACSCalibur flow cytometer (Becton Dickinson, San Jose, CA) using CellQuest software. The mean red:green fluorescence was calculated using FlowJo software (TreeStar Inc., Ashland, OR). MCF-7 cells gamma-irradiated at 25˚C using a Cs-137 irradiator at a dose-rate of 243 cGy/min were used as a positive control 24 h after irradiation.

Statistical Analyses

Statistical analyses were conducted using Prism software version 4.0 (Graphpad, San Diego, CA.) and a level of $P < 0.05$ was considered statistically significant. Apoptosis data were analyzed using one-way ANOVA followed by a Tukey's post-hoc test. CalcuSyn 2.0 was use to determine synergy values.

RESULTS

α-TEA and *t*-RES, alone and in combination induce apoptosis in MDA-MB-435-F-L-GFP cells

Separate treatments with *t*-RES at 44 and 88 μM and α-TEA at 10.3 and 20.5 μM significantly induced MDA-MB-435-F-L cells to undergo apoptosis in comparison to vehicle control (Fig 1A) ($P < 0.01$; $P < 0.001$; $P < 0.05$; and $P < 0.001$; respectively). Likewise, treatments with *t*-RES at 44 and 88 μM in combination with α-TEA at 10.3 or 20.5 μM significantly enhanced apoptosis in comparison to vehicle ($P < 0.05$; $P < 0.001$; $P < 0.001$, and $P < 0.001$, respectively). The combination data were entered into CalcuSyn to determine a combination index value (CI) and synergy. The CI value was 0.742 for

the 88 μM *t*-RES + 20.5 μM α-TEA combination which indicates a synergistic relationship as defined as CI < 1.

Pre-treatment with *t*-RES and α-TEA alone and together sensitize MDA-MB-435 cancer cells to Fas and TRAIL mediated apoptosis.

In an effort to better understand how separate and combination treatments with *t*-RES and α-TEA induce apoptosis, Fas and TRAIL mediated apoptosis was investigated. Cells were pre-treated with VEH, *t*-RES, α-TEA and a co-treatment for 6 h and then replaced with Fas, or TRAIL activating antibodies, or irrelevant antibody control, cultured for 48 hrs and then analyzed for apoptosis. Vehicle cells cultured with Fas or TRAIL activating antibodies did not undergo apoptosis, suggesting that MDA-MB-435 cells were non-responsive to Fas or TRAIL induced apoptosis (Fig 1B). However, pre-treatment of the cells with *t*-RES, α-TEA alone and in combination, followed by treating with Fas or TRAIL activating antibodies significantly enhanced apoptosis over vehicle and irrelevant antibody controls (Fig 1B). These data show that pretreatment of MDA-MB-435 cells with *t*-RES or α-TEA alone and in combination sensitize the cells to Fas and TRAIL induced apoptosis. Levels of significance for Fas and TRAIL activating antibodies with the following pre-treatments were: *t*-RES, $P< 0.01$ and $P< 0.01$; α-TEA, $P< 0.05$ and $P< 0.001$; α-TEA + *t*-RES, $P< 0.01$ and $P< 0.001$, respectively.

α-TEA alone and in combination with *t*-RES enhances DR5, TRAIL, and Fas protein levels.

MDA-MB-435 cells were treated for 6, 12, 24 and 48 h with VEH, *t*-RES, α-TEA and co-treatment. At 24 and 48 h, both α-TEA and co-treatment upregulated DR5 protein levels by 2.4 and 2.3 fold and 4.2 and 4.2 fold, respectively (Fig 1C, top panel). TRAIL ligand was also upregulated beginning at 24 h in the co-treatment (1.5 fold) and by 1.8, 1.8 and 2.2 fold by *t*-RES, α-TEA and co-treatment, respectively at 48 h (Fig 1C,

second panel). *t*-RES and α-TEA treatments enhanced Fas protein levels at 24 h (1.7 and 1.8 fold, respectively) and by all treatments at 48 h (1.7, 1.2 and 1.2 fold) (Fig 1C, third panel). In contrast, *t*-RES and combination treatments at 12 and 24 h decreased levels of FasL, 2.7 and 3.0 fold for 12 hours, and 12 and 10.5 fold at 24 hours, respectively. α-TEA reduced Fas L 1.5 fold at 24 hours, and all treatments decreased FasL at 48 hrs. (Fig 1C, fourth panel).

α-TEA alone and in combination, but not *t*-RES, induces caspase cleavage.

Cells were treated with α-TEA and *t*-RES, alone and together, for 6, 12, 24 and 48 h to evaluate the role of caspases in the induction of apoptosis. *t*-RES alone did not activate caspases (Fig 2A). Of the three key caspases normally involved in apoptotic signaling (caspases-3, -8, and-9), caspase-8 was the first to show cleavage. Cleavage of caspase-8 was detected at 12 h in cells treated with α-TEA and co-treatment, with co-treatment giving a 1.7 fold increased caspase 8 cleavage fragment (Fig 2A, top panel). Both treatments showed caspase 8 cleavage at 24 and 48 h, with a 1.6 fold increase in cleavage fragment by α-TEA than the co-treatment at 24 h, and a 1.1 fold increase in the cleavage fragment by the co-treatment at 48 h (Fig 2A, top panel). Caspase-9 cleavage was detected at 24 and 48 h in the α-TEA and co-treatment groups. Treatment with *t*-RES induced cleavage of caspase- 9 at 48 h treatment (Fig 2A, second panel). Cleavage fragments for caspase-3 were detected at 24 and 48 h in the α-TEA and co-treatment cells. At both time-points, in comparison to α-TEA treatment, co-treatment enhanced caspase-3 cleavage fragments 7.0 and 2.8 fold at 24 and 48 h treatment, respectively (Fig 2A, third panel). The disappearance of pro-caspase-2 was detected beginning at 6 h with the co-treatment (1.2 fold reduction in comparison to VEH). At each progressive time-point, the co-treatment had less pro-caspase-2 than both VEH and the individual treatments, and at 48 h there was a 23.8, 11.1, and 8.6 fold decrease in caspase 2

compared to VEH, *t*-RES and α-TEA, respectively (Fig 2A, fourth panel). Despite repeated efforts, a cleavage band was not found for caspase-2 at any time-point. PARP cleavage by the co-treatment was detected at 12, 24 and 48 hours. All treatments gave PARP cleavage at 24 and 48h, with co-treatment giving the greatest amount of PARP cleavage (Fig 2A, fifth panel).

α-TEA and co-treatment induced apoptosis is caspase-dependent.

As an alternate approach to the involvement of activated caspases in treatment induced apoptosis (data depicted in Fig 2A), cells were pre-treated with caspase-3, -8 and -9 specific inhibitors and a general pan-caspase inhibitor and levels of apoptosis quantified (Fig 2B). Each of the four inhibitors significantly reduced apoptosis in α-TEA and co-treated cells, with the greatest reduction seen in the co-treatment (Fig 2 B). In the absence of an effective caspase-2 specific inhibitor, cells were transfected with caspase-2 siRNA, followed by α-TEA and *t*-RES alone and together. Following treatment, cells were subdivided into two groups with one group DAPI stained and assayed for apoptosis, and cell lysates assayed by western immunoblotting in the other group to verify effectiveness of siRNA. Caspase 2 siRNA reduced levels of caspase-2 (Fig 2C) and significantly reduced levels of apoptosis induced by α-TEA and co-treatments (α-TEA, $P < 0.01$ and co-treatment, $P < 0.05$). (Fig 2D). Although caspase 2 siRNA reduced the level of apoptosis induced by *t*-RES treatment, there was no significant difference from the negative siRNA control (Fig 2D).

Apoptosis induced by *t*-RES is caspase-independent. Despite inducing cleavage of caspase-9 after 48 h treatment (Fig 2A), it appears that apoptosis induced by *t*-RES is caspase-independent. When cells were pre-treated with caspase-3, -8 and -9 specific inhibitors and a general pan-caspase inhibitor, there was not a statistical decrease in the percentage of apoptosis detected after *t*-RES treatment (Fig 2B). Also, caspase 2 siRNA

reduced the levels of cellular caspase-2 (Fig 2C) but did not significantly reduce levels of apoptosis induced by *t*-RES (Fig 2D).

_t_-RES and α-TEA alone and together down-regulate pro-survival c-FLIP$_L$ and survivin protein levels.

t-RES and α-TEA alone and together decreased pro-survival c-FLIP and survivin protein levels, with the co-treatment showing the largest decrease of both proteins at each time point (Fig 3A). At 12 h, there was a 2.1, 1.5 and 4.9 fold decrease in c-FLIP for *t*-RES, α-TEA, and co-treatment. By 48 h there was a 2.1 and 10.6 fold decrease for *t*-RES and α-TEA and undetectable levels in the co-treatment. Similar to the results seen for c-FLIP, the co-treatment was the most effective at each time-point in decreasing survivin. At 12 h there was a 1.6 fold decrease in survivin in co-treated cells. At 48 hrs treatment, there was a 4.1 fold decrease by *t*-RES, a 2.3 fold decrease by α-TEA, and undetectable levels of survivin in the co-treated cells (Fig 3A).

To determine if c-FLIP$_L$ and survivin are integral to *t*-RES and α-TEA treatment induced apoptosis, c-FLIP$_L$ and survivin were overexpressed in the MDA-MB-435 cells. Elevated levels of c-FLIP$_L$ and survivin in the transfected cells were confirmed by western blotting (Fig 3 B &C). Cells expressing either vector control, survivin, or c-FLIP$_L$ over-expression vectors were treated with α-TEA and *t*-RES alone or together and evaluated for apoptosis. Levels of apoptosis were significantly reduced in the co-treated cells expressing c-FLIP$_L$ and survivin ($P < 0.01$ and $P < 0.05$) (Fig 3D). Cells treated with α-TEA showed a 43 and 46% decrease for survivin and c-FLIP$_L$ over-expression, respectively, compared to α-TEA treated vector control cells, but this difference was not statistically significant (Fig 3D). Over expression of c-FLIP$_L$ or survivin had no effect on *t*-RES induced apoptosis (Fig 3D).

Effects of siRNA to Fas, DR5, c-FLIP$_L$ and survivin on treatment-induced apoptosis.

Western immunoblot analyses were used to verify that transfection of MDA-MB-435 cells with siRNA to Fas, DR5, c-FLIP$_L$, and survivin reduced levels of each protein, respectively (Fig 4A). Next, cells transfected with siRNA to Fas, DR5, c-FLIP$_L$ and survivin were treated with VEH, *t*-RES, α-TEA, or co-treatment and then evaluated for apoptosis. Knockdown of c-FLIP$_L$ and survivin significantly enhanced the ability of *t*-RES to induce the cells to undergo apoptosis, ($P< 0.0001$ and $P< 0.01$). Knockdown of DR5 and Fas had no significant effect on *t*-RES-induced apoptosis (Fig 4B). Knockdown of DR5 and Fas reduced α-TEA induced apoptosis by 46 and 36%, respectively, and knockdown of c-FLIP$_L$ and survivin significantly enhanced α-TEA induced apoptosis ($P< 0.01$, and $P< 0.0001$; Fig 4B). For the co-treated cells, knockdown of Fas and DR5 significantly reduced treatment induced apoptosis ($P< 0.01$, and $P< 0.01$). While there was an increase in apoptosis in the co-treated cells transfected with siRNA to c-FLIP (26 %) and survivin (31 %) the increase was not significantly different from the negative control transfected or α-TEA treated cells (Fig 4B).

***t*-RES and co-treatments induce low levels of autophagic vacuoles.**

The above data show that *t*-RES induces apoptosis as determined by PARP cleavage and DNA fragmentation, but apoptosis does not appear to be mediated by caspase activation. Next, based on studies showing *t*-RES to induce autophagocytosis in human ovarian cancer cells [54], treatment induced autophagocytosis was investigated in breast cancer cells. A2780 cisplatin sensitive ovarian cancer cells treated with cisplatin or *t*-RES were used as positive controls for apoptosis and autophagocytosis (Fig 5A and B). MDA-MB-435-F-L breast cancer cells were treated with VEH, *t*-RES, α-TEA or co-treatment and then evaluated for the presence of autophagic vacuoles (AV) using TEM (Fig 5 C-G). Cells treated with *t*-RES (Fig 6D) showed low levels of AV and no nuclear

condensation compared to control (Fig 5C). In contrast, cells treated with α-TEA showed no AV but showed nuclear condensation and invaginations of the nuclear membrane compared to control (Fig 5F compared to Fig 5C). Co-treated cells showed AV similar to that of *t*-RES (Fig 5E compared to Fig 5D) and apoptotic profile similar to α-TEA (Fig 5G compared to Fig 5F)).

Autophagy proteins do not increase in response to *t*-RES in MDA-MB-435-F-L cells.

Although AV were seen with *t*-RES treatments using TEM analyses, only low levels of AV were seen in individual cells. Next, LAMP-1, Beclin-1, and MAP-LC3 proteins known to be associated with autophagocytosis were examined using western blotting. As a positive control, MCF-7 cells were treated with 0.15 μM camptothecin (CPT [132]) and *t*-RES. CPT treatment gave a time-dependent increase in LAMP-1 (2.2, 3.3 and 2.2 fold), beclin-1 (1.6 and 1.9 fold), and MAP-LC3 (1.8 and 2.0 fold) (Fig 6A). In MCF-7 cells treated with *t*-RES there was an increase in beclin-1 and MAP-LC3 proteins beginning at 6 h. LAMP-1 protein levels were not significantly changed (Fig 6A). In MDA-MB-435-F-L breast cancer cells, *t*-RES treatment increased beclin-1 protein levels at 6 (2.4 fold) and 12 h (1.6 fold), which decreased to basal levels at 24 h (Fig 6B). LAMP-1 and MAP-LC3 protein levels were not significantly changed (Fig 6B).

Mean red:green fluorescence does not increase after treatment with *t*-RES, α-TEA or co-treatment.

In one final effort to quantitate AV, MDA-MB-435 cells were treated with acridine orange, a dye that localizes and accumulates in vacuoles, and is used an indictor for AV. MCF-7 cells gamma-irradiated were used as a positive control. Twenty-one percent of the MCF-7 gamma irradiated cells showed high red fluorescence The mean red:green ratio increased from 1.36 to 2.34 in these cells (Fig 7 A & B). Using these same

conditions, MDA-MB-435 cells were treated with VEH, *t*-RES, α-TEA or co-treatment. All treatments showed a decrease in the mean red:green ratio and a decrease in high red fluorescent cells from VEH treated cells (Fig 7 C-F). Taken together, there is little support for *t*-RES -induced autophagy in MDA-MB-435 cells.

DISCUSSION

Combinations of *t*-RES and α-TEA synergize to produce increased levels of cell death by apoptosis in MDA-MB-435-F-L human breast cancer cells *in vitro*. MDA-MB-435 cells are insensitive to both Fas and DR5/TRAIL induced apoptosis, but pretreatment of the cells with α-TEA or α-TEA + *t*-RES sensitizes the cells to both Fas and DR5 apoptotic signaling. α-TEA alone and in combination with *t*-RES enhances levels of DR5, TRAIL and Fas, and all three treatments reduce Fas ligand protein levels. *t*-RES alone induced increased levels of TRAIL at 48 hrs of treatment. α-TEA alone and in combination with *t*-RES apoptotic signaling via these membrane receptors involves activation of caspases-8, -9, -3, and -2. Treatment reduction of caspase-2 levels is indicative of activation of caspase-2. *t*-RES alone induces the cells to undergo apoptosis in a Fas/DR5/caspase independent manner. α-TEA and *t*-RES alone and in combination down-regulate pro-survival c-FLIP$_L$ and survivin. siRNA knockdown of c-FLIP$_L$ and survivin significantly enhances *t*-RES-induced apoptosis. Decreased levels of c-FLIP$_L$ and survivin proteins are proposed as one mechanism for combination treatment induced synergistic apoptotic effects. Autophagy was ruled out as a mechanism whereby *t*-RES induces apoptosis in a caspase-independent manner.

One possible explanation for treatment-induced decreases in Fas is the translocation of FasL to the cell exterior, as reported by our lab following treatment with vitamin E succinate (VES), a vitamin E derivative [89]. Overall, the Fas/TRAIL/caspase data for α-TEA reported here are consistent with previous reports for VES and α-TEA

[88-89, 121, 124-125]. *t*-RES-induced enhanced levels of TRAIL is supported by data in the literature showing *t*-RES to sensitize neuroblastoma cells to TRAIL induced apoptosis [11], and to involve Fas and TRAIL induced apoptosis in colon cancer cells, without an increase in receptor levels [126]. While *t*-RES induced cleavage of pro-caspase-2 and -9, neither caspase was required for cell death. This is consistent with previous reports that *t*-RES induces caspase-independent apoptosis [55, 93, 127].

Data show that both *t*-RES and α-TEA decrease cellular levels of survivin and c-FLIP and that a combination of the two decreases the levels of these two proteins to undetectable levels. Although both α-TEA and *t*-RES reduce c-FLIP$_L$ and survivin protein levels, overexpression of these two proteins decreased α-TEA and combination induced apoptosis, but did not affect levels of *t*-RES induced apoptosis suggesting that while the decrease in these proteins by *t*-RES plays a role in the synergy, *t*-RES alone does not require a decrease in c-FLIP$_L$ or survivin to induce cell death.

To further evaluate whether DR5, Fas, c-FLIP and survivin are important to the synergy effect, levels of these proteins were knocked down using siRNA. A statistical decrease in apoptosis was seen in co-treated cells where Fas and DR5 were knocked down and smaller but not significant decreases were seen in *t*-RES and α-TEA treated cells. There was also a statistical increase in apoptosis in *t*-RES and α-TEA treated cells after survivin and c-FLIP siRNA transfections were done. α-TEA has been shown to reduce levels of survivin and c-FLIP [125], and *t*-RES has been shown to reduce levels of survivin [11, 17, 128]. To our knowledge, there are no reports showing a decrease in c-FLIP following *t*-RES treatment.

In an effort to explore alternative death pathways to explain how *t*-RES induces cell death independent of Fas/DR5/caspases/c-FLIP and survivin, three different approaches were used to determine if autophagocytosis was involved in *t*-RES-induced

apoptosis in MDA-MB-435 cells. Although TEM analyses showed low levels of *t*-RES-induced autophagocytosis, this data was not confirmed by western immunoblotting of proteins known to be involved in autophagy, and acridine orange stained lysosomes. Based on the data generated by these three approaches, it was concluded that autophagocytosis is not a major player in *t*-RES-induced apoptosis in human MDA-MB-435 breast cancer cells.

As more types of cell death and overlap between types of cell death are discovered, it becomes increasingly evident that it is difficult to neatly categorize cell death induced by a particular agent. An increasing amount of work suggests an interdependence between multiple signaling pathways and in some cases there appear to be multiple paths to the same end. Exclusive definitions are difficult to make and probably do not represent the true nature of cell death due to the overlap and shared signaling pathways [48]. Based on the results reported here, we propose a signaling model where the synergy between α-TEA and *t*-RES is due to both classical apoptosis and caspase-independent events (Fig 8). The ability of both *t*-RES and α-TEA to reduce c-FLIP$_L$ and survivin levels could contribute to combination treatment synergy. Secondly, we propose that *t*-RES kills cells via a caspase-independent cell death (CICD) pathway. *t*-RES data presented here are consistent with cells undergoing CICD, i.e. low levels of DNA condensation and fragmentation, absence of caspase activation, and no DISC formation [6]. Percent *t*-RES treated cells showing DNA condensation and fragmentation under TEM analyses and DAPI staining were low. While studies of DISC formation were not performed, siRNA knockdown of DR5 and Fas, and caspase inhibitors had little effect on *t*-RES induced apoptosis, suggesting that DISC formation and caspase activity are not required for cell death induced by *t*-RES.

Future studies will focus on caspase-independent death signaling mechanisms in *t*-RES treated cells and caspase-2 signaling in α-TEA treated cells since both of these signaling mechanisms are poorly understood and appear important to the synergy between *t*-RES and α-TEA. One theory for CICD signaling is that TRADD and RIP are recruited to TNFα receptor to activate cathepsin B, which then interacts with the mitochondria to release AIF, SMAC/DIABLO, EndoG, and Omi/HtrA2. These proteins can then either inhibit IAPs in the cytoplasm or enter the nucleus to induce DNA condensation and fragmentation. One theory for caspase-2 signaling is that it is activated in a p53-dependent PIDDosome formation, though Vakifahmetoglu *et al* have reported PIDDosome formation in both $p53^{(+/+)}$ and $p53^{(-/-)}$ cells [129]. PIDDosome formation is thought to occur when p53 recruits PIDD, RRAID and caspase-2 to Fas receptor, which activates caspase-2 [120, 129-130]. Active caspase-2 acts upstream of the mitochondria to cleave bid and induce bax translocation and cytochrome c release [130-131]. Clearly, more work needs to be done for a better understanding of CICD, the function of caspase-2, and their roles in cell death. In a recent paper, *t*-RES was shown to induce apoptosis in human estrogen responsive MCF-7 breast cancer cells in a caspase-independent manner [55]. Data suggest that *t*-RES-induced apoptosis in MCF-7 cells involves an oxidative, caspase-independent mechanism, whereby inhibition of P13K signaling converges to Bcl2 through NF-kappaB and calpain protease activity. Future studies are needed to determine if PI3K/AKT, Bcl-2 and NF-kappaB are targets of *t*-RES induced apoptosis in estrogen non-responsive MDA-MB-435 breast cancer cells.

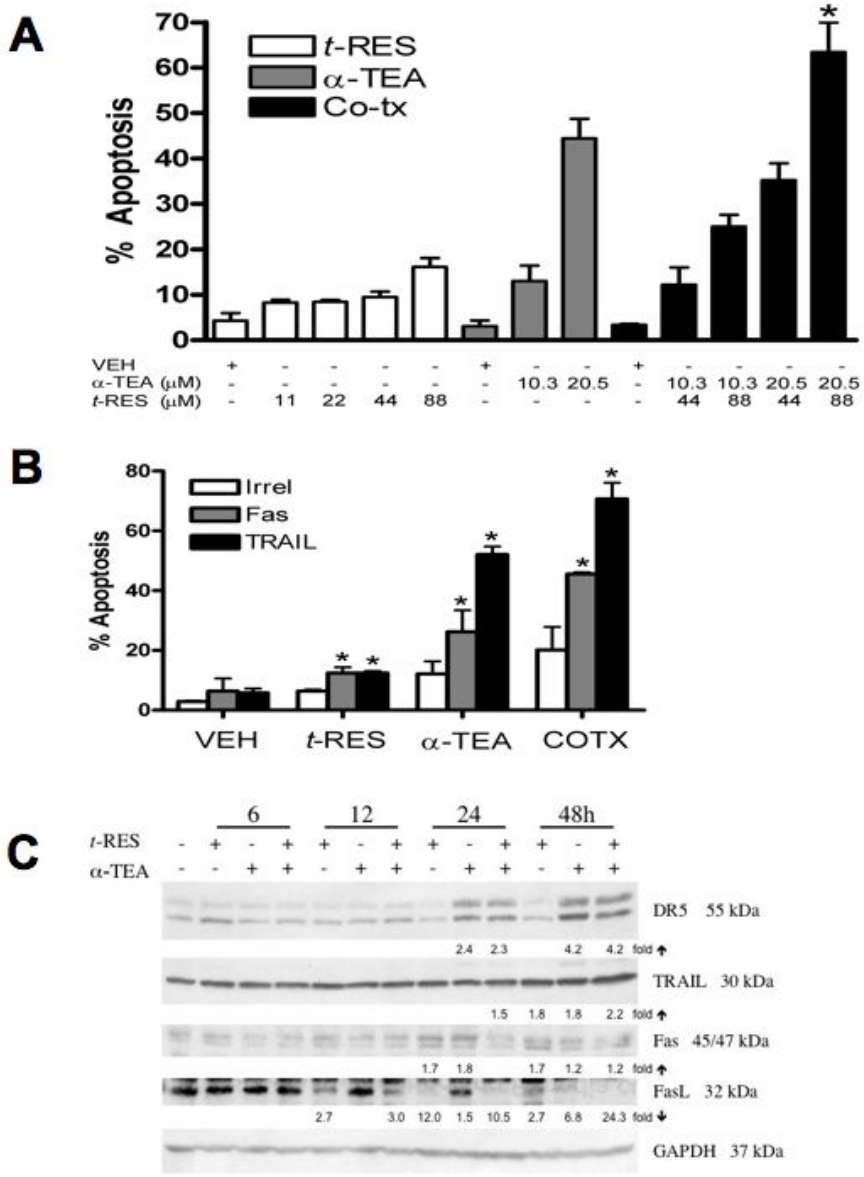

Figure 5.1. α–TEA and *t*-RES induce apoptosis and sensitize cells to Fas and DR5 mediated cell death. *A*, Apoptosis induced following treatment with various concentrations of α–TEA, *t*-RES, and combinations. Densitometry values indicate fold difference from VEH. * indicates synergy (CI= 0.742). *B*, Treatments statistically increase apoptosis in sensitivity assay. * $p < 0.05$ compared to irrelevant control for that treatment. *C,* Western blot of DR5, Fas, TRAIL, and FasL protein levels after treatment. Densitometric analyses were performed, using GAPDH, to quantitate protein increases or decreases. A & B data are depicted as the mean ± S. D. of three independent experiments. C data are representative of three independent experiments.

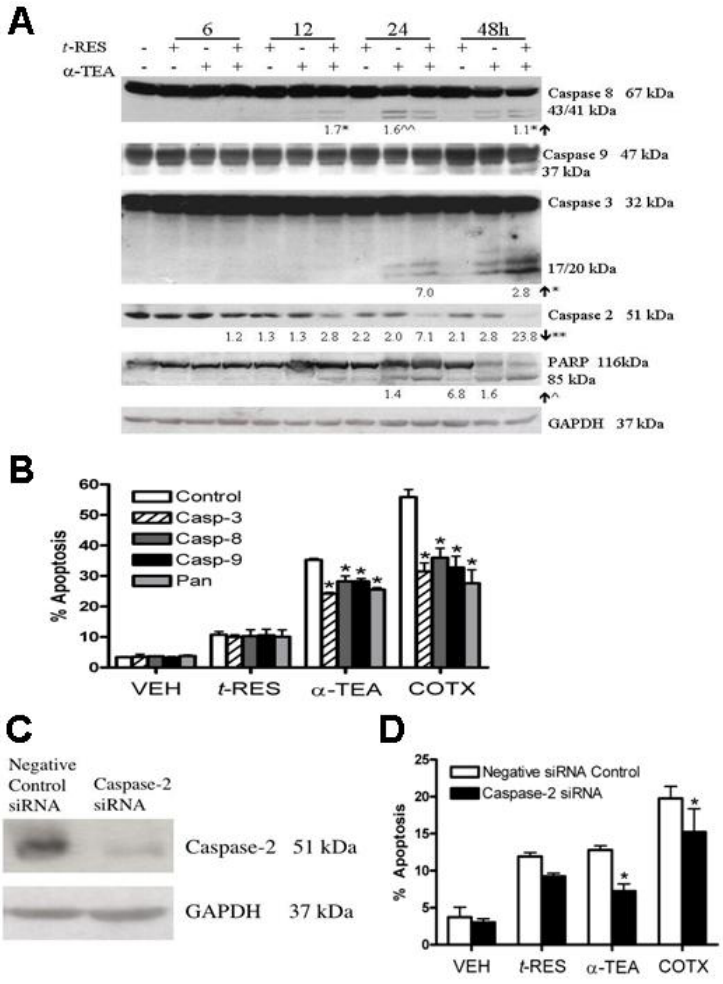

Figure 5.2. Caspase activation. *A,* Western blot analyses for cleavage of caspases-8, -9, -3, -2. and PARP. * indicates fold increase of co-treatment over α-TEA, ** indicates fold decrease from control, ^ indicates fold increase of co-treatment over individual treatments, ^^ indicates fold increase of α-TEA treatment over co-treatment. Data are representative of three independent experiments. *B*, Cells were pretreated with caspase inhibitors (2 μM) for 2 h before treatment with VEH, *t*-RES (88 μM), α-TEA (20.5 μM) or co-treatment for 2 days, DAPI stained and apoptosis determined. Data are depicted as the mean ± S. D. of three independent experiments. * = significantly different from control, $P < 0.05$. *C*, Western blot analyses showing caspase-2 knockdown after siRNA transfection. Data are representative of 3 independent experiments. *D*, Cells were transfected with caspase-2 siRNA and then treated with VEH, *t*-RES (88 μM), α-TEA (20.5 μM) or co-treatment for 1 day. Cells were DAPI-stained and percentage apoptosis was determined. Data are depicted as the mean ± S. D. of three independent experiments. * $p < 0.05$ compared to negative siRNA control for each respective treatment.

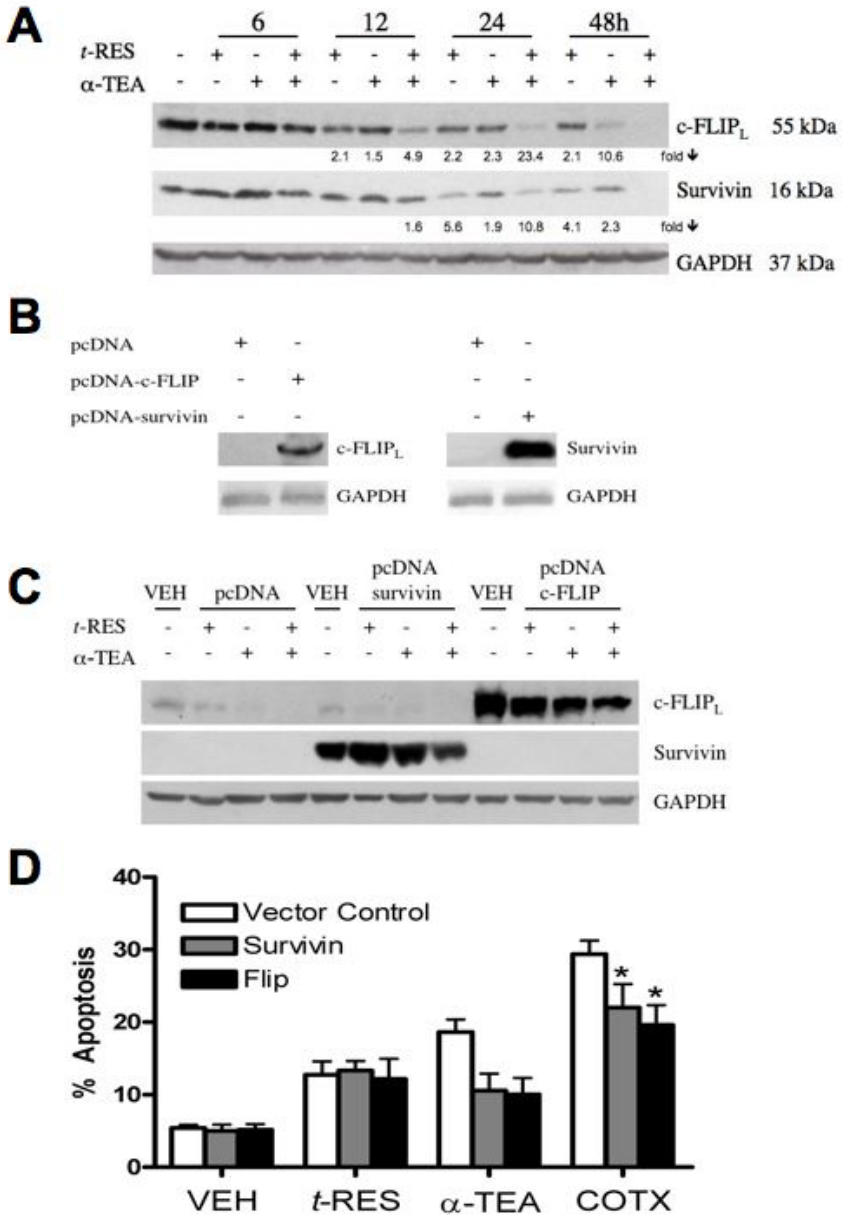

Figure 5.3. Importance of survivin and c-FLIP. *A*, Western blot showing decrease in survivin and c-FLIP following treatment for 6, 12, 24 or 48 h with VEH, *t*-RES (88 μM), α-TEA (20.5 μM) or co-treatment. Densitometry values indicate fold decrease from VEH. *B-C*, Western blots showing over-expression of survivin and c-FLIP. *D*, Apoptosis induced by VEH, *t*-RES (88 μM), α-TEA (20.5 μM) or co-treatment following overexpression of survivin and c-FLIP. A, B, and C data are representative of three independent experiments. D data are depicted as the mean ± S. D. of three independent experiments. *$p < 0.05$ compared to vector control for each respective treatment.

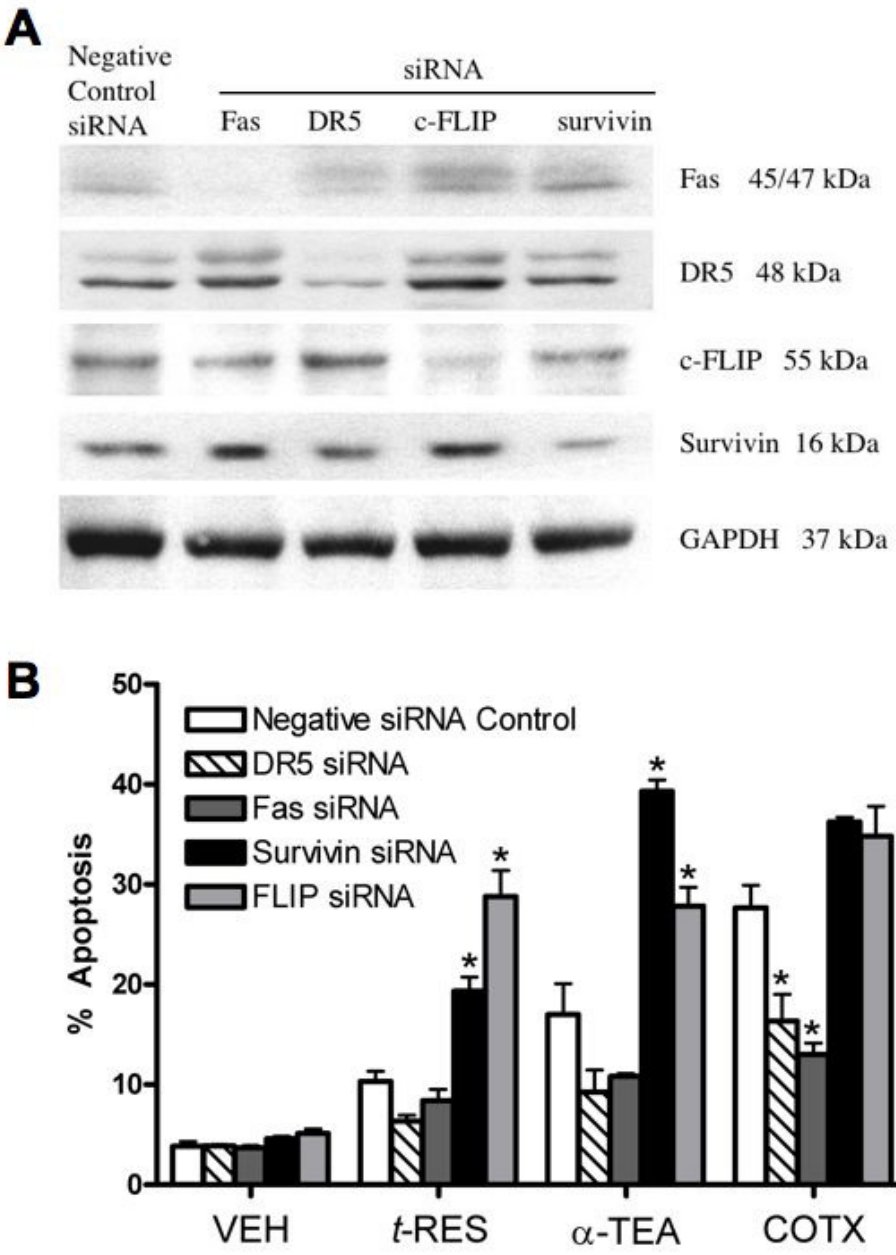

Figure 5.4. siRNA knockdown of Fas, DR5, c-FLIP, and survivin. *A*, Western blot for proteins knocked down following siRNA transfection. *B*, Apoptosis induced by VEH, *t*-*t*-RES (88 μM), α-TEA (20.5 μM), or combination in DR5, Fas, Survivin, and FLIP siRNA transfected cells. A data are representative of three independent experiments. B data are depicted as the mean ± S. D. of three independent experiments. * $p < 0.05$ compared to negative siRNA control for each respective treatment.

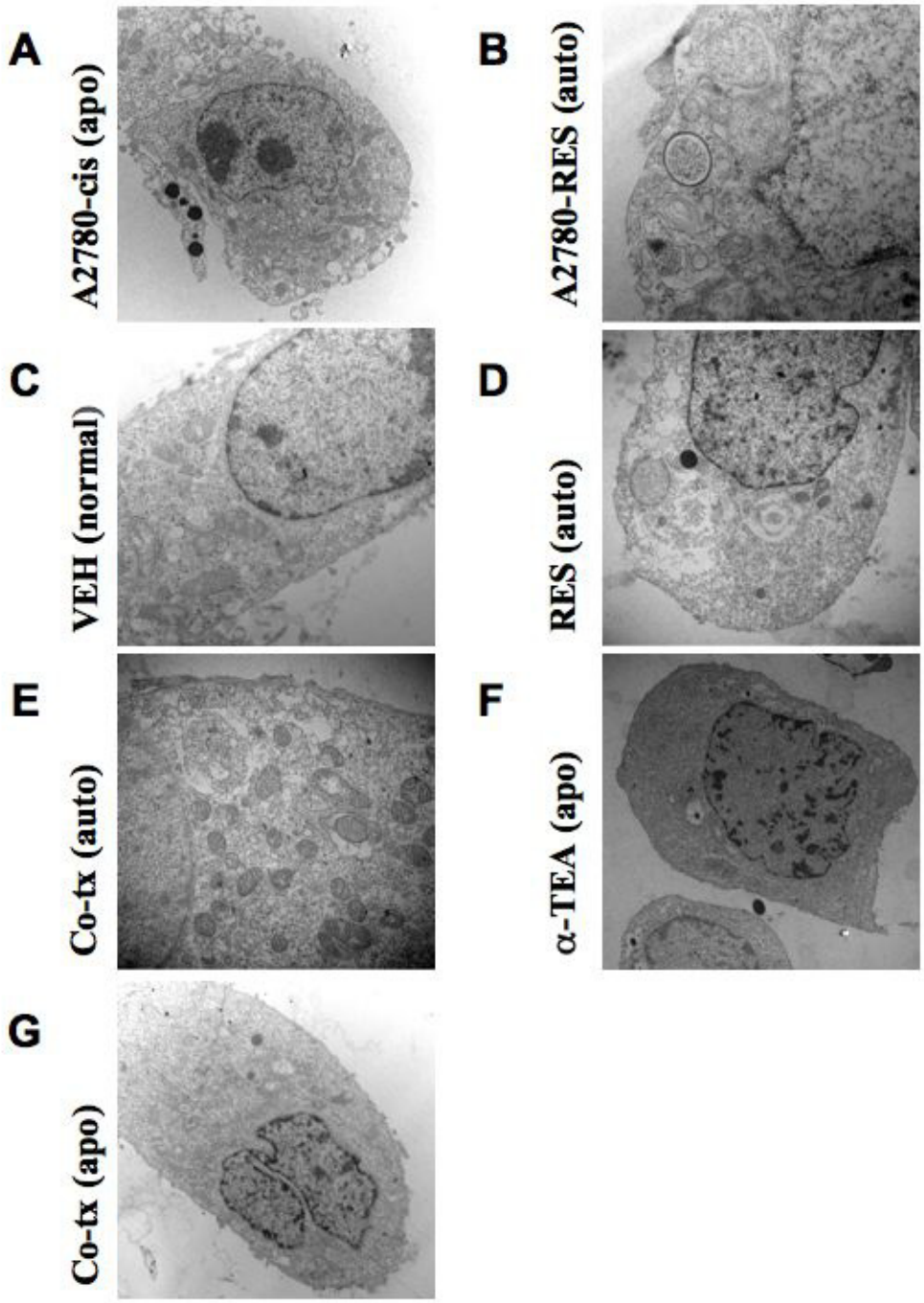

Figure 5.5. TEM analysis of autophagic vacuoles. *A-B*, A2780 cells were treated with cisplatin or *t*-RES as positive controls for apoptosis and autophagocytosis, respectively. *C-G*, MDA-MB-435 cells treated with VEH, *t*-RES (88 μM), α-TEA (20.5 μM), or co-treatment to look for the presence of autophagic vacuoles (AV).

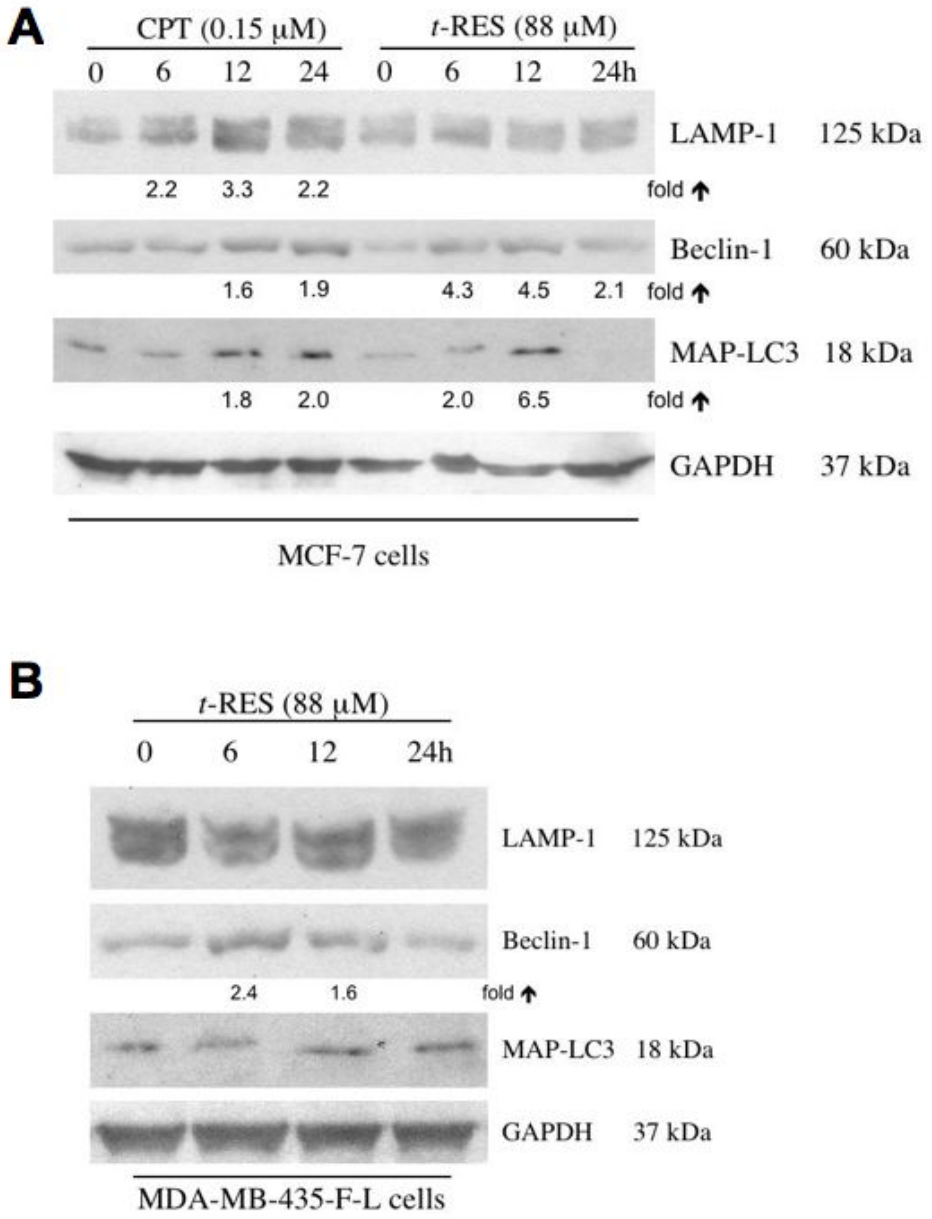

Figure 5.6. Western immunoblotting for autophagy associated proteins. *A*, MCF-7 cells were treated with CPT or *t*-RES for 0, 6, 12 or 24 h and then analyzed by western blotting for LAMP-1, Beclin-1 or MAP-LC3. Cells treated with CPT served as a positive control for autophagy. *B*, MDA-MB-435-F-L cells were treated with *t*-RES for 6, 12, and 24 h, and western immunoblotting was conducted on cell lysates, Densitometry values indicate fold increase from VEH (O h time point). A and B data are representative of three independent experiments.

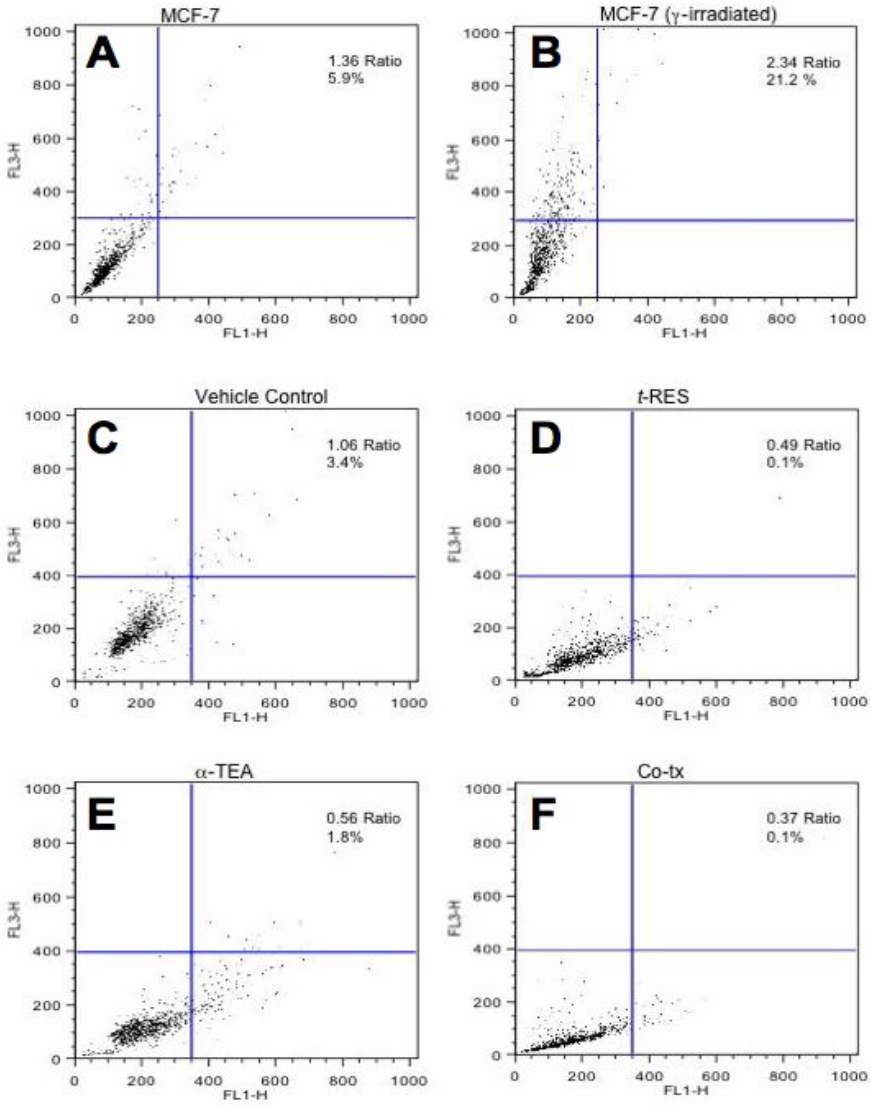

Figure 5.7. Lysosomal activity measured by acridine orange. Acridine orange in its free form is a weak base that becomes trapped inside of acidic vacuoles. The accumulation of these molecules results in bright red fluorescence (>650 nm). Increases in mean red:green fluorescence therefore reflects an increase in lysosomal volume. Cells were analyzed using flow cytometry to look for an increase in bright red fluorescent cells and an increase in the mean red:green ratio. *A-B*, MCF-7 cells were either untreated or gamma-irradiated and analyzed after 24 h as a positive control. *C-F*, MDA-MB-435 cells were treated with VEH, *t*-RES (88 μM), α-TEA (20.5 μM), or co-treatment for 24 h. Percentage indicates cells that show bright red fluorescence.

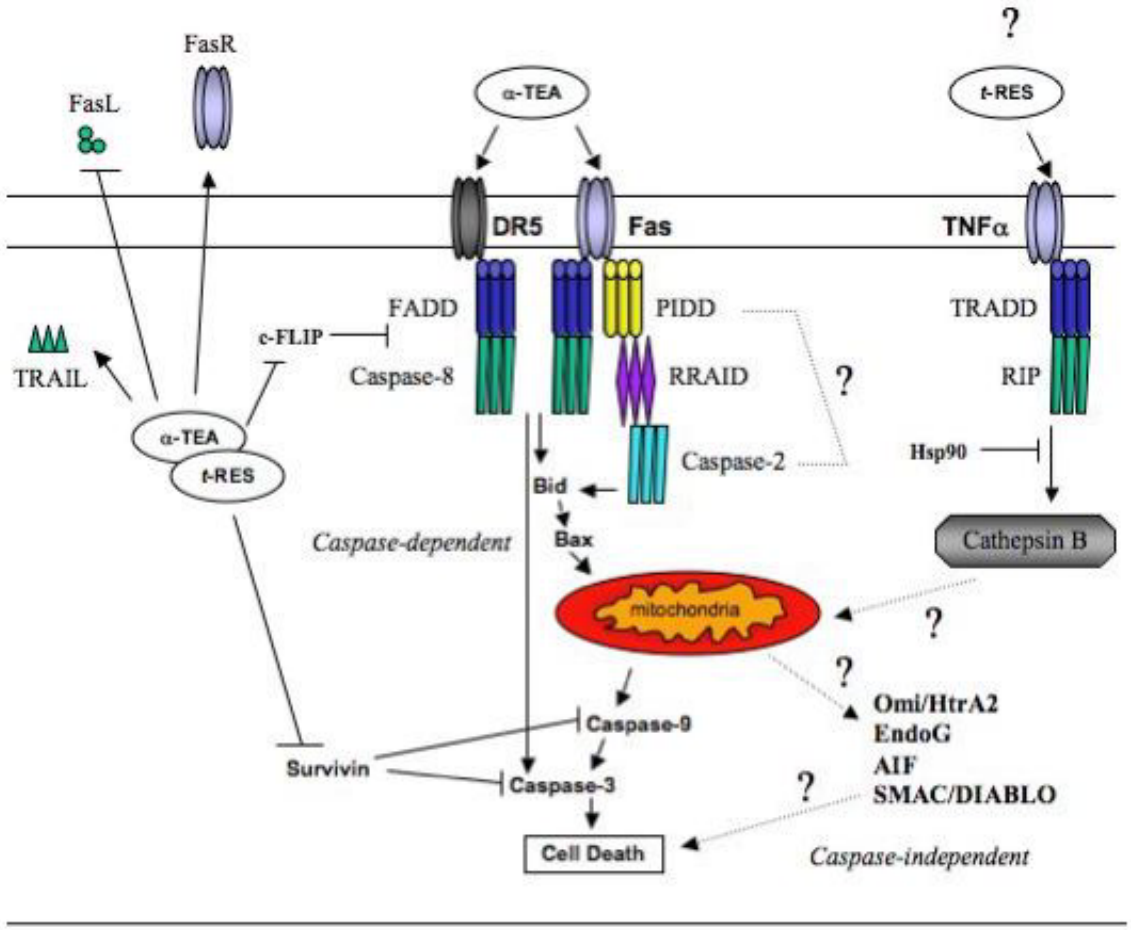

Figure 5.8. Proposed Signaling Mechanism for α-TEA and *t*-RES induced cell death. α-TEA induces apoptosis via the Fas and DR5 death receptors, which leads to activation caspases-2, -3, -8, and -9. *t*-RES activates cell death through the caspase-independent cell death (CICD) pathway. Both α-TEA and *t*-RES decrease levels of survivin and c-FLIP, increase TRAIL and Fas receptor, and decrease cellular FasL. α-TEA also increases DR5 levels in cells. Future studies will focus on caspase-2 and CICD signaling and are represented by dashed arrows and question marks.

Chapter 6: Summary and Future Directions

SUMMARY

Cancer is currently the most common cause of death in women under the age of 85. Breast cancer specifically will have the highest incidence of reported new cases in 2006 (32%) and be responsible for about 15 percent of cancer deaths in women [1]. More than 90% of these cancer deaths will be due to metastatic lesions that have arisen from aggressive tumor cells that have escaped and survived earlier attempts at treatment [87]. As we continue to understand more about the nature of tumor cells, signaling mechanisms, and the heterogeneity of tumors, it becomes increasingly clear that treatment with a single agent or method will not eliminate all of the cells of a tumor, and that perhaps a cocktail of treatments would be more effective. The goal of these studies was to further the understanding of the molecular mechanisms of α-TEA and explore its potential in combination with two other natural based chemotherapeutic agents, MSC/MSA and *t*-RES, to induce cell death in cancer cells.

α-TEA was first developed in our lab with the hope of finding a clinically useful vitamin E-based chemotherapeutic agent that could be administered in a clinically relevant manner. It is structurally similar to natural vitamin E, RRR-α-tocopherol but contains a non-hydrolysable ether-linked acetic acid moiety at carbon 6 of the chroman head, allowing it to remain stable *in vivo*. α-TEA has repeatedly been shown to induce human ovarian, cervical, breast, endometrial, prostate, lung, colon and lymphoid cells to undergo apoptosis without toxicity in normal PrEC and HMEC epithelial cells [38-39]. Several recent reports have also shown it to be an effective inhibitor of tumor and metastatic growth *in vivo* [40-44]. The studies reported here provide evidence to support

the efficacy of α-TEA as a chemopreventive and chemotherapeutic agent in human breast cancer cells.

Chapter 1 is an introductory chapter that introduces types of cancer cell death, specifically apoptosis and autophagocytosis. It also provides background information on the function, structure and metabolism of α-TEA, *t*-RES, and MSC/MSA. Various animal models and the main cell line used in the investigations presented in this dissertation were also reviewed.

Chapter 2 focuses on the initial studies that characterized how α-TEA, *t*-RES, and MSC/MSA inhibit proliferation and induce apoptosis in various breast and prostate cancer cell lines. Specifically we investigated the ability of α-TEA alone and together with MSA and *t*-RES to prevent proliferation and induce apoptosis and differentiation in human MDA-MB-435-F-L breast cancer cells. All three compounds induced apoptosis individually and synergistic apoptosis was seen in combinations. Other human breast (MDA-MB-231, MCF7, and T47D) and human prostate (LnCaP, PC-3, and DU-145) cancer cell lines were also tested and similar enhancements were seen. No apoptosis was seen in primary cultures of human mammary epithelial cells (HMECs). Western immunoblotting confirmed that all three compounds individually and in combination induced poly(ADP-ribose) polymerase cleavage with more complete cleavage seen in the combination. In studies of DNA synthesis arrest, clonegenic assay, and cell differentiation, all three compounds produced dose-dependent responses individually and enhanced responses in combinations. We concluded that the combination of α-TEA, MSA, and *t*-RES is more effective than single treatments for inhibiting cell proliferation, and inducing differentiation and apoptosis of human cancer cells in culture.

Chapter 3 investigated the ability of α-TEA, alone and together with MSC and *t*-RES, to reduce tumor burden, induce apoptosis, and prevent proliferation of MDA-MB-

435-F-L cells, *in vivo*. We showed that α-TEA and low doses of *t*-RES reduce tumor burden in athymic nude mice but that combinations of the three compounds are not as effective as α-TEA or *t*-RES alone. Immunohistochemistry of tumors showed an increase in TUNEL positive cells and a decrease in Ki-67 positive cells after treatment. Additionally, treatments were effective at reducing macroscopic and microscopic metastatic lung and lymph node lesions. This chapter also showed that the diet is important to the overall tumor growth because we found that the efficacy of *t*-RES administered at low (10 mg/kg bw) and high (100 mg/kg bw) concentrations was diet related. We concluded that when α-TEA, MSC, and *t*-RES are administered together to MDA-MB-435-F-L cells *in vivo*, the combination was not as effective as the individual treatments at reducing tumor burden, but all treatments prevent metastases to the lungs and lymph nodes. We also conclude that careful analysis of rodent diets should be made prior to any *in vivo* studies.

Chapter 4 focuses on the effectiveness of several natural compounds, α-TEA, MSA and *t*-RES, to prevent the formation of DMBA-induced lesions in the MMOC model and to prevent MNU-induced lesions in a rat mammary carcinogenesis model. In the MMOC model, α-TEA, MSA and *t*-RES were each effective at inhibiting the incidence and multiplicity of alveolar lesions and the multiplicity of ductal lesions. Four combinations of co-treatments were also made and analyzed for increased efficacy over individual treatments. A combination of α-TEA + *t*-RES was most effective against alveolar and ductal lesions. Based on these results, α-TEA + *t*-RES were combined in the MNU-induced rat mammary carcinogenesis model. Treatments lasted for 39 days at which time there were 45, 55 and 65% fewer tumors in the α-TEA, *t*-RES and Co-tx groups compared to the control. Even though a statistical difference was not seen between Co-tx, α-TEA and *t*-RES, the co-treatment group had 36% fewer tumors than α-

TEA and 22% fewer than *t*-RES. Weight loss was also looked at in this study as a measure of toxicity. Neither α-TEA nor *t*-RES caused significant weight loss, nor did α-TEA cause significant loss in tissue weight for spleen, heart, ovaries/uterus, lungs or kidneys. Together, these results suggest that α-TEA and *t*-RES may be an effective chemopreventive regimen.

Chapter 5 reports studies showing how *t*-RES and α-TEA synergize to produce increased levels of cell death in MDA-MB-435-F-L human breast cancer cells *in vitro*. Here we attempt to elucidate some of the signaling events that may contribute to this event. We found that pretreatment with *t*-RES, α-TEA or co-treatment can sensitize cells to Fas and TRAIL mediated apoptosis. Treatment with *t*-RES, α-TEA and co-treatment also increases levels of DR5, TRAIL, and Fas receptor and decreases FasL. α-TEA and co-treatment induced cell death was dependent on activation of caspases-2, -3, -8, and -9 while that for *t*-RES was not. Both *t*-RES and α-TEA decreased survivin and c-FLIP levels and a combination of the two decreased the levels of these proteins to undetectable levels. To further evaluate whether DR5, Fas, c-FLIP and survivin are important to the synergy effect, levels of these proteins were knocked down using siRNA. A statistical decrease in apoptosis was seen in co-treated cells where Fas and DR5 were knocked down and a statistical increase in apoptosis in *t*-RES and α-TEA treated cells after survivin and c-FLIP were knocked down. We also used TEM to evaluate the possible activation of autophagocytosis to explain the results seen for *t*-RES. Using TEM we saw low levels of AV in cells treated with *t*-RES and the co-treatment but not in α-TEA treated cells. Western-blot analyses showed *t*-RES to increase levels of beclin-1 but not LAMP-1 or MAP-LC3, but we were unable to confirm autophagy using flow cytometry. Based on the results reported here, we propose a signaling model (Fig 6.1) where the

synergy between α-TEA and *t*-RES is due to a combination of apoptosis and caspase-independent cell death (CICD).

FUTURE DIRECTIONS

Taken together, these studies suggest that α-TEA, in combination with other pro-cell death agents such as *t*-RES and MSC/MSA, can reduce human breast cancer growth *in vitro* and *in vivo* more effectively than any of the agents alone. These studies add insight into the complex mechanisms that regulate cell death in human breast cancer cells and provide a basis for future breast cancer treatments and prevention regimens. Future studies will focus on caspase-independent death signaling mechanisms in *t*-RES treated cells and caspase-2 signaling in α-TEA treated cells since both of these signaling mechanisms are poorly understood and appear important to the synergy between *t*-RES and α-TEA. One theory for CICD signaling is that TRADD and RIP are recruited to TNFα receptor to activate cathepsin B, which then interacts with the mitochondria to release AIF, SMAC/DIABLO, EndoG, and Omi/HtrA2. These proteins can then either inhibit IAPs in the cytoplasm or enter the nucleus to induce DNA condensation and fragmentation. One theory for caspase-2 signaling is that it is activated in p53-dependent PIDDosome formation, though it has been reported in both p53 $^{(+/+)}$ and p53 $^{(-/-)}$ cells [129]. PIDDosome formation is thought to occur when p53 recruits PIDD, RRAID and caspase-2 to Fas receptor, which activates caspase-2 [120, 129-130]. Active caspase-2 acts upstream of the mitochondria to cleave bid and induce bax translocation and cytochrome c release [130-131]. Clearly, more work needs to be done on understanding CICD and the function of caspase-2 and how they may act to enhance cell death.

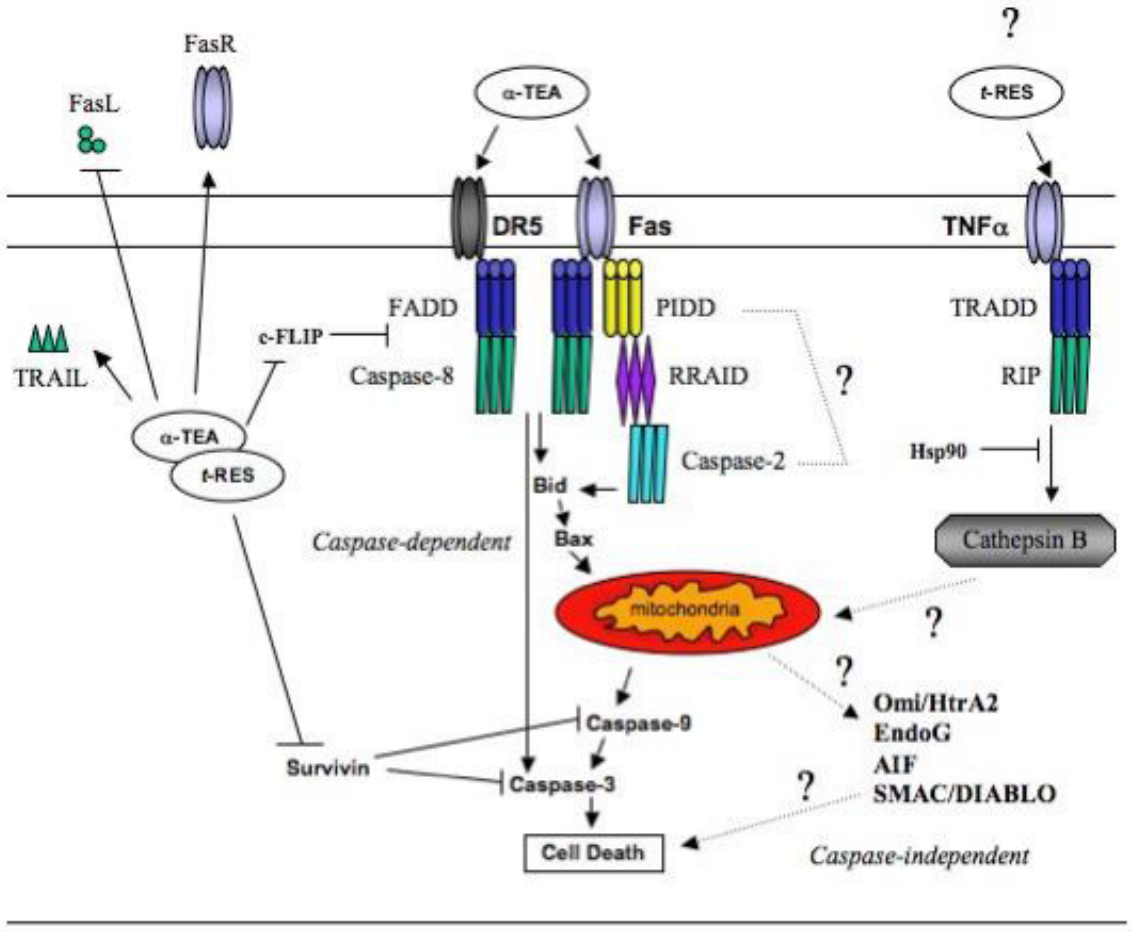

Figure 6.1. Proposed Signaling Mechanism for α-TEA and *t*-RES induced cell death and Future Studies. α-TEA induces apoptosis via the Fas and DR5 death receptors, which leads to activation caspases-2, -3, -8, and -9. *t*-RES activates cell death through the caspase-independent cell death (CICD) pathway. Both α-TEA and *t*-RES decrease levels of survivin and c-FLIP, increase TRAIL and Fas receptor, and decrease cellular FasL. α-TEA also increases DR5 levels in cells. Future studies will focus on caspase-2 and CICD signaling and are represented by dashed arrows and question marks.

References

1. Jemal, A., et al., *Cancer statistics, 2006.* CA Cancer J Clin, 2006. **56**: p. 106-30.

2. Aggarwal, B.B. and S. Shishodia, *Molecular targets of dietary agents for prevention and therapy of cancer.* Biochem Pharmacol, 2006. **71**: p. 1397-421.

3. Clarke, P. and S. Clarke, *Historic Apoptosis.* Nature, 1995. **378**: p. 230.

4. Bras, M., B. Queenan, and S.A. Susin, *Programmed cell death via mitochondria: different modes of dying.* Biochem (Moscow), 2005. **70**: p. 231-9.

5. Broker, L.E., F.A. Kruyt, and G. Giaccone, *Cell death independent of caspases: a review.* Clin Cancer Res, 2005. **11**: p. 3155-62.

6. Melino, G., R.A. Knight, and P. Nicotera, *How many ways to die? How many different models of cell death?* Cell Death Differ, 2005. **12**: p. 1457-62.

7. Edinger, A.L., and C.B. Thompson, *Death by design: apoptosis, necrosis, autophagy.* Curr Opin Cell Biol, 2004. **16**: p. 663-9.

8. Bursch, W., et al., *Programmed cell death (PCD): Apoptosis, autophagic PCD, or others?* Ann N Y Acad Sci, 2000. **926**: p. 1-12.

9. Hetz, C.A., V. Torres, and A.F.G. Quest, *Beyond apoptosis: nonapoptotic cell death in physiology and disease.* Biochem Cell Biol, 2005. **83**: p. 579-88.

10. Kim, R., M. Emi, and K. Tanabe, *Role of mitochondria as the gardens of cell death.* Cancer Chemother Pharmacol, 2005. **57**: p. 545-53.

11. Fulda, S., and K.M. Debatin, *Sensitization for tumor necrosis factor-related apoptosis-inducing ligand-induced apoptosis by the chemopreventative agent resveratrol.* Cancer Res, 2004. **64**: p. 337-46.

12. Peter, M.E., and P.H. Krammer, *The CD95 (APO-1/Fas) DISC and beyond.* Cell Death Differ, 2003. **10**: p. 26-35.

13. Kimberley, F.C., and G.R. Screaton, *Following a TRAIL: update on a ligand and its five receptors.* Cell Res, 2004. **14**: p. 359-72.

14. Kelley, S.K., and A. Ashkenazi, *Targeting death receptors in cancer with Apo2L/TRAIL.* Curr Opin Pharmacol, 2004. **4**: p. 333-9.

15. Wang, S., and W.S. El-Deiry, *TRAIL and apoptosis induction by TNF-family death receptors.* Oncogene, 2003. **22**: p. 8628-33.

16. Altieri D.C., *Survivin, versatile modulation of cell division and apoptosis in cancer.* Oncogene, 2003. **22**: p. 8581-9.

17. Fulda, S., and K.M. Debatin, *Resveratrol-mediated sensitization to TRAIL-induced apoptosis depends on death receptor and mitochondrial signaling.* Eur J Cancer, 2005. **41**: p. 786-98.

18. Yu, W., et al., *alpha-TEA inhibits survival and enhances death pathways in cisplatin sensitive and resistant human ovarian cancer cells.* Apoptosis, 2006. [In Press].

19. Mizushima, N., *Methods for monitoring autophagy.* Int J Biochem Cell Biol, 2004. **36**: p. 2491-502.

20. Lockshin, R.A., and Z. Zakeri, *Apoptosis, autophagy, and more.* Int J Biochem Cell Biol, 2004. **36**: p. 2405-19.

21. Boya, P., et al., *Inhibition of macroautophagy triggers apoptosis.* Mol Cell Biol, 2005. **25**: p. 1025-40.

22. Kabeya, Y., et al., *LC3, a mammalian homologue of yeast Apg8p, is localized in autophagosome membranes after processing.* EMBO J, 2000. **19**: p. 5720-8.

23. Tsujimoto, Y., and S. Shimizu, *Another way to die: autophagic programmed cell death.* Cell Death Differ, 2005. **12**: p. 1528-34.

24. Meijer, A.J., and P. Codogno, *Regulation and role of autophagy in mammalian cells.* Int J Biochem Cell Biol, 2004. **36**: p. 2445-62.

25. Scarlatti, F., et al., *Ceremide-mediated macroautophagy involves inhibition of protein kinase and up-regulation of beclin-1.* J Biol Chem, 2004. **279**: p. 18384-91.

26. Pattingre, S., and B. Levine, *Bcl-2 inhibition of autophagy: a new route to cancer?* Cancer Res, 2006. **66**: p. 2885-8.

27. Liang, X.H., et al., *Induction of autophagy and inhibition of tumorigenesis by beclin-1.* Nature, 1999. **402**: p. 672-6.

28. Kanzawa, T., et al*., Role of autophagy in temozolomide-induced cytotoxicity for malignant glioma cells.* Cell Death Differ, 2004. **11**: p. 448-57.

29. Paglin, S., et al., *A novel response of cancer cells to radiation involves autophagy and formation of acidic vesicles.* Cancer Res, 2001. **61**: p. 439-44.

30. Eskelinen, E.L., et al., *Role of LAMP-2 in lysosomal biogenesis and autophagy.* MBC, 2002. **13**: p. 3355-68.

31. "Selenium." Wikipedia. The Free Encyclopedia. 2 Aug 2006, 07:08 UTC. Wikimedia Foundation, Inc. 5 Aug 2006.

32. Institute of Medicine (2000) Dietary Reference Intakes for Vitamin C, Vitamin E, Selenium, and Carotenoids (A Report of the Panel on Dietary Antioxidants and Related Compounds). P 1-486. National Academy Press, Washington, D.C.

33. Brigelius-Flohe, R., et al., *The european perspective on vitamin E: current knowledge and future research.* Am J Clin Nutr, 2002. **76**: p. 703-16.

34. Brigelius-Flohe, R., and M. Traber, *Vitamin E: function and metabolism.* FASEB J, 1999. **13**: p. 1145-55.

35. Azzi, A., and A. Stocker, *Vitamin E: non-antioxidant roles.* Prog Lipid Res, 2000. **39**: p. 231-55.

36. Wang, X., and P.J. Quinn, *Vitamin E and its function in membranes.* Prog lipid Res, 1999. **38**: p. 309-36.

37. Kline, K., W. Yu, and B.G. Sanders, *Vitamin E and breast cancer.* J Nutr, 2004. **134**: p. 3458S-62S.

38. Kline, K., et al., *Vitamin E and breast cancer prevention: current status and future potential.* J Mammary Gland Biol Neoplasia, 2003. **8**: p. 91-102.

39. Anderson, K., et al., *Differential response of human ovarian cancer cells to induction of apoptosis by vitamin E succinate and vitamin E analog, alpha-TEA.* Cancer Res, 2004. **64**: p. 4263-9.

40. Lawson, K.A., et al., *Novel vitamin E analog decreases syngeneic mouse mammary tumor burden and reduces lung metastasis.* Mol Cancer Ther, 2003. **2**: p. 437-44.

41. Lawson, K.A., et al., *Comparison of vitamin E derivatives -TEA and VES in reduction of mouse mammary tumor burden and metastasis.* Exp Biol Med, 2004. **229**: p. 954-63.

42. Lawson, K.A., et al., *Novel vitamin E analog and 9-nitro-camptothecin administered as liposome aerosols decrease syngeneic mouse mammary tumor*

burden and inhibit metastasis. Cancer Chemother Pharmacol, 2004. **54**: p. 421-31.

43. Zhang, S., et al., *Vitamin E analog α-TEA and celecoxib alone and together reduce human MDA-MB-435-GFP-FL breast cancer and metastasis in nude mice.* Breast Cancer Res and Treatment, 2004. **87**: p. 111-21.

44. Anderson, K., et al., *Alpha-TEA plus cisplatin reduces human cisplatin-resistant ovarian cancer cell tumor burden and metastasis.* Exp Biol Med, 2004. **229**: p. 1169-76.

45. Baur, J.A., and D.A. Sinclair, *Therapeutic potential of resveratrol: the in vivo evidence.* Nat Rev Drug Discov, 2006. **5**: p. 493-506.

46. She, Q.B., et al., *Resveratrol-induced activation of p53 and apoptosis is mediated by extracellular signal-regulated protein kinases and p38 kinase.* Cancer Res, 2001. **61**: p. 1604-10.

47. Jang, M., et al., *Cancer chemopreventative activity of resveratrol, a natural product derived from grapes.* Science, 1997. **275**: p. 218-20.

48. Sgambato, A., et al., *Resveratrol, a natural phenolic compound, inhibits cell proliferation and prevents oxidative DNA damage.* Mutat Res, 2001. **496**: p. 171-80.

49. Mahyar-Roemer, M., et al., *Resveratrol induces colon tumor cell apoptosis independently of p53 and preceded by epithelial differentiation, mitochondrial proliferation and membrane potential collapse.* Int J Cancer, 2001. **94**: p. 615-22.

50. Hsieh, T.C., et al., *Cell cycle effects and control of gene expression by resveratrol in human breast carcinoma cell lines with different metastatic potentials.* Int J Oncol, 1999. **15**: p. 245-52.

51. Juan, M.E., M.P. Vinardell, and J.M. Planas, *The daily oral administration of high doses of trans-resveratrol to rats for 28 days is not harmful.* J Nutr, 2002. **132**: p. 257-60.

52. Asensi, M., et al., *Inhibition of cancer growth by resveratrol is related to its low bioavailability.* Free Radic Biol Med, 2002. **33**: p. 387-98.

53. Bhat, K.P., et al., *Estrogenic and antiestrogenic properties of resveratrol in mammary tumor models.* Cancer Res, 2001. **61**: p. 7456-63.

54. Opipari, A.W., et al., *Resveratrol-induced autophagocytosis in ovarian cancer cells.* Cancer Res, 2004. **64**: p. 696-703.

55. Pozo-Guisado, E., et al., *Resveratrol-induced apoptosis in MCF-7 human breast cancer cells involves a caspase-independent mechanism with down-regulation of bcl-2 and NF-kB.* Int J Cancer, 2005. **115**: p. 74-84.

56. Banerjee, S., C. Bueso-Ramos, and B.B. Aggarwal, *Suppression of 7,12-dimethylbenz(a)anthracene-induced mammary carcinogenesis in rats by resveratrol: role of nuclear factor-kB, cyclooxygenase 2, and matrix metalloprotease 9.* Cancer Res, 2002. **62**: p. 4945-54.

57. Kimura, Y., and H. Okuda, *Resveratrol isolated from Polygonum cuspidatum root prevents tumor growth and metastasis to lung and tumor-induced neovasculatization in Lewis lung carcinoma-bearing mice.* J Nutr, 2001. **131**: p. 1844-9.

58. Savouret, J.F., and M. Quesne, *Resveratrol and cancer: a review.* Biomed Pharmacother, 2002. **56**: p. 84-7.

59. Yu, C., et al., *Human, rat, and mouse metabolism of resveratrol.* Pharm Res, 2002. **19**: p. 1907-14.

60. Walle, T., et al., *High absorption but very low bioavailability of oral resveratrol in humans.* Drug Metab Dispos, 2004. **32**: p. 1377-82.

61. Spallholz, J.E., B.J. Shriver, and T.W. Reid, *Dimethyldiselenide and methylselininic acid generate superoxide in an in vitro chemiluminescence assay in the presence of glutathione: implications for the anticarcinogenic activity of L-selenomethionine and L-Se-methylselenocysteine.* Nutr Cancer, 2001. **40**: p. 34-41.

62. Ip, C., et al., *Chemical form of selenium, critical metabolites, and cancer prevention.* Cancer Res, 1991. **51**: p. 595-600.

63. Sinha, R., et al., *Methylselininic acid, a potent growth inhibitor of synchronized mouse mammary epithelial tumor cells in vitro.* Biochem Pharmacol, 2001. **61**: p. 311-17.

64. Dong, Y., et al., *Characterization of the biological activity of γ-glutamyl-Se-methylselenocysteine: a novel, naturally occurring anticancer agent from garlic.* Cancer Res, 2001. **61**: p. 2923-8.

65. Ip, C., et al., *Chemoprevention of mammary cancer with Se-allylselenocysteine and other selenoamino acids in the rat.* Anticancer Res, 1999. **19**: p. 2875-80.

66. Ip, C., and H.E. Ganther, *Comparison of selenium and sulfur analogs in cancer prevention.* Carcinogenesis, 1992. **13**: p. 1167-70.

67. Dong, Y., et al., *Identification of molecular targets associated with selenium-induced growth inhibition in human breast cells using cDNA microarrays.* Cancer Res, 2002. **62**: p. 708-14.

68. Medina, D., et al., *Se-methylselenocysteine: a new compound for chemoprevention of breast cancer.* Nutr Cancer, 2001. **40**: p. 12-7.

69. Jiang, C., et al., *Selenium-induced inhibition of angiogenesis in mammary cancer at chemoprevetive levels of intake.* Mol Carcinogenesis, 1999. **26**: p. 213-25.

70. "Tocopherol." Wikipedia. The Free Encyclopedia. 4 Aug 2006, 19:38 UTC. Wikimedia Foundation, Inc. 5 Aug 2006.

71. Ip, C., et al., *In vitro and in vivo studies of methylselininic acid: evidence that a monomethylated selenium metabolite is critical for cancer chemoprevention.* Cancer Res, 2000. **60**: p. 2882-6.

72. Ip, C., et al., *Chemical Speciation Influences Comparative Activity of Selenium-Enriched Garlic and Yeast in Mammary Cancer Prevention.* J Agric Food Chem, 2000. **48**: p. 2062-70.

73. Bandyopadhyay, A., et al., *Development and gene expression profiling of a metastatic variant of the human breast cancer MDA-MB-435 cells.* Cancer Biol Ther, 2005. **4**: p. 168-74.

74. Flanagan, S.P.*, 'Nude,' a new hairless gene with pleiotrophic effects in the mouse.* Genet Res, 1966. **8**: p. 295-309.

75. Nehls, M., et al., *New member of the winged-helix protein family disrupted in mouse and rat nude mutations.* Nature, 1994. **372**: p. 103-7.

76. Greiner, D.L., R.A. Hesselton, and L.D. Schultz, *SCID mouse models of human stem cell engraftment.* Stem Cell, 1998. **16**: p. 166-7.

77. Nonoyama, S., et al., *Strain-dependent leakiness of mice with severe combined immune deficiency.* J Immunol, 1993. **150**: p. 3817-24.

78. Ishigaki, Y., et al., *Enhanced human tumor cell transplantability in a new congenic immunodeficient mouse; KSN-BNX.* Folia Microbiol (Praha), 1998. **43**: p. 493-4.

79. Thompson, H.J., and M. Singh, *Rat models of premalignant breast disease.* J Mammary Gland Biol Neoplasia, 2000. **5**: p. 409-20.

80. Ginsburg, E., and B.K. Vonderhaar, "Whole organ culture of the mouse mammary gland." Methods in mammary gland biology and breast cancer research. Kluwer Academic, New York: 2000.

81. Mehta, R.G., M.E. Hawthorne, and V.E. Steele, *Induction and prevention of carcinogen-induced precancerous lesions in mouse mammary gland organ culture.* Methods Cell Sci, 1997. **19**: p. 19-24.

82. Mehta, R.G., et al., *Induction of atypical ductal hyperplasia in mouse mammary gland organ culture.* J Natl Cancer Inst, 2001. **93**: p. 1103-6.

83. Thompson, H.J., et al., *Rapid induction of mammary intraductal proliferations, ductal carcinoma in situ and carcinomas by the injection of sexually immature female rats with 1-methyl-1-nitrosourea.* Carcinogenesis, 1995. **16**: p. 2407-11.

84. Thompson, H.J., and H. Adlakha, *Dose-responsive induction of mammary gland carcinomas by the intraperitoneal injection of 1-methyl-1-nitrosourea.* Cancer Res, 1991. **51**: p. 3411-5.

85. Thompson, H.J., et al., *Temporal sequence of mammary intraductal proliferations, ductal carcinomas in situ and adenocarcinomas induced by 1-methyl-1-nitrosourea in rats.* Carcinogenesis, 1998. **19**: p. 2181-5.

86. Thompson, H.J., M. Singh, and J. McGinley, *Classification of premalignant and malignant lesions developing in the rat mammary gland after injection of sexually immature rats with 1-Methyl-1-nitrosourea.* J Mammary Gland Biol Neoplasia, 2000. **5**: p. 201-10.

87. Fidler, I.J., and C.M. Balch, *The biology of cancer metastases and implications for therapy.* Curr Probl Surg, 1987. **24**: p. 129-209.

88. Yu, W., et al., *Vitamin E succinate (VES) induces Fas sensitivity in human breast cancer cells: role for Mr 43,000 Fas in VES-triggered apoptosis.* Cancer Res, 1999. **59**: p. 953-61.

89. Israel, K., B.G. Sanders, and K. Kline, *RRR-alpha-tocopheryl succinate inhibits the proliferation of human prostatic tumor cells with defective cell cycle/differentiation pathways.* Nutr Cancer, 1995. **24**: p. 161-9.

90. Charpentier, A., et al., *RRR-alpha-tocopheryl succinate inhibits proliferation and enhances secretion of transforming growth factor-beta (TGF-beta) by human breast cancer cells.* Nutr Cancer, 1993. **19**: p. 225-39.

91. You, H., et al., *Role of extracellular signal-regulated kinase pathway in RRR-α-tocopheryl succinate-induced differentiation of human MDA-MB-435 breast cancer cells.* Mol Carcinogenesis, 2002. **33**: 228-36.

92. You, H., et al., *RRR- -tocopheryl succinate induces MDA-MB-435 and MCF-7 human breast cancer cells to undergo differentiation.* Cell Growth Differ, 2001. **12**: p. 471-80.

93. Wang, Q., et al., *Resveratrol promotes differentiation and induces Fas-independent apoptosis of human medulloblastoma cells.* Neurosci Lett, 2003. **351**: p. 83-6.

94. Clarke, R., *Issues in experimental design and endpoint analysis in the study of experimental cytotoxic agents in vivo in breast cancer and other models*. Breast Cancer Res Treat, 1997. **46**: p. 255-78.

95. Signorelli, P., and R. Ghidoni, *Resveratrol as an anticancer nutrient: molecular basis, open questions, and promises.* J Nutr Biochem, 2005. **16**: p. 449-66.

96. Knight, V., et al., *Anticancer effect of 9-nitrocamptothecin liposome aerosol on human cancer xenografts in nude mice.* Cancer Chemother Pharmacol, 1999. **44**: p. 177-86.

97. Weidner, N., *Intratumor microvessel density as a prognostic factor in cancer.* Am J Pathol, 1995. **147**: p. 9-19.

98. Busquets, S., et al., *Resveratrol, a natural diphenol, reduces metastatic growth in an experimental cancer model.* Cancer Lett, 2006. **[In Press]**.

99. Garvin, S., K. Ollinger, and C. Dabrosin, *Resveratrol induces apoptosis and inhibits angiogenesis in human breast cancer xenografts in vivo.* Cancer Lett, 2006. **231**: p. 113-22.

100. Sato, M., et al., *Prepubertal resveratrol exposure accelerates N-methyl-N-nitrosourea-induced mammary carcinoma in female Sprague-Dawley rats.* Cancer Lett, 2003. **202**: p. 137-45.

101. Thigpen, J.E., et al., *Phytoestrogen content of purified. Open- and closed-formula laboratory animal diets.* Lab Anim Sci, 1999. **49**: p. 530-6.

102. Barnes, S., *Effects of genistein on in vitro and in vivo models of cancer.* J Nutr, 1995. **125**: p. 777S-83S.

103. Barnes, S., et al., *Soybeans inhibit mammary tumors in models of breast cancer.* Clin Biol Res, 1990. **347**: p. 239-53.

104. Barnes, S., et al., *Potential role of dietary isoflavones in the prevention of cancer.* Adv Exp Med Biol, 1994. **354**: p. 135-47.

105. Kim, H., et al., *Chemoprevention by grape seed extract and genistein in carcinogen-induced mammary cancer in rats is diet dependent.* J Nutr, 2004. **134**: p. 3445S-52S.

106. Boettger-Tong, H., et al., *A case of a laboratory animal feed with high estrogenic activity and its impact on in vivo responses to exogenously administered estrogens.* EHP, 1998. **106**: p. 369-73.

107. Ley, F.J., et al., *Sterilization of laboratory animal diets using gamma radiation.* Lab Anim, 1969. **3**: p. 221-54.

108. Rose, D.P., et al., *Effects of diets containing different levels of linoleic acid on human breast cancer growth and lung metastases in nude mice.* Cancer Res, 1993. **53**: p. 4686-90.

109. Connolly, J.M., and D.P. Rose, *Effects of fatty acids on invasion through reconstituted basement membrane ('Matrigel') by a human breast cancer cell line.* Cancer Lett, 1993. **75**: p. 137-42.

110. Rose, D.P., and J.M. Connolly, *Influence of dietary linoleic acid on experimental human breast cancer cell metastases in athymic nude mice.* Int J Oncol, 1998. **13**: p. 1179-83.

111. Rose, D.P., J.M. Connolly, and X.H. Liu, *Effects of linoleic acid on the growth and metastases of two human breast cancer cell lines in nude mice and the invasive capacity of these cell lines in vitro.* Cancer Res, 1994. **54**: p. 6557-62.

112. Benton, C., *Phytoestrogens and cancer research.* Harlan Teklad.

113. Eldridge, A.C., and W.F. Kwolek, *Soybean isoflavones: effect of environment and variety on composition.* J Agric Food Chem, 1983. **31**: p. 394-6.

114. Steele, V.E., et al., *Use of in vitro assays to predict the efficacy of chemopreventive agents in whole animals.* J Cell Biochem, 1996. **26S**: p. 29-53.

115. Russo, J., et al., *Tumours of the mammary gland.* IARC Sci Publ, 1990. **99**: p. 47-78.

116. Tirmenstein, M.A., et al., *Sensitive method for measuring tissue alpha-tocopherol and alpha-tocopheryloxybutyric acid by high-performance liquid chromatography with fluorometric detection.* J Chromatogr B Biomed Sci Appl, 1998. **707**: p. 308-11.

117. Tirmenstein, M.A., and S.D. Nelson, *Subcellular binding and effects on calcium homeostasis produced by acetaminphen and a nonhepatotoxic regioisomer, 3'-hydroxyacetanilide, in mouse liver.* J Biol Chem, 1989. **264**: p. 9814-9.

118. Manson, M.M., et al., *Innovative agents in cancer prevention.* RRCR, 2005. **166**: p. 257-75.

119. Chipuk, J.E., and D.R. Green, *Do inducers of apoptosis trigger caspase-independent cell death?* Nat Rev Mol Cell Biol, 2005. **6**: p. 268-74.

120. Kroemer, G., and S.J. Martin, *Caspase-independent cell death.* Nat Med, 2005. **11**: p. 725-30.

121. Shun, M.C., et al., *Pro-apoptotic mechanisms of action of a novel vitamin E analog (alpha-TEA) and a naturally occurring form of vitamin E (delta-Tocotrienol) in MDA-MB-435 human breast cancer cells.* Nutr Cancer, 2004. **48**: p. 95-105.

122. Dan, H.C., et al., *Phosphatidylinositol-3-OH kinase/AKT and surviving pathways as critical targets for geranylgeranyltransferase I inhibitor-induced apoptosis.* Oncogene, 2004. **23**: p. 706-15.

123. Kim, Y., et al., *An inducible pathway for degradation of FLIP protein sensitizes tumor cells to TRAIL-induced apoptosis.* J Biol Chem, 2002. **277**: p. 22320-9.

124. Yu, W., B.G. Sanders, and K. Kline, *RRR-α-tocopheryl succinate-induced apoptosis of human breast cancer cells involves Bax translocation to mitochondria.* Cancer Res, 2003. **63**: p. 2483-91.

125. Shun, M.C., et al., *Pro-apoptotic mechanisms of action of a novel vitamin E analog (alpha-TEA) and a naturally occurring form of vitamin E (delta-Tocotrienol) in MDA-MB-435 human breast cancer cells.* Nutr Cancer, 2004. **48**: p. 95-105.

126. Delmas, D., et al., *Redistribution of CD95, DR4 and DR5 in rafts accounts for the synergistic toxicity of resveratrol and death receptor ligands in colon carcinoma cells.* Oncogene, 2004. **23**: p. 8979-86.

127. Liu, J., et al., *Differential regulation of CYP1A1 and CYP1B1 expression in resveratrol-treated human medulloblastoma cells.* Neurosci Lett, 2004. **363**: p. 257-61.

128. Fulda, S., and K.M. Debatin, *Sensitization for anticancer drug-induced apoptosis by the chemopreventive agent resveratrol.* Oncogene, 2004. **23**: p. 6702-11.

129. Vakifahmetoglu, H., et al., *Functional connection between p53 and caspase-2 is essential for apoptosis induced by DNA damage.* Oncogene, 2006. [In Press].

130. Tinel, A., and J. Tschopp, *The PIDDosome, a protein complex implicated in activation of caspase-2 in response to gentoxic stress.* Science, 2004. **304**: p. 843-6.

131. Lavrik, I.N., et al., *Caspase-2 is activated at the CD95 death-inducing signaling complex in the course of CD95-induced apoptosis.* Blood, 2006. **108**: p. 559-65.

132. Lamparska-Przybysz, M., B. Gajkowska, and T. Motyl, *Cathepsins and bid are involved in the molecular switch between apoptosis and autophagy in breast cancer MCF-7 cells exposed to camptothecin.* J Physiol Pharmacol, 2005. **56**: p. 159-79S.

Vita

Rachel Marie Snyder was born in San Antonio, Texas on October 20, 1979 to Jerry Ray Saunders and Nancy Jane Saunders. She has two younger brothers, Nathan John Saunders and Matthew Nelson Saunders who were born June 27, 1984 and April 29, 1986. Rachel's family moved to Garland, Texas shortly before her first birthday and a few years later to another suburb of Dallas, Rowlett, where she lived until graduating from Garland High School, Garland, Texas in 1998. In the fall of that year she began her secondary education at The University of Texas at Austin and in the summer of 2000 met her future husband Michael Garrett Snyder while taking a Physics lab course. She received her Bachelor of Science in Microbiology from The University of Texas in 2001 and began work as a veterinary technician at University Animal Clinic in Austin, Texas. Before beginning her graduate work, Rachel worked for a short time as a technician in the lab of Drs. Bob G. Sanders and Kimberly Kline where she remained throughout her graduate career. Michael and Rachel married on May 4, 2003.

Permanent address: 3607 Lily Lane, Rowlett, TX 75089

This dissertation was typed by Rachel Marie Snyder